

Anonymous Referee #1:

In this study, the authors examined light absorption of black carbon (BC) under clean and polluted conditions based on observations. They found that we found that the aging degree and light absorption capability of BC containing particles increased by 26-73% and 13-44% respectively, due to more coating materials on the BC surface. This work is interesting and merits publication after following comments addressed.

We would like to thank the reviewer for the valuable and constructive comments, which helps us to improve the manuscript. Listed below are our responses to the comments point-by-point, as well as the corresponding changes made to the revised manuscript. The reviewer's comments are marked in black and our answers are marked in blue, and the revision in the manuscript is further formatted as *Italics*.

1. General Comments

The authors reported a large amount of BC was originated from sources outside Beijing based on effective emission intensity. It is true in this analysis. But the authors need to caution that they were comparing the contributions from a small region (Beijing) and a large region (outside Beijing or adjacent regions). In addition, the authors evaluated the contribution of local photochemical production by the changes of O₃ concentrations in the atmosphere. They found that the O₃ concentrations showed a different temporal trend. It only means weak photochemical production of O₃ due to high aerosol concentrations blocking sunlight. It does not mean the local aging of BC is weak because high concentrations of aerosols may compensate the adverse conditions for BC aging. Anyway, the authors should provide uncertainty values for the numbers.

Response: We thanks the reviewer for raising these questions and we hope the reviewer will be clear after our detailed clarification below.

(1) In terms of comparing the contributions of BC from a small region (Beijing) and a large region (outside Beijing or adjacent regions), we agree with the reviewer that we need to caution. Noted that we are not paying attention to the difference between the contributions of BC from local Beijing and other regions (For example, the contributions of BC from local Beijing (~37%) during polluted period was smaller than that from other regions (~63%), partly due to comparing the contributions from a small region (Beijing) and a large region (outside Beijing)). In this study, we focus on comparing the contributions of BC from outside Beijing (considered as regional origins in this study) among different pollution levels (i.e., clean, slight polluted and polluted period). During polluted period, we found that the BC amount from regional origins (i.e., other regions not including local Beijing) accounted for ~21%, ~39% and ~63% of total BC amount in the site during the clean, slightly polluted and polluted periods, respectively. This revealed that the regional contribution to BC over Beijing increased as the air pollution levels increased.

To make this point clear, the related discussion has been revised in the manuscript, as “*In this study, the spatial origin of total BC in the site was classified into local Beijing and other regions (i.e., adjacent areas, considered as regional origins in this study). Noted that the local region (i.e., Beijing) defined in this study is smaller than areas outside Beijing (e.g., Hebei, Tianjin, Shanxi and Inner Mongolia (Fig. S1)). Table 1 lists the contribution of BC from regional origins (i.e., $EEI_{outside}/EEI_{total}$ ratio). During polluted period, the contributions of BC from regional origins was ~63%, larger than that from local Beijing (~37%). This was partly due to comparing the contributions from a small region (Beijing) and a large region (outside Beijing). In this study, we focus on comparing the contributions of BC from outside Beijing (considered as regional origins in this study) among different pollution levels (i.e., clean, slight polluted and polluted period). The BC amount from regional origins (i.e., outside Beijing) accounted for ~21%, ~39% and ~63% of total BC amount in*

the site during the clean, slightly polluted and polluted periods, respectively. This revealed that the regional contribution to BC over Beijing increased as the air pollution levels increased.”

- (2) In terms of evaluating the contribution of local photochemical production by the changes of O₃ concentrations in the atmosphere, we have revised the related discussion, as *“When PM₁ concentrations were higher than ~120 μg m⁻³, O₃ concentrations decreased to ~2 ppb. Zheng et al. (2015) has demonstrated the weakened importance of photochemistry in the production and aging of secondary aerosols in Beijing under polluted conditions due to decrease of oxidant concentrations. This indicated that the photochemical processing in BC aging may be weakened under higher polluted levels (i.e., PM₁>120μg m⁻³). Noted that photochemical processing is not the only possible pathway in BC aging process and other pathways were not discussed in this study. The local aging process of BC might be enhanced by other pathways. For example, high concentrations of aerosols under polluted environment may compensate the adverse photochemical conditions for BC aging.”*

2. Specific comments

- (1) Page 1 Line 14: It 'is' well known.

Response: Many thanks. We have revised it.

- (2) Page 2 Line 22: What is the 'lens effect'?

Response: Thanks for the comment. We have stated/defined the “lens effect” in the revised manuscript according to the literatures (Bond et al., 2006; Fuller et al., 1999; Jacobson, 2001; Lack and Cappa, 2010): *“The non-BC species (i.e., coating materials) on the surface of BC can enhance BC light absorption via the lens effect (namely, the*

coating materials act as a lens to focus more photons on BC, Bond et al., 2006; Fuller et al., 1999; Jacobson, 2001; Lack and Cappa, 2010)”

(3) Page 7 Line 27: Missing ‘)’.

Response: Thanks. We apologize for the typo and have revised it.

(4) Page 8 Line 21: How many samples are there for different PM1 conditions?

Response: Thanks for the comments. In order to obtain the evolution of D_p/D_c ratio and E_{ab} of BC-containing particles with size-resolved rBC cores with pollution development (shown in Fig. 2a), we used 28 different PM1 conditions.

To make this point clear, we revised the statement in the caption of Fig. 2a in the revised manuscript, as “*Figure 2. (a) The aging degree (D_p/D_c ratio) and light absorption capability (E_{ab}) of BC-containing particles with size-resolved rBC cores (D_c) under different PM₁ concentration (28 samples).*”

(5) Page 9 Line 27: It should be ‘Figure 4’. The unit of EEI is ‘t/grid/year’ shown in the figure. What does the ‘t’ stand for?

Response: Thanks. We apologize for the typo and have changed “Figure 5” in P9/L27 into “*Figure 4*”. The “t” stand for “ton”, the unit of amount of air pollutant emission. We have changed “t/grid/year” into “*ton/grid/year*”.

(6) Page 9 Line 30: ‘account for’ what? Does that mean the rest of the contribution is from Beijing’s own emissions or emissions from other non-adjacent regions? As I understand, there are three emission source regions, emissions from Beijing, adjacent regions, and other regions. Please clarify.

Response: Thanks to the reviewer to point this out. The “account for” here represents the proportion of BC amount from adjacent regions in total BC amount in the site. In

this study, the spatial origin of total BC in the site was classified into local Beijing and other regions (e.g., Hebei, Tianjin, Shanxi and Inner Mongolia).

To make it clear, we have revised the manuscript, as *“In this study, the spatial origin of total BC in the site was classified into local Beijing and other regions (i.e., adjacent areas, considered as regional origins in this study). Noted that the local region (i.e., Beijing) defined in this study is smaller than areas outside Beijing (e.g., Hebei, Tianjin, Shanxi and Inner Mongolia (Fig. S1)). Table 1 lists the contribution of BC from regional origins (i.e., $EEI_{outside}/EEI_{total}$ ratio). During polluted period, the contributions of BC from regional origins was ~63%, larger than that from local Beijing (~37%). This was partly due to comparing the contributions from a small region (Beijing) and a large region (outside Beijing). In this study, we focus on comparing the contributions of BC from outside Beijing (considered as regional origins in this study) among different pollution levels (i.e., clean, slight polluted and polluted period). The BC amount from regional origins (i.e., outside Beijing) accounted for ~21%, ~39% and ~63% of total BC amount in the site during the clean, slightly polluted and polluted periods, respectively. This revealed that the regional contribution to BC over Beijing increased as the air pollution levels increased.”*

(7) Page 10 Line 1: Does EEI_{total} include the contribution from Beijing’s own emissions?

Response: Thanks and yes. The EEI_{total} includes the contribution from Beijing’s own emissions, calculated by Eq. (8) in the manuscript.

(8) Page 10 Line 3: I am confused that EEI_{total} increased by a factor of 4.6, but after that, the authors said BC from adjacent area. Should it be $EEI_{adjacent}$? In addition, I think it needs a supplement to the conclusion that the increased BC is due to transport of polluted air mass, not the adverse local meteorology. It is true for a very small region, based on the analysis of this study, because the authors were comparing the

contributions from a small region and a large region. Also, polluted events always occur over a larger region, even spread the whole eastern China. They are definitely caused by adverse meteorology. The more transport of pollutants into Beijing is probably a consequence of increased pollutants due to adverse meteorology in other regions. For example, Yang et al. (2017) analyzed the source-receptor relationship of BC in China and found that, during polluted days in winter, the increases in BC over the North China Plain (including Beijing) is dominated by its local emissions instead of regions outside North China Plain. The weakening of winds can explain it.

Response: Thanks for the comments. The EEI given here is the total EEI (EEI_{total} , calculated by Eqs. (7) and (8) in the manuscript) including BC from Beijing and other regions. The EEI_{total} can be used to characterize the total BC amount (unit of ton/year, not the BC concentrations) transported to the site. The EEI_{total} strongly depends on BC emission of source origins (including local Beijing and other regions) and dry/wet deposition during atmospheric transport. Considering the change of BC emission from local Beijing under different pollution levels was slight, the variations in EEI_{total} was dominated by BC from different regional origins (i.e., higher EEI_{total} due to BC from regional origins with higher emission (e.g., south of Hebei) and lower EEI_{total} due to BC from regional origins with lower emission (e.g., Mongolia)). On the other hand, the effect of local meteorology on EEI_{total} is slight. However, BC concentration in the site strongly depends on both total BC amount (transported from local Beijing and other regions, characterized by EEI_{total} in this study) and local meteorology. In this study, we found that the EEI_{total} and BC concentrations from the clean period to the polluted period increase by ~4.6 times and ~7.4 times, respectively, revealing that the increase of EEI_{total} account for ~62% of the increase in BC mass concentration. This indicated that the adverse local meteorology contributed ~38% of the increase in BC mass concentration in the site from the clean period to the polluted period.

We agreed with the reviewer that less effect of adverse local meteorology is due to that local Beijing is smaller than other regions (e.g., Hebei, Tianjin, Shanxi and Inner

Mongolia). Polluted events always occur over a larger region and are definitely caused by adverse meteorology. For our case, the adverse meteorology during polluted days in the whole large region including Beijing and other adjacent areas can lead to the increase of pollutants and then more transport of pollutants into Beijing.

Following the reviewer's suggestion, we have revised the statement to assess the effect of regional transport and adverse local meteorology on BC increase under polluted conditions, as *“Table 1 shows that the EEI_{total} was 4.6 times higher during the polluted period than during the clean period, revealing that polluted air mass brought more BC to Beijing. BC concentration in the site strongly depends on both total BC amount (transported from local Beijing and other regions, characterized by EEI_{total} in this study) and local meteorology. Table 1 shows that the BC concentrations from the clean period to the polluted period increase by ~7.4 times. The increase of EEI_{total} (~4.6 times) accounted for ~62% the increase in BC mass concentrations (~7.4 times). This indicated that the adverse local meteorology contributed ~38% of the increase in BC mass concentration in the site from the clean period to the polluted period. Compared with regional transport, less effect of adverse local meteorology might be attributed to relatively small areas defined as the local region (i.e., Beijing) in this study. Polluted events in China always occur over a large region, e.g., North China Plain (Yang et al., 2017; Zheng et al., 2015). For our case, the adverse meteorology during polluted days in the whole large region including Beijing and other areas can lead to the increase of pollutants and then more transport of pollutants into Beijing. Yang et al. (2017) found that the increases in BC concentration under polluted conditions over the North China Plain (including Beijing and other adjacent areas) is dominated by its local emissions due to adverse meteorology.”*

(9) Page 11 Line 1: What does the normalized EEI mean? Is it a percent value or some index?

Response: Thanks to the reviewer to point this out. In this study the EEI_{total} was normalized by scaling by a factor of 10^{-3} , namely $EEI_{total,normalized} = EEI_{total}/1000$. To make it clear, we have added the statement in the caption in Fig.6 in the revised manuscript, as “*The normalized EEI_{total} ($EEI_{total,normalized}$) was calculated by scaling by a factor of 10^{-3} , namely $EEI_{total,normalized} = EEI_{total}/1000$.*”

(10) Page 11 Line 19: I see the author calculated DRF by scaling the average DRF (0.32 W m^{-2}) of externally mixed BC with an average MAC of $7.5 \text{ m}^2 \text{ g}^{-1}$ from various climate models (Bond et al., 2013). Is the DRF value global average with a fixed BC climatology? The author should make it clear, or the readers may think the value is the DRF over Beijing during the analyzed clean and polluted days.

Response: We thank the reviewer for raising the important issue. In this study, the DRF (0.31 W m^{-2}) of externally mixed BC was the global averages from the global climate models listed in Table R1 in the response (Table S1 in the revised manuscript). The calculated DRF of BC-containing particles (shown in the Fig.7 in the revised manuscript) was obtained by scaling the average DRF (0.31 W m^{-2}) of externally mixed BC from various global climate models (Bond et al. 2013) with a scaling factor of E_{ab} under different PM_{10} concentrations. Noted that the DRF values calculated here did not consider the change of BC amount under different pollution levels. In this study, we focused on investigating the effect of BC light-absorption capability on DRF. Therefore, the increase in DRF of BC with increasing pollution levels just considered the change in light-absorption capability of BC.

Table R1 (Table S1 in the revised manuscript) The DRF of externally mixed BC from global climate models. The modeled values were taken from Bond et al. (2013).

Global climate Model	Mixing state	Modeled MAC ($\text{m}^2 \text{ g}^{-1}$)	Modeled DRF (W m^{-2})	Reference
AeroCom models				
GISS	External	8.4	0.22	Schulz et al. (2006)
LOA	External	8.0	0.32	Schulz et al. (2006)
LSCE	External	4.4	0.30	Schulz et al. (2006)

SPRINTARS	External	9.8	0.32	Schulz et al. (2006)
UIO-CTM	External	7.2	0.22	Schulz et al. (2006)
UMI	External	6.8	0.25	Schulz et al. (2006)
Other models				
BCC_AGCM	External	4.3	0.10	Zhang et al. (2012)
CAM3 ECA	External	10.6	0.57	Kim et al. (2008)
GISS-GCM II	External	7.8	0.51	Chung and Seinfeld (2002)
Average values		7.5	0.31	

To make it clear, we added the Table S1 and the related discussion in the revised manuscript, as “*The DRF values for BC-containing particles at different pollution levels were obtained by scaling the average DRF (0.31 W m^{-2}) of externally mixed BC from various climate models (Bond et al. 2013) with a scaling factor of the calculated E_{ab} under different PM_{10} concentrations (Fig. 2b). The DRF (0.31 W m^{-2}) of externally mixed BC was the global averages from the global climate models listed in Table S1. In order to point out the effect of BC light-absorption capability on DRF under different PM_{10} concentrations, we did not consider the changes of BC amount for DRF calculation.*”

(11) Page 12 Line 15: Delete 'by'.

Response: Thanks. We have revised it.

(12) Page 13 Line 19: It was defined as transport-controlled 'period'.

Response: Thanks. We have changed “region” into “period”.

References:

Bond, T. C., Doherty, S. J., Fahey, D. W., Forster, P. M., Berntsen, T., DeAngelo, B. J., Flanner, M. G., Ghan, S., Kärcher, B., Koch, D., Kinne, S., Kondo, Y., Quinn, P. K., Sarofim, M. C., Schultz, M. G., Schulz, M., Venkataraman, C., Zhang, H., Zhang, S., Bellouin, N., Guttikunda, S. K., Hopke, P. K., Jacobson, M. Z., Kaiser, J. W., Klimont, Z., Lohmann, U., Schwarz, J. P., Shindell, D., Storelvmo, T., Warren, S. G., and Zender, C. S.: Bounding the role of black carbon in the climate system: A scientific assessment, *J. Geophys. Res.-Atmos.*, 118, 5380-5552, 10.1002/jgrd.50171, 2013.

Bond, T. C., Habib, G., and Bergstrom, R. W.: Limitations in the enhancement of visible light absorption due to mixing state, *J. Geophys. Res.-Atmos.*, 111, 2006.

Chung, S. H., and Seinfeld, J. H.: Global distribution and climate forcing of carbonaceous aerosols, *J. Geophys. Res.-Atmos.*, 107, AAC 14-11-AAC 14-33, 10.1029/2001JD001397, 2002.

Dongchul, K., Chien, W., L., E. A. M., C., B. M., and J., R. P.: Distribution and direct radiative forcing of carbonaceous and sulfate aerosols in an interactive size - resolving aerosol - climate model, *J. Geophys. Res.-Atmos.*, 113, doi:10.1029/2007JD009756, 2008.

Fuller, K. A., Malm, W. C., and Kreidenweis, S. M.: Effects of mixing on extinction by carbonaceous particles, *J. Geophys. Res.-Atmos.*, 104, 15941-15954, 1999.

Jacobson, M. Z.: Strong radiative heating due to the mixing state of black carbon in atmospheric aerosols, *Nature*, 409, 695-697, 2001.

Kim, D., Wang, C., Ekman, A. M. L., Barth, M. C., and Rasch, P. J.: Distribution and direct radiative forcing of carbonaceous and sulfate aerosols in an interactive size-resolving aerosol-climate model, *J. Geophys. Res.-Atmos.*, 113, 10.1029/2007JD009756, 2008.

Lack, D. A., and Cappa, C. D.: Impact of brown and clear carbon on light absorption enhancement, single scatter albedo and absorption wavelength dependence of black carbon, *Atmos. Chem. Phys.*, 10, 4207-4220, 2010.

Schulz, M., Textor, C., Kinne, S., Balkanski, Y., Bauer, S., Berntsen, T., Berglen, T., Boucher, O., Dentener, F., Guibert, S., Isaksen, I. S. A., Iversen, T., Koch, D., Kirkevåg, A., Liu, X., Montanaro, V., Myhre, G., Penner, J. E., Pitari, G., Reddy, S., Seland, Ø.,

Stier, P., and Takemura, T.: Radiative forcing by aerosols as derived from the AeroCom present-day and pre-industrial simulations, *Atmos. Chem. Phys.*, 6, 5225-5246, 2006.

Yang, Y., Wang, H., Smith, S. J., Ma, P.-L., and Rasch, P. J.: Source attribution of black carbon and its direct radiative forcing in China, *Atmos. Chem. Phys.*, 17, 4319-4336, 2017.

Zhang, H., Wang, Z., Wang, Z., Liu, Q., Gong, S., Zhang, X., Shen, Z., Lu, P., Wei, X., Che, H., and Li, L.: Simulation of direct radiative forcing of aerosols and their effects on East Asian climate using an interactive AGCM-aerosol coupled system, *Clim. Dyn.*, 38, 1675-1693, 10.1007/s00382-011-1131-0, 2012.

Zheng, G. J., Duan, F. K., Su, H., Ma, Y. L., Cheng, Y., Zheng, B., Zhang, Q., Huang, T., Kimoto, T., Chang, D., Pöschl, U., Cheng, Y. F., and He, K. B.: Exploring the severe winter haze in Beijing: the impact of synoptic weather, regional transport and heterogeneous reactions, *Atmos. Chem. Phys.*, 15, 2969-2983, 2015.

Anonymous Referee #2:

We would like to thank the reviewer for the valuable and constructive comments, which helps us to improve the manuscript. Listed below are our responses to the comments point-by-point, as well as the corresponding changes made to the revised manuscript. The reviewer's comments are marked in black and our answers are marked in blue, and the revision in the manuscript is further formatted as '*Italics*'.

1. Summary

The authors present measurements from Beijing, focusing on analysis and interpretation of data from a single particle soot photometer. They use the SP2 measurements to infer light absorption and light absorption amplification factors. The technical analysis is of reasonably high quality. The interpretation and discussion could benefit from some stronger quantitative analysis to discern process-based information. The authors also need to clarify how they have calculated averages, and whether they are mass-weighted or not. My specific comments follow below.

Response: We thank the reviewer for raising the important issue. In the revised manuscript, the average values of the D_p/D_c ratio, the calculated E_{ab} , MAC, SFE and DRF were mass-weighted across all sizes above the detection limit of SP2 incandescence (i.e., rBC larger than ~75 nm). The mass-weighted averages were shown in the new Fig. 2b, Fig. 6, Fig. 7 and Table 1. The change rate of E_{ab} shown in the Fig. 4 was also obtained based on the mass-weighted averages of the calculated E_{ab} .

2. Specific comments

(1) General comment on terminology: Throughout the manuscript, the authors need to clarify when they are talking about actual absorption measurements or absorption enhancement measurement, and when they are talking about calculated/theoretical values. There are many, many points where this distinction needs to be made clearly, starting from the abstract and continuing through the conclusions. I will note only a few points where this is necessary as examples, but there are many more beyond what I have noted.

P1 L20 & 27, and P2 L1 & L3: This should be changed to “theoretical light absorption capability”

Response: Thanks for the suggestion. Throughout the manuscript, we have clarified the statement on actual absorption measurements and theoretical values.

(2) P2, L14: The Moffett study does not directly measure light absorption. Their conclusions are based on theoretical calculations. Thus, it is not appropriate here. Same for the Zhang et al. 2016 reference.

Response: Thanks and we agree with the reviewer. The references of Moffett et al. (2009) and Zhang et al. 2016 (2016) have been removed. We have added some other citations (Knox et al., 2009; Peng et al. 2016; Schnaiter et al. 2005), which reported the directly measure light absorption.

(3) P2, L15: It is unclear as written when the authors are referring to theoretical studies versus observations studies. This must be clarified.

Response: Thanks. Following the suggestion, the statement has been changed as “*Previous theoretical (Jacobson, 2001; Moffet et al., 2009; Zhang et al., 2016) and observation studies (Cappa et al., 2012; Peng et al., 2016; Knox et al., 2009) showed a broad range of absorption enhancements (1.05-3.05) of BC during the atmospheric aging process.*”

(4) P2, L23: This should be revised to clarify that the concept of “more coating materials results in stronger light absorption capability” depends on whether one considers coatings on individual particles versus coatings averaged over the ensemble of particles.

Response: Thanks for the comments. To clarify it, we have revised the statement as *“In terms of individual BC particle, more coating materials results in its stronger light absorption capability.”*

(5) P2 ,L29: It should be clarified that the idea that more materials coat BC under polluted conditions is only true so far as the total amount of BC does not scale equally with the overall amount of pollution. If there were more secondary aerosol but also more BC particles, then it is possible that the average coating per particle is unchanged in more versus less polluted conditions. Also, this statement oversimplifies issues related to mixing state, and whether that secondary material condenses on BC versus on non-BC containing particles. The authors oversimplify here, in my opinion.

Response: Thanks the reviewer to point this out. To clarify it, the sentence has been revised as *“Whether the changes of secondary aerosols with air pollution will affect the coating materials on the BC is complex, which not only depends on the increase in BC amount versus secondary aerosols but also controlled by secondary material condensation on BC versus non-BC containing particles.”*

(6) P2, L31: it is unclear what “quasi-atmospheric” means. Also, this study ultimately indicates very simply that when you have greater amounts of coating on monodisperse particles the absorption enhancement is larger.

Response: Thanks. To make it clear, we have changed “quasi-atmospheric” into *“Recent BC aging measurements in Beijing and Houston using an environmental chamber (flowing ambient air to feed with lab-generated fresh BC particles)....”*

(7) P4, L3: Fig. S2 indicates that the uncertainty in the aethelometer measurements is 10% based on the uncertainty in the “compensation factors.” However, this inherently assumes that the measurements by the reference instrument, a MAAP, are perfect and without uncertainty, which is not true. The actual uncertainty is larger and this should be noted. Also, this assumes that the MAAP perfectly accounts for filter-loading and multiple-scattering effects.

Response: Thanks for the comment and we agree with the reviewer. In this study, we also corrected the MAAP data using the algorithm reported by Hyvärinen et al. (2013). As the reviewer said, the uncertainty in the compensation factors of AE measurements obtained in our study depends on the uncertainty in MAAP measurements. Hyvärinen et al. (2013) compared the results from a PAS against those derived from the MAAP in Beijing, and estimated the uncertainty of ~15% in absorption coefficients derived from MAAP based on the developed algorithm. Therefore, we estimated that the factor C derived by comparing AE and MAAP measurement would exhibit an uncertainty of ~15%.

To make the statement more appropriate, the related statement in the supplementary has been revised as *“In this study, the uncertainty in the factor C was dominated by the uncertainty in MAAP measurements. We corrected the MAAP data using the algorithm reported by Hyvärinen et al. (2013). They estimated that the uncertainty in absorption coefficients derived from MAAP based on the developed algorithm was ~15% by comparing the results from a PAS against those derived from the MAAP in Beijing. This indicated that the factor C used in our study (~2.6) would exhibit an uncertainty of ~15% from the uncertainty in MAAP measurements. Considering the uncertainty on the AE33 measurements was mainly from the factor C , the absorption coefficient from AE33 was estimated to have an uncertainty of ~15%.”*

(8) Eqn. 1: This is not so much an equation as a relationship. It does not seem to me that it needs to be called out as an equation.

Response: Thanks. We have removed the relationship (1) and added the related discussion “*In Mie calculation, the D_p is retrieved from C_s , the size of rBC core (D_c) and the refractive indices of the non-BC shell (RI_s) and rBC core (RI_c).*”

(9) SP2 limits: The authors indicate a lower size limit of 75 nm in the main text. But, Fig. S4 makes clear that the lowest two size bins are strongly biased low in terms of their concentrations since there is no physical reason for such a sharp falloff in concentration below 95 nm. It is unclear whether this is taken into account, which would be particularly important when the [PM1] is $< 50 \text{ ug/m}^3$. Fig. S4 makes clear that there is a counting artifact in the SP below 95 nm, where the detection efficiency falls off rapidly giving rise to an apparent sharp decrease in concentration.

Response: Thanks and we agree with the reviewer. Considering the counting artifact in SP2 for smaller BC particles, the rBC mass concentration was corrected for SP2 detection efficiency. Figure R1 shows the SP2 detection efficiency concentration (η) in each rBC size-bin. In our study, the SP2 detection efficiency was determined with a DMA-SP2/CPC system. Monodispersed Aquadag particles generated by DMA were simultaneously measured by SP2 and CPC. The size-resolved η was calculated by dividing the particle number concentration from SP2 measurement by that from CPC measurement.

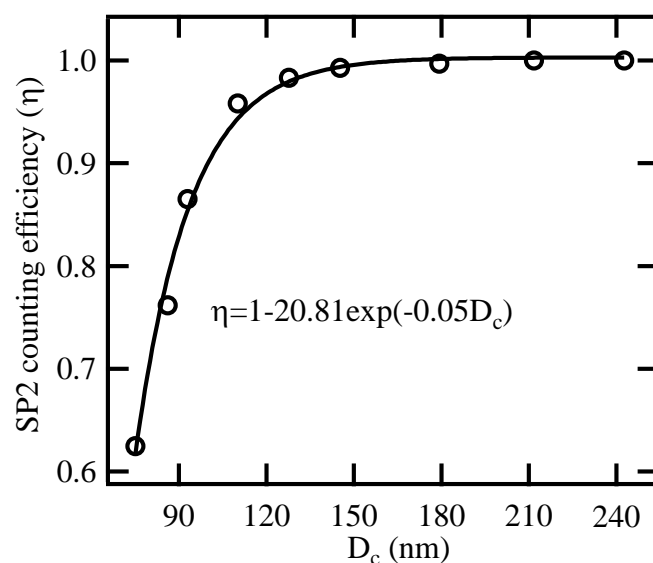


Figure R1 (Fig. S3 in the revised manuscript). SP2 detection efficiency of particle (η) in each rBC size-bin.

To make this point clear, we have added the Fig. S3 (Fig. R1 in the response) and its related discussion in the revised manuscript: “*The mass concentration of rBC is calculated from the particle-to-particle mass of rBC and the sampled flow (~0.12 lpm). Note that the SP2 detection efficiency (Fig. S3) have been considered in the calculation of rBC mass concentration.*”

(10) Fig. S7 and P6/L5: it is unclear how this figure addresses uncertainties in the absorption calculations. However, the authors do argue in the supplemental that the “absorption: : was underestimated by no more than 50%.” A 50% uncertainty is very large and this information should not be buried in the supplemental. Further, additional details are required as to how this was determined. The MAC from Mie theory varies as a function of particle size while that from RDG is constant. The RDG MAC for bare BC, using the RI given here, is 3.2 m²/g at 880 nm. This is relatively small to begin with, so how is the 50% number determined. Also, the argument that “the uncertainty

of BC light absorption from the calculation of bare BC properties using Mie theory is no more than 2%” is demonstrably not correct. If the absolute absorption can be underestimated by 50%, then the uncertainty cannot be only 2%. Just because there were few times that bare BC particles were observed does not change this fundamental issue. The uncertainty in the absolute absorption from the calculations is much larger than 2%. And then on P8, L5 it is stated that the uncertainty is 10%. It is ultimately unclear what the actual uncertainty on the calculations is.

Response: Thanks to the reviewer to point this out. We have recalculated the uncertainties on the calculated light absorption. In this study, the MAC for bare BC derived from Mie calculation, using the RI given here, is 3.8-4.5 m²/g at 880 nm with an average of ~4.3 m²/g (Fig. R2 in the response). Bond and Bergstrom (2006) suggested a value of 7.5 m²/g for the MAC of bare BC at 550 nm. Considering that the absorption is inversely proportional to wavelength (Bond and Bergstrom, 2006), the MAC of bare BC at 880 nm is estimated to be ~4.7 m²/g, which was slightly greater than that (~4.3 m²/g) obtained from Mie calculation in our study. This indicated the uncertainty of MAC for bare BC from Mie calculation was ~8%.

Correspondingly, we deleted the Fig. S7 and added the new Fig. S9 and related discussion in the revised supplement, as “*Based on Mie calculation, we obtained the MAC of rBC core (MAC_c) at 880 nm in the range of 3.8-4.5 m²/g with an average of ~4.3 m²/g during the campaign period (Fig. S9). Bond and Bergstrom (2006) suggested a value of 7.5 m²/g for the MAC of bare BC at 550 nm. Considering that the absorption is inversely proportional to wavelength (Bond and Bergstrom, 2006), the MAC of bare rBC at 880 nm is estimated to be ~4.7 m²/g, which was slightly greater than that (~4.3 m²/g) obtained from Mie calculation in our study. This indicated the uncertainty of MAC for bare rBC from Mie calculation was ~8%. We estimated that the uncertainties of calculated BC light absorption related to MAC of bare rBC from Mie calculation was ~8%.*”

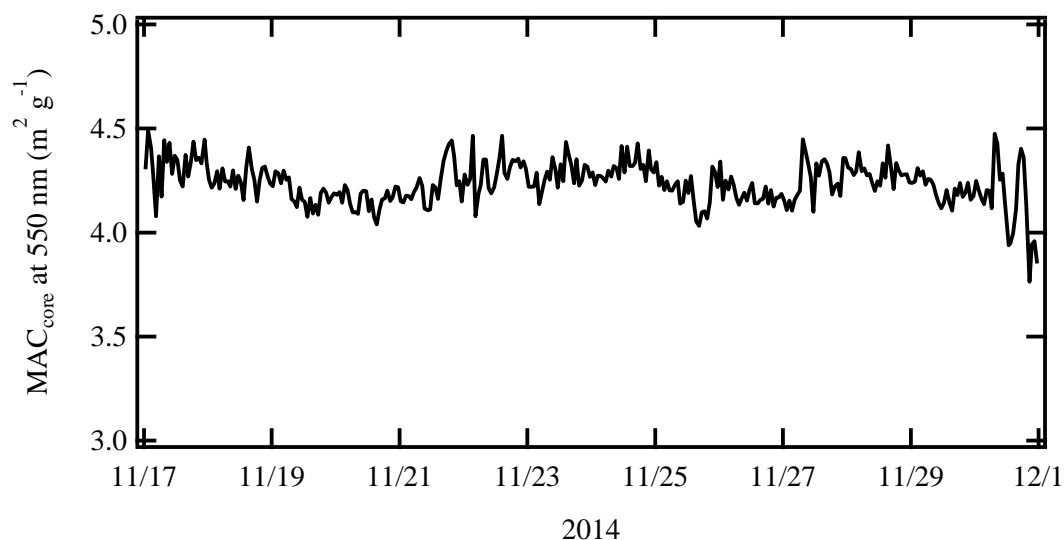


Figure R2 (Fig. S9 in the revised manuscript). The time series of MAC derived from Mie calculation for BC cores (i.e., bare BC) at 880 nm.

(11) P7/L19: This should be Fig. S4a.

Response: We apologize for the typo and have revised it.

(12) P7/L26: This should say “calculated absorption coefficient.”

Response: Thanks. We have revised it.

(13) P8/L2: As noted above, the uncertainty on the AE33 measurements is >10%.

Response: Thanks. As explained in the response to comment 7, we agree with the reviewer that the uncertainty on the AE33 measurements may be larger than 10%. We estimated the uncertainty in factor *C* was ~15% (see the response to comment 7). Considering the uncertainty on the AE33 measurements was mainly from the factor *C*, the absorption coefficient from AE33 was estimated to have an uncertainty of ~15%.

To make the statement here more appropriate, we revised the discussion on the uncertainty in the AE33 measurements, see the response to comment 7.

(14) P8/L5: is the agreement similarly good at the other wavelengths?

Response: Thanks to the reviewer for raising this concern. We have compared the light absorption coefficient (σ_{ab}) at other wavelength (i.e., 660 nm) obtained from Mie calculation with that from AE33 measurement (Fig. R in the response). We found that the calculated σ_{ab} and measured σ_{ab} showed better correlation at a wavelength of 880 nm ($\sigma_{ab,calculated} = 0.90\sigma_{ab,measured}$ ($R^2=0.98$), shown in the Fig. 1c in the manuscript) than at a wavelength of 880 nm ($\sigma_{ab,calculated} = 0.74\sigma_{ab,measured}$ ($R^2=0.97$), shown in the Fig. R3 in the response). At the wavelength of 880 nm, other aerosol particles (carbonaceous or mineral) absorb significantly less and absorption can be attributed to BC alone. In this study, the calculated σ_{ab} based on Mie theory characterized the absorption of rBC. Therefore, we just compared the calculated σ_{ab} at 880 nm with the measured σ_{ab} using AE33 at 880 nm.

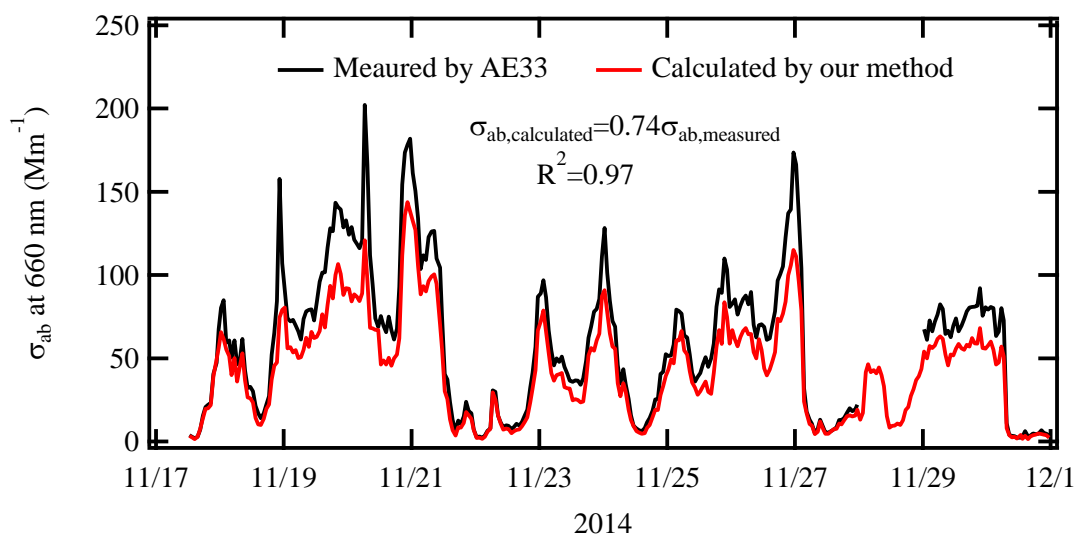


Figure R3 (Fig. S7 in the revised manuscript). The correlation between the calculated σ_{ab} ($\sigma_{ab, \text{calculated}}$) at 660 nm using Mie theory combined with SP2 measurements and the measured σ_{ab} ($\sigma_{ab, \text{measured}}$) by the AE33.

(15) P8/L9: It should be clarified that these are all theoretical studies of the enhancement. None of the citations is to a direct measurement of the enhancement.

Response: Thanks for the suggestion. We have revised the sentence as “*Previous theoretical studies reported that the coating materials on the BC surface can significantly enhance the light absorption of BC via the lens effect (Fuller et al., 1999; Jacobson, 2001; Lack and Cappa, 2010; Moffet et al., 2009).*”

(16) P8/L14: It should be clarified to “the calculated E_{ab} ”.

Response: Thanks. Throughout the manuscript, we have revised it.

(17) P8/L16: It would be helpful to show a graph that explicitly has the D_p/D_c and calculated E_{ab} s as a function of PM1 concentration, to help illustrate this point. This could be shown as a mean across all sizes, a weighted mean across all sizes, or for a few select sizes. This would help to illustrate the magnitude of the changes.

Response: Following the reviewer’s suggestion, we have added a graph that explicitly has the D_p/D_c and calculated E_{ab} as a function of PM1 concentration (Fig. R4 in the response and new Fig. 2b in the revised manuscript). The D_p/D_c and calculated E_{ab} values shown in the Fig. R3 are the mass-weighted averages across all sizes above the detection limit of SP2 incandescence (i.e., rBC larger than ~75 nm).

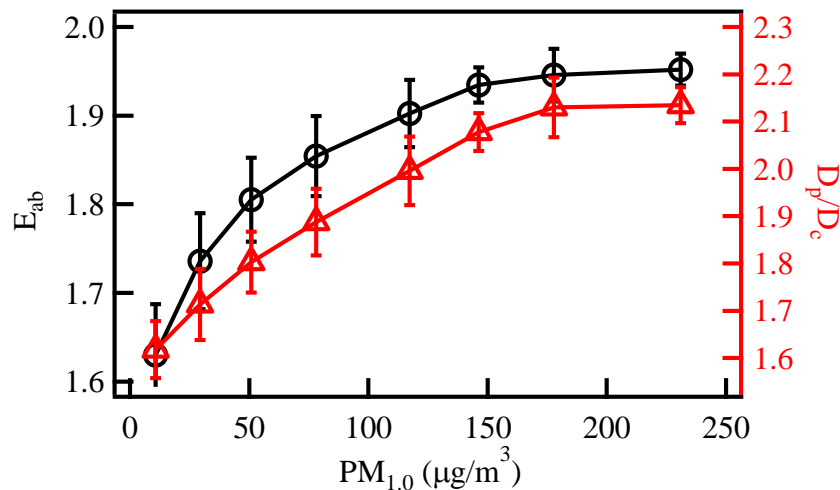


Figure R4 (Fig. 2b in the revised manuscript). Variations in the D_p/D_c and calculated E_{ab} of BC-containing particles with the $PM_{1.0}$ concentration. The D_p/D_c and calculated E_{ab} values shown in the Fig. 2b are the mass-weighted averages across all sizes above the detection limit of SP2 incandescence (i.e., rBC larger than ~ 75 nm).

Correspondingly, the related discussion on the new Fig. 2b in the revised manuscript has been added “On average (i.e., mass-weighted mean across rBC core size larger than ~ 75 nm), the D_p/D_c and calculated E_{ab} for observed BC-containing particles in SP2 under different $PM_{1.0}$ concentrations during the campaign period varied in the range of 1.6-2.2 and 1.6-2.0, respectively (Fig. 2b). Correspondingly, the mass-averaged values of the D_p/D_c and calculated E_{ab} of BC-containing particles increased by $\sim 33\%$ and $\sim 18\%$, respectively, with increasing $PM_{1.0}$ concentrations from $\sim 10 \mu\text{g m}^{-3}$ to $\sim 230 \mu\text{g m}^{-3}$.”

(18) P8/L24: I find the term “aging degree” to be ambiguous because it could apply to almost anything. I suggest that here, and throughout, the authors change to a more specifically descriptive language. Perhaps “coating-to-core ratio”?

Response: Thanks for the suggestion. We have stated in the Methods section that the aging degree of BC-containing particles was characterized by the D_p/D_c ratio in this

study. Throughout the manuscript, we have changed some “aging degree” into “ D_p/D_c ratio”.

(19) P8/L25: It would be helpful to frame this in the context of the overall size distribution, i.e. to report the weighted-average values based on the observed PM₁-dependent BC core size distributions.

Response: Thanks for the suggestion. We have added the new Fig. 2b in the revised manuscript (Fig. R4 in the response) to show the weighted-average values of D_p/D_c and calculated E_{ab} based on the observed PM₁-dependent BC core size distributions. Please see the response to the comment 17.

(20) P8/L23: Better as “exponential function with a y-offset”. However, this by itself gives little physical insight. In Metcalf et al. (2013), for example, there was a comparison to the expected decay based on the SA/V ratio of the particles and diffusion controlled growth. Here, the authors mention this study but do not connect to it quantitatively. The authors should strongly consider introducing a physical explanation using a semiquantitative analysis, rather than just an empirical fit. I believe this would strengthen the paper.

Response: This is a very good point. We have deleted the empirical fit. Following the reviewer’s suggestion, we have introduced a physical explanation using a semiquantitative analysis (Fig. R5 in the response and new Fig. 3 in the revised manuscript). The method of semiquantitative analysis shown here was similar with that using in Metcalf et al. (2013) and is described below.

According to the diffusion-controlled growth law (Seinfeld and Pandis 2006), the evolution of the size of BC-containing particles (D_p) is shown:

$$\frac{dD_p}{dt} = \frac{A}{D_p} \quad (1)$$

in which, $\frac{dD_p}{dt}$ represents the diffusion-controlled growth rate; A is a parameter.

Integrating Eq. (1) with $D_p(t = 0) = D_c$:

$$D_p^2 = D_c^2 + 2At = D_c^2 + B \quad (2)$$

in which, D_c is rBC core diameter; B (i.e., $2At$) is a parameter, varying under different PM_{10} concentrations.

Following Eq. (2), the D_p/D_c ratio is given:

$$\frac{D_p}{D_c} = \left(\frac{B}{D_c^2} + 1\right)^{1/2} \quad (3)$$

where the parameter B is determined by the value of the measured D_p/D_c ratio with D_c of 160 nm under different PM_{10} concentrations.

The increase ratio of the D_p/D_c ($IR_{Dp/Dc}$) for BC-containing particles with PM_{10} concentration increasing from $10 \mu\text{g m}^{-3}$ to $230 \mu\text{g m}^{-3}$ can be calculated by Eq. (4):

$$IR_{Dp/Dc} = \frac{\left(\frac{D_p}{D_c}\right)_{230} - \left(\frac{D_p}{D_c}\right)_{10}}{\left(\frac{D_p}{D_c}\right)_{10}} = \frac{\left(\frac{B_{230}}{D_c^2} + 1\right)^{1/2} - \left(\frac{B_{10}}{D_c^2} + 1\right)^{1/2}}{\left(\frac{B_{10}}{D_c^2} + 1\right)^{1/2}} \quad (4)$$

where $\left(\frac{D_p}{D_c}\right)_{230}$ and $\left(\frac{D_p}{D_c}\right)_{10}$ represent the D_p/D_c ratio when PM_{10} concentrations are $230 \mu\text{g m}^{-3}$ and $10 \mu\text{g m}^{-3}$, respectively; B_{230} and B_{10} are parameter B with PM_{10} concentrations of $230 \mu\text{g m}^{-3}$ and $10 \mu\text{g m}^{-3}$, respectively.

The increase ratio of E_{ab} (IR_{Eab}) for BC-containing particles with PM_{10} concentration increasing from $10 \mu\text{g m}^{-3}$ to $230 \mu\text{g m}^{-3}$ can be derived based on $E_{ab}=k \times (D_p/D_c)$, as expressed in Eq. (5):

$$IR_{Dp/Dc} = \frac{\left(\frac{D_p}{D_c}\right)_{230} - \left(\frac{D_p}{D_c}\right)_{10}}{\left(\frac{D_p}{D_c}\right)_{10}} = \frac{k_{230} \times \left(\frac{B_{230}}{D_c^2} + 1\right)^{1/2} - k_{10} \times \left(\frac{B_{10}}{D_c^2} + 1\right)^{1/2}}{k_{10} \times \left(\frac{B_{10}}{D_c^2} + 1\right)^{1/2}} \quad (5)$$

We compared the calculated $IR_{Dp/Dc}$ and IR_{Eab} based on Eqs. (4) and (5) with those from SP2 measurements, as shown in Fig R5 (new Fig.3 in the manuscript). The agreement indicated that the increase of the D_p/D_c and E_{ab} for BC-containing particles with increasing PM_{10} concentrations follow the diffusion-controlled growth law.

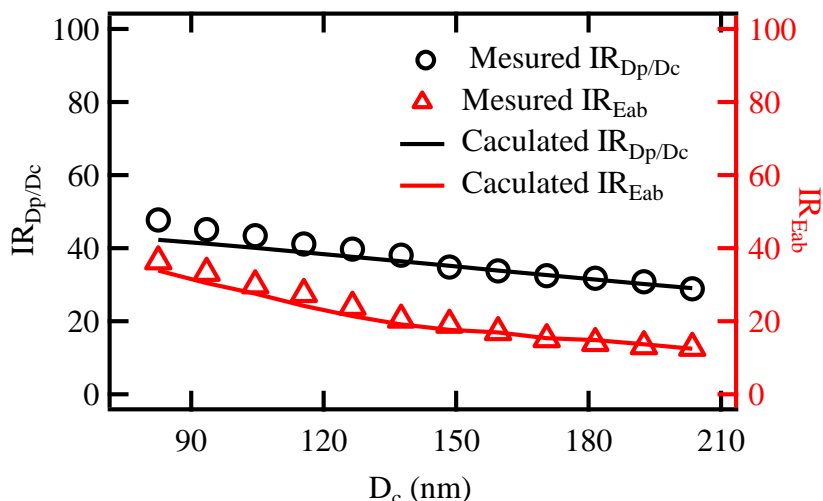


Figure R5 (new Fig. 3 in the revised manuscript). The increase ratio of the D_p/D_c and E_{ab} (IR_{D_p/D_c} and $IR_{E_{ab}}$) for BC-containing particles with PM_1 concentration increasing from $10 \mu\text{g m}^{-3}$ to $230 \mu\text{g m}^{-3}$. The calculated IR_{D_p/D_c} and $IR_{E_{ab}}$ was determined based on Eqs. (4) and (5). The measured IR_{D_p/D_c} and $IR_{E_{ab}}$ was obtained from SP2 measurements.

Correspondingly, the added discussion on physical explanation for the increase of the D_p/D_c and E_{ab} for BC-containing particles with increasing PM_1 concentrations, as “Figure 3 shows the increase of the D_p/D_c and calculated E_{ab} for BC-containing particles with increasing PM_1 concentrations from $10 \mu\text{g m}^{-3}$ to $230 \mu\text{g m}^{-3}$ (IR_{D_p/D_c} and $IR_{E_{ab}}$) as a function of rBC core size. Based on the D_p/D_c ratio and calculated E_{ab} of BC-containing particles with size-resolved rBC cores in SP2 measurement under different PM_1 concentration (shown in Fig. 2a), we can obtain the IR_{D_p/D_c} and $IR_{E_{ab}}$ as a function of rBC core size. When PM_1 concentration increasing from $\sim 10 \mu\text{g m}^{-3}$ to $\sim 230 \mu\text{g m}^{-3}$ during the campaign period, the D_p/D_c ratio and calculated E_{ab} of BC-containing particle with rBC cores at 75-200 nm increased by 28-48% and 13-36%, respective. The size-dependent increase of D_p/D_c ratio and calculated E_{ab} associated with air pollution indicated that the aging process of smaller rBC was relatively more sensitive to air pollution levels. This could be attributed to the fact that the condensational growth associated with air pollution due to the formation of secondary

components is more effective for smaller particles in terms of increasing the diameter (Metcalf et al., 2013).

Meanwhile, following a semiquantitative analysis using in Metcalf et al. (2013), we calculated the IR_{D_p/D_c} and $IR_{E_{ab}}$ based on diffusion-controlled growth law (Seinfeld and Pandis 2006).

According to the diffusion-controlled growth law (Seinfeld and Pandis 2006), the evolution of the size of BC-containing particles (D_p) is shown:

$$\frac{dD_p}{dt} = \frac{A}{D_p} \quad (10)$$

in which, $\frac{dD_p}{dt}$ represents the diffusion-controlled growth rate; A is a parameter.

Integrating Eq. (10) with $D_p(t=0) = D_c$:

$$D_p^2 = D_c^2 + 2At = D_c^2 + B \quad (11)$$

in which, D_c is rBC core diameter; B (i.e., $2At$) is a parameter, varying under different PM_1 concentrations.

Following Eq. (11), the D_p/D_c ratio is given:

$$\frac{D_p}{D_c} = \left(\frac{B}{D_c^2} + 1\right)^{1/2} \quad (12)$$

where the parameter B is determined by the value of the measured D_p/D_c ratio with D_c of 160 nm under different PM_1 concentrations.

The increase ratio of the D_p/D_c (IR_{D_p/D_c}) for BC-containing particles with PM_1 concentration increasing from $10 \mu\text{g m}^{-3}$ to $230 \mu\text{g m}^{-3}$ can be calculated by Eq. (13):

$$IR_{D_p/D_c} = \frac{\left(\frac{D_p}{D_c}\right)_{230} - \left(\frac{D_p}{D_c}\right)_{10}}{\left(\frac{D_p}{D_c}\right)_{10}} = \frac{\left(\frac{B_{230}}{D_c^2} + 1\right)^{1/2} - \left(\frac{B_{10}}{D_c^2} + 1\right)^{1/2}}{\left(\frac{B_{10}}{D_c^2} + 1\right)^{1/2}} \quad (13)$$

where $\left(\frac{D_p}{D_c}\right)_{230}$ and $\left(\frac{D_p}{D_c}\right)_{10}$ represent the D_p/D_c ratio when PM_1 concentrations are $230 \mu\text{g m}^{-3}$ and $10 \mu\text{g m}^{-3}$, respectively; B_{230} and B_{10} are parameter B with PM_1 concentrations of $230 \mu\text{g m}^{-3}$ and $10 \mu\text{g m}^{-3}$, respectively.

The increase ratio of E_{ab} ($IR_{E_{ab}}$) for BC-containing particles with PM_1 concentration increasing from $10 \mu\text{g m}^{-3}$ to $230 \mu\text{g m}^{-3}$ can be derived based on $E_{ab}=k \times (D_p/D_c)$, as expressed in Eq. (5):

$$IR_{D_p/D_c} = \frac{\left(\frac{D_p}{D_c}\right)_{230} - \left(\frac{D_p}{D_c}\right)_{10}}{\left(\frac{D_p}{D_c}\right)_{10}} = \frac{k_{230} \times \left(\frac{B_{230}}{D_c^2} + 1\right)^{1/2} - k_{10} \times \left(\frac{B_{10}}{D_c^2} + 1\right)^{1/2}}{k_{10} \times \left(\frac{B_{10}}{D_c^2} + 1\right)^{1/2}} \quad (14)$$

We compared the calculated IR_{D_p/D_c} and $IR_{E_{ab}}$ based on Eqs. (13) and (14) with those from SP2 measurements, as shown in Fig.3. The agreement indicated that the increase of the D_p/D_c and E_{ab} for BC-containing particles with increasing PM_{10} concentrations follow the diffusion-controlled growth law. ”

(21) P8/L30: it is unclear how the “change rates” were calculated. Are these point-by-point differences? And, how is the E_{ab} calculated? Is this a weighted average? Also, it’s not entirely demonstrated how this is an especially meaningful metric. Isn’t the same general information obtained by plotting E_{ab} vs. r_{BC} (for example)? Assuming this is from point-by-point differences, then one would expect that:

$$k_{E_{ab}}/k_{PM_{10}} = \frac{(E_{ab,t2} - E_{ab,t1})/E_{ab,t1}}{(PM_{10,t2} - PM_{10,t1})/PM_{10,t1}} = \frac{(PM_{10,t1})/E_{ab,t1}}{(PM_{10,t2} - PM_{10,t1})} \frac{(E_{ab,t2} - E_{ab,t1})}{E_{ab,t1}}$$

How is this generally useful? This could be elaborated upon. Also, given that negative values are allowed, it could be clarified that these are not just “growth” rates. This is really just a susceptibility curve.

Response: Thanks and yes. We determined the change rates from point-by-point differences, i.e., $k_{E_{ab}} = (E_{ab,t2} - E_{ab,t1}) / (E_{ab,t1} * (t2 - t1))$, $k_{PM_{10}} = (PM_{10,t2} - PM_{10,t1}) / (PM_{10,t1} * (t2 - t1))$ and $k_{r_{BC}} = (C_{r_{BC},t2} - C_{r_{BC},t1}) / (C_{r_{BC},t1} * (t2 - t1))$. We have calculated the hourly E_{ab} values with weighted average and used them to determine the change rates. The $k_{E_{ab}}$, $k_{PM_{10}}$ and $k_{r_{BC}}$ values represent an apparent change rate of calculated E_{ab} , PM_{10} concentration and r_{BC} mass concentration, respectively. The $k_{E_{ab}}/k_{PM_{10}}$ characterizes the sensitivity of the change of calculated E_{ab} with increasing/decreasing PM_{10} concentrations. The same general information obtained by plotting $k_{E_{ab}}$ vs. $k_{r_{BC}}$ (i.e., the sensitivity of the change of calculated E_{ab} with increasing/decreasing r_{BC} mass concentration). We agree the reviewer that the $k_{E_{ab}}$, $k_{PM_{10}}$ and $k_{r_{BC}}$ values shown in Fig.

3 (new Fig. 4 in the revised manuscript) are not just “growth” rates. We have changed the “growth rate” into “change rate” in the manuscript.

To make these points clear, we have added the statement on the “change rates” in the caption of new Fig. 4 in the revised manuscript, as “*The k_{Eab} , k_{PM1} and k_{rBC} values represent an apparent change rate of calculated E_{ab} , PM_1 concentration and rBC mass concentration, respectively, and are from point-by-point differences of hourly E_{ab} , namely $k_{Eab} = (E_{ab,t2} - E_{ab,t1}) / (E_{ab,t1} * (t2 - t1))$, $k_{PM1} = (PM_{1,t2} - PM_{1,t1}) / (PM_{1,t1} * (t2 - t1))$ and $k_{rBC} = (C_{rBC,t2} - C_{rBC,t1}) / (C_{rBC,t1} * (t2 - t1))$. The sensitivity of the change of calculated E_{ab} with changing PM_1 and rBC concentrations was obtained by plotting k_{Eab} vs. k_{PM1} (i.e., k_{Eab}/k_{PM1} , the slope shown in (a)) and k_{rBC} (i.e., k_{Eab}/k_{rBC} , the slope shown in (b)), respectively.*”

(22) P8/L31: The units on the equation are incorrect. It is $k_{Eab} = 4.8k_{PM1}$, not 4.8%.

The percents cancel.

Response: Thanks. Figure 3a shows the linear relationship between k_{Eab} and k_{PM1} with a slope of 0.048, i.e. $k_{Eab} = 0.048k_{PM1}$. To make this point clear, we have revised the equation as “ $k_{Eab} = 0.048k_{PM1}$ ”.

(23) P9/L1: The statement here relates to one point on a graph of hundreds of points.

What is the uncertainty on a single point? Is this meaningful to state? I question whether it is especially meaningful to state the results for this one point. I could randomly pick another point, based on the maximum k_{PM1} (for example) and conclude that k_{Eab} varies slowly with k_{PM1} . This feels to me too selective to be meaningful to include and I suggest it is removed or put in a fuller context.

Response: Thanks for the comment and we agree with the reviewer. Following reviewer's suggestion, this sentence has been removed from the revised manuscript.

(24) P9/L2: The authors relate their observations to other studies. However, I do not understand why they only consider values with $k_{Eab} > 0$. Why exclude the negative numbers? Also, to reiterate my above point, are the individual points truly meaningful once one accounts for the uncertainty in the individual points? Using confidence intervals for the slopes would, in my opinion, be more meaningful. Or looking at the distribution of k_{Eab} values. It is evident from Fig. 3 that if a histogram of k_{Eab} values was made the peak would be around zero, i.e. that the particles are shrinking as often as they are growing, on average. While I do see some value in providing the range of values here, a much more statistical picture would provide much greater value.

Response: Thanks. In the revised manuscript, we have considered k_{Eab} values including both positive and negative numbers. Following reviewer's suggestion, we have removed the statement on the results based on the individual points and have added some statistical results (distributions of k_{Eab} , k_{PM1} , and k_{Eab}/k_{PM1} values (Fig. R6 in the response and new Fig. 4b in the revised manuscript).

Correspondingly, the related discussion on the statistical results has been added in the revised manuscript “*Figure 4b shows frequency distribution of k_{Eab} , k_{PM1} , and k_{Eab}/k_{PM1} . During the campaign period, most of k_{Eab} and k_{PM1} values were in the range of -50% - $50\% h^{-1}$ and -4% - $4\% h^{-1}$, respectively, revealing a lower change rate for BC aging than that for PM_1 concentration. The peak value of frequency distribution of k_{Eab} was around zero, indicating the BC particles are shrinking as often as they are growing. The k_{Eab}/k_{PM1} ratio characterized the sensitivity of the change of calculated E_{ab} with changing PM_1 concentrations. The frequency distribution of k_{Eab}/k_{PM1} ratio showed that $\sim 60\%$ values were in the range of 0-1, with a peak value around 0.05. Smaller values of k_{Eab}/k_{PM1} ratio indicated that the change of calculated E_{ab} was not sensitive to variations in PM_1 concentrations.*”

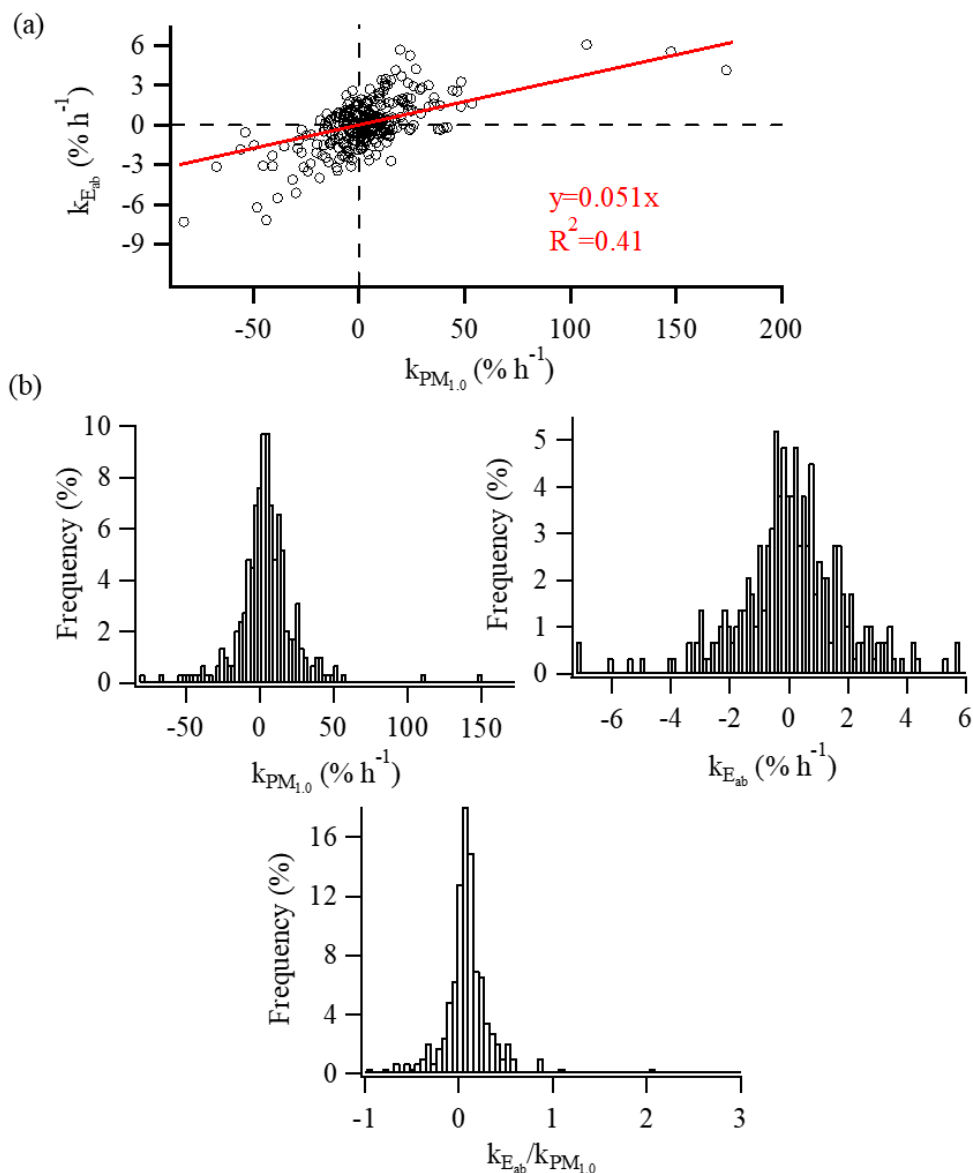


Figure R6 (new Fig. 4 in the revised manuscript). (a) Correlation between the changing rate of calculated E_{ab} ($k_{E_{ab}}$) and the changing rates of PM_1 concentrations (k_{PM_1}) during the campaign period. (b) Frequency distribution of $k_{E_{ab}}$, k_{PM_1} , and $k_{E_{ab}}/k_{PM_1}$. The $k_{E_{ab}}$ and k_{PM_1} values represent an apparent change rate of E_{ab} , PM_1 concentration and rBC mass concentration, respectively, and are from point-by-point differences of hourly E_{ab} , namely $k_{E_{ab}} = (E_{ab,t2} - E_{ab,t1}) / (E_{ab,t1} * (t2 - t1))$ and $k_{PM_1} = (PM_{1,t2} - PM_{1,t1}) / (PM_{1,t1} * (t2 - t1))$. The sensitivity of the change of E_{ab} with changing PM_1 concentrations was obtained by plotting $k_{E_{ab}}$ vs. k_{PM_1} (i.e., $k_{E_{ab}}/k_{PM_1}$, the slope shown in (a)).

(25) Fig. S9 and P9/L5: If the authors were to introduce a more quantitative picture that included an interpretation of why this type of behavior might be expected that would be most welcome. Most likely, this is simply because the net change in diameter for a given amount of material deposited decreases with the size of the particle due to surface-to-volume scaling. Since the particles are larger when PM1 is larger, one would expect the $\Delta D_p/\text{time}$ to decrease with PM1 and thus the E_{ab}/time would also decrease. Of course, this oversimplifies because E_{ab} is not a linear function of ΔD_p . But, it would be great if the authors could introduce some physical discussion of why this observed behavior is/is not expected this would increase the value of this observation.

Response: Thanks. Following the reviewer's suggestion, we have introduced a more quantitative picture (Fig. R7 in the response and new Fig. S9b in the revised manuscript) and added some physical discussion on why the change rate of calculated E_{ab} decreased with $PM_{1.0}$, as “*This can be explained by larger BC particles when $PM_{1.0}$ concentration is higher (Fig. S9b). The net change in diameter for a given amount of material deposited decreases with increasing particle size due to surface-to-volume scaling, which would expect the growth rate of particles to decrease with increasing $PM_{1.0}$ concentration and thus the $k_{E_{ab}}$ would also decrease (Fig. S9a).*”

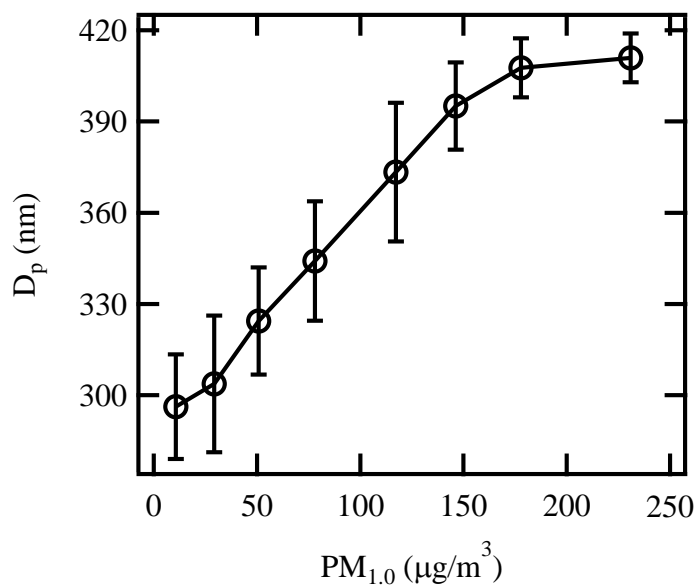


Figure R7 (new Fig. S9b in the revised manuscript). (b) Variations in the diameter of BC-containing particles (D_p) with the normalized PM_{10} concentrations.

(26) P9/L9: I find this discussion about previous studies “ignoring” an aspect to be unclear and suggest it be expanded/clarified. How does the current observation help, specifically, explain these previous studies? It is not abundantly clear. Consider that the variability in the calculated E_{ab} is actually only 15% between the low and high PM_{10} periods in the size range that matters (the BC mass weighted size), based on Fig. 2. These previous measurements would not have been able to discern a 15% difference easily, most likely, in their data anyway. While the current study finds a large theoretical enhancement, what is not found is substantial variability in the enhancement (Fig. 2). The variability in the “growth rate” is inconsequential in the context of the actual enhancement dependence on PM_{10} (Fig.2). Related, it is not clear where the 28% on L19 comes from. What matters is the mass-weighted enhancement. Assuming this is a straight average over the points in Fig. 2, this is not relevant to the actual measurement of the enhancement, which is weighted. I suggest that the authors rethink this discussion entirely.

Response: Thanks for the comments. Following the reviewer's suggestion, we have rethink this discussion entirely and revised the statement in P9/L9-19, as “The evolution of theoretical light absorption of BC with pollution levels depends on the change in both rBC mass concentrations and calculated E_{ab} . *Figure S13 shows markedly smaller $k_{E_{ab}}$ than k_{rbc} ($k_{E_{ab}} \approx 0.027 k_{rbc}$), indicating the change of calculated E_{ab} was significantly slower than that of rBC mass concentrations under different pollution levels. Due to less sensitive for calculated E_{ab} to change in air pollution levels compared with that for rBC mass concentrations, some previous measurements (McMeeking et al., 2011; Ram et al., 2009; Wang et al., 2014b; Andreae, et al., 2008) would not have been able to discern a difference of E_{ab} easily among different pollution levels and thus just focus on the change of BC mass concentration. This would lead to uncertainties in estimation of BC light absorption. In our case, we found the mass-*

weighted average of E_{ab} increased by ~18% with PM_{10} concentration increasing from $10 \mu\text{g m}^{-3}$ to $230 \mu\text{g m}^{-3}$ (Fig. 2b). If the change of calculated E_{ab} of BC with PM_{10} increase was neglected in our study, the theoretical light absorption of BC-containing particles would be underestimated by ~18% under polluted conditions.”

(27) Related to the previous comment, it is unclear how the references on P9/L9 relate to the references on P9/L13. The authors appear to be linking these, I think, but it is not clear. Also, this seems selective, as there are studies (e.g. Liu et al. 2015) in which variability was observed. The authors should aim to provide a more comprehensive picture. Finally, it is not at all clear that the conditions in the cited studies are similar enough to those here to be relevant. This aspect needs to be discussed.

Response: Thanks to the reviewer for raising this concern. We have revised the statement in P9/L9-19, please see the comment (26).

(28) P9/L27: Should be Figure 4.

Response: We apologize for the typo and have revised it.

(29) Figure 4: The site location should be clearly indicated. In addition, the boundaries of the in-region vs. out of region should be indicated clearly. Also, it is not clear whether these regions are defined based on some physical parameter (e.g. as air basins) or simply based on political boundaries. It would be useful if this were addressed.

Response: Thanks for the comment. We have indicated the site location and the boundaries of the in-region (i.e., Beijing) vs. out of region (i.e., other areas such as Tianjin, Hebei, Inner Mongolia, Shanxi, Shandong), shown in Fig. S1 (Fig. R8 in the response). These regions are defined based on political boundaries.

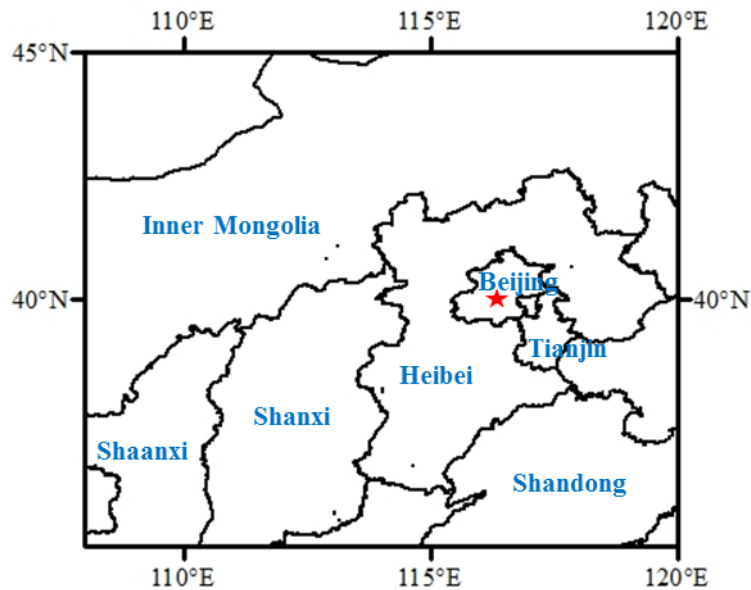


Figure R8 (Fig. S1 in the manuscript). Location of the observation site (red star).

To clarify it clear, we have added the statement in the caption of Fig. 5 in the revised manuscript, as “*The site location and the boundaries of the in-region (i.e., Beijing) vs. out of region (i.e., other areas such as Tianjin, Hebei, Inner Mongolia, Shanxi, Shandong), shown in Fig. S1. Noted that these regions are defined based on political boundaries.*”

(30) P10/L3: It is unclear where the 62% number comes from.

Response: Thanks for the comment. The percentage of 62% is obtained from the ratio between the 4.6-fold increase in EEI_{total} and 7.4-fold increase in rBC mass concentration. Table 1 shows that rBC mass concentration increased by 7.4-fold from clean period ($0.82 \mu\text{g m}^{-3}$) to polluted period ($6.07 \mu\text{g m}^{-3}$). The increase in rBC mass concentration can be attributed to more BC transported to the site and the adverse local meteorology. In this study, the amount of BC transported to the site was characterized by EEI_{total} . Table 1 shows that nomalized EEI_{total} increased by 4.6-fold from clean period (3.68) to polluted period (16.87), revealing that the increase in amount of BC

transported to the site contributed 62% of increase in rBC mass concentration with air pollution development.

To make it clear, the sentence has been revise as “*Table 1 shows that the BC concentrations from the clean period to the polluted period increase by ~7.4 times. The increase of EEI_{total} (~4.6 times) accounted for ~62% the increase in BC mass concentrations (~7.4 times).*”

(31) P10/L14: It is unclear how Fig. 4c indicates that there were “higher aging rates.” Can this be clarified?

Response: Thanks. Fig. 4c in the manuscript shows that the BC particles transported to the site during polluted period were mainly from Hebei province, which is one of the polluted regions in China. Peng et al. (2015) pointed out higher BC aging rates under more polluted environments, indicating that BC particles passing though polluted regions would show higher aging rates during atmospheric transport compared to that from clean regions.

To clarify it, the statement has been revised as “*On the other hand, compared with the BC carried in the clean air mass from the northwest of Beijing during the clean period (Fig. 4a), the BC in the polluted air mass underwent regional transport from the region south of Beijing (i.e., Hebei, one of the most polluted provinces in China with high pollutant emission) during the polluted period. Peng et al. (2015) pointed out higher BC aging rates under more polluted environments, indicating that BC particles passing though polluted regions would show higher aging rates during atmospheric transport than that from clean regions.*”

(32) P10/L15: “observed” should be “calculated.” Also, is this a weighted average? A straight average across size? This needs to be clarified. A weighted average is most appropriate. This comment applies to everywhere in the manuscript that values for E_{ab} or D_p/D_c are mentioned. What sort of averages are these? This needs to be clarified.

Response: Thanks for the comment. We have changed “observed” into “calculated”. Here and elsewhere in the manuscript that values for calculated E_{ab} or D_p/D_c are mentioned, we have showed their mass-weighted average values.

To make it clear, the sentence has been revise as “*The mass-average value of calculated E_{ab} for BC-containing particles observed at our site were ~1.66, ~1.81 and ~1.91 during the clean, slightly polluted and polluted periods, respectively (Table 1)....*”

(33) P10: I find the discussion with respect to O₃ is somewhat lacking in detail and nuance. While O₃ is lower during the polluted events, the concentration of precursors may be higher and this would contribute to aging. Additionally, photochemical processing is not the only possible pathway. Have the authors considered to what extent NO₃ oxidation at night might be important?

Response: Thanks for the reviewer for raising this concern. We agree with the reviewer that photochemical process is not the only possible pathway and other chemical processes may be important. However, in this study, we focused on the effect of regional transport on BC aging process. We just roughly discussed the chemical process during BC aging. The chemical process of BC aging under polluted environment in china is complex, which involved photochemical oxidation and heterogeneous chemical production (Zheng et al. 2015). We will investigate the chemical process of BC aging under polluted environment in future.

In the revised manuscript, we have toned down the related discussion on the chemical process of BC aging, as “*When PM_1 concentrations were higher than $\sim 120 \mu\text{g m}^{-3}$, O_3 concentrations decreased to ~ 2 ppb. Zheng et al. (2015) has demonstrated the weakened importance of photochemistry in the production and aging of secondary aerosols in Beijing under polluted conditions due to decrease of oxidant concentrations. This indicated that the photochemical processing in BC aging may be weakened under higher polluted levels (i.e., $PM_1 > 120 \mu\text{g m}^{-3}$). Noted that photochemical processing is not the only possible pathway in BC aging process and*

other pathways were not discussed in this study. The local aging process of BC might be enhanced by other pathways.”

(34) P10/L24: The meaning of “taking more EEI_{total} more BC” is unclear.

Response: Thanks. In this study, the amount of BC transported to the site was characterized by EEI_{total} (calculated by Eq. (8) in the manuscript). Larger EEI_{total} values at a certain time (Fig. 5a in the manuscript) revealed that more BC in the site was transported from regional origins.

To make this point clear, the sentence has been revised as “*On the other hand, the changes in the amount of BC from regional transport was characterized by variation of EEI_{total} , which was used to evaluate the contributions of regional transport to BC aging.*”

(35) P11/L17: Is the MAC range given here the increase over the baseline or the actual MAC range at 550 nm? I find this unclear. Also, is this mass weighted? The MAC varies with particle size.

Response: Thanks for the comment. The MAC range of BC-containing particles given here is the calculated MAC range at 550 nm based on Mie theory. We have shown the mass-weighted MAC values in Fig. R9 in the response (new Fig. 7a in the revised manuscript). To make it clear, the statement has been revised as “*Figure 7 shows that with increasing pollution levels (i.e., PM_{10} increasing from $\sim 10 \mu\text{g m}^{-3}$ to $\sim 230 \mu\text{g m}^{-3}$) during the campaign period, the mass-averaged values of calculated MAC at 550 nm for BC-containing particles increased from $\sim 11 \text{ m}^2 \text{ g}^{-1}$ to $\sim 14 \text{ m}^2 \text{ g}^{-1}$, which resulted in the SFE of BC-containing particles increasing from $\sim 0.7 \text{ m}^2 \text{ g}^{-1} \text{ nm}^{-1}$ to $\sim 0.9 \text{ m}^2 \text{ g}^{-1} \text{ nm}^{-1}$.*”

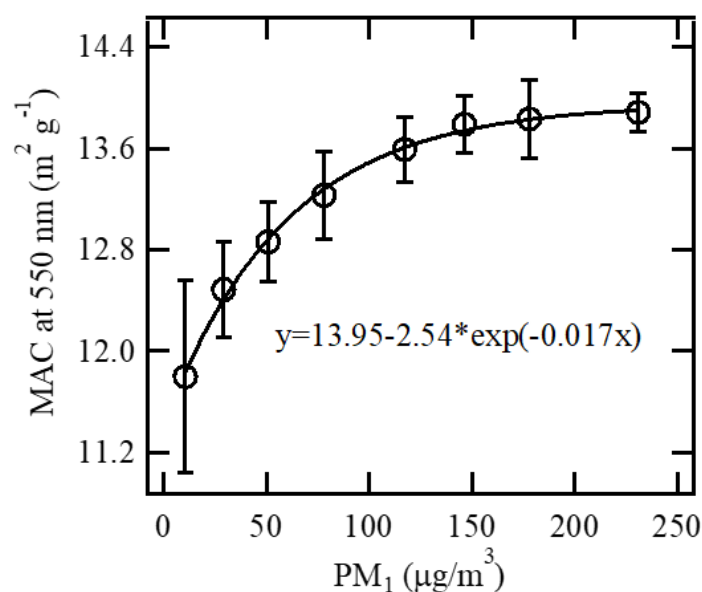


Figure R9 (new Fig. 7a in the revised manuscript). Variations in the *MAC* at 550 nm of BC-containing particles with the PM_1 concentrations.

(36) P11/L19: Are the DRF values given related to the total BC? It is surprising that the increase is so small, given that the BC concentration itself increased by a factor of 7 or so. This could be clarified.

Response: We thank the reviewer for raising the important issue. The DRF values given here was not related to the total BC. In this study, we focused on investigating the effect of BC light-absorption capability on DRF. Therefore, the increase in DRF of BC with increasing pollution levels shown in the Fig.7c (in the revised manuscript) just considered the change in light-absorption capability of BC. The DRF values for BC-containing particles at different pollution levels were obtained by scaling the average *DRF* (0.31 W m^{-2}) of externally mixed BC from various climate models (Bond et al. 2013) with a scaling factor of E_{ab} under different PM_1 concentrations. To make it clear, we added the statement in the caption of Fig. 7 in the manuscript, as “*The DRF values for BC-containing particles at different pollution levels were obtained by scaling the average DRF (0.31 W m^{-2} , Table S1) of externally mixed BC from various climate models (Bond et al. 2013) with a scaling factor of E_{ab} under different PM_1 concentrations. In order to point out the effect of BC light-absorption capability on*

DRF under different PM₁ concentrations, we did not consider the changes of total BC amount for DRF calculation in Fig. 7c.”

Following the reviewer’s suggestion, we also estimated the change in DRF of BC related to both the mass concentration and theoretical absorption capability of BC. The related discussion was added in the revised manuscript, as “*Fig. 7c shows the DRF of BC increased by ~15% during the polluted period compared with that during the clean period. Meanwhile, the BC mass concentration increased by ~7 times (Table 1). If assuming the DRF of BC during the clean period to be ~0.5 W m⁻² based on calculation shown in Fig. 7c, it would increase to ~4 W m⁻² under polluted conditions, taking the increase in both of the mass concentration and theoretical absorption capability of BC.”*

(37) P12/L5 and P12/L8: It is not clear to me that the authors have demonstrated that there is a “speeding up” or “acceleration” of the coating process in the more polluted air. In fact, they seem to be arguing that photochemical processing is slower, but that there is longer time. This would actually go against the idea that there is a speeding up. This should be revisited. Associated with this, it is not clear to me that Fig. 7 is necessarily correct. The EEI analysis indicates that the contribution from the regional sources is smaller during less polluted periods. This does not mean that those particles from regional sources are less coated just because the overall particle distribution has less coating during low pollution periods. In fact, it is possible that the regional particles are more coated due to higher photochemical activity (potentially). But, because their fractional contribution is smaller the net impact on the coating amount appears smaller in the average, which is now dominated by the local sources. I think that Fig. 7 and the discussion section need to be rethought a little bit to provide a more nuanced picture of what might be happening. It may be that the authors are correct, but I do not think that they have fully justified their conclusion here.

Response: Thanks for the reviewer for raising this concern. Considering more coating precursors (e.g, SO₂, NO_x and VOCs) in more polluted air mass, we pointed out a

“speeding up” or “acceleration” of the coating process during atmospheric transport for regional BC particles in the polluted air compared with that in the clean air. Peng et al. (2016) has revealed that compared with clean urban environments (i.e, Houston), the more efficient BC growth under polluted urban environments (i.e, Beijing) was attributable to higher concentrations of gaseous aerosol precursors.

It is noted that a “speeding up” or “acceleration” of the coating process mentioned here was just for regional BC. Under polluted period, the BC particles transported to the site was dominated by polluted regions (i.e., high emission areas such as south of Heibei province and Tianjin). However, under clean period, the BC particles transported to the site was dominated by clean regions (i.e., low emission areas such as Inner Mongolia). Polluted air mass from polluted regions exhibit more coating precursors. For regional BC particles, we evaluated their chemical activities (i.e., photochemical and other processes) based on the amount of coating precursors in air mass. We cannot separately estimate the photochemical and other processes during regional transport. The photochemical process under polluted conditions may be weakened during regional transport. However, photochemical process is not the only possible pathway and other chemical processes may be important. Zheng et al., (2015) has demonstrated the importance of both regional transport and heterogeneous chemistry in secondary aerosol production. On the other hand, although we discussed the photochemical production based on O₃ concentration in this study, this discussion just focused on local BC particles in Beijing.

Following the reviewer’s suggestion, we have revised the Fig. 7 (Fig. R10 in the response) and related discussion to provide a more nuanced picture of what might be happening, as *“As shown in Fig. 8, this amplification effect on BC light absorption associated with air pollution is caused by increasing BC concentration and at the same time enhanced light absorption capacity of BC-containing particles by more coating production in the more polluted air. Variation of both the mass concentration and light absorption capability of BC associated with air pollution strongly depend on the air pollutant emission (e.g., BC, SO₂, NO_x and VOC). Under polluted environment,*

polluted air mass from high emission areas not only brings more BC, but also more coating materials on BC surface due to more precursors of secondary components.”

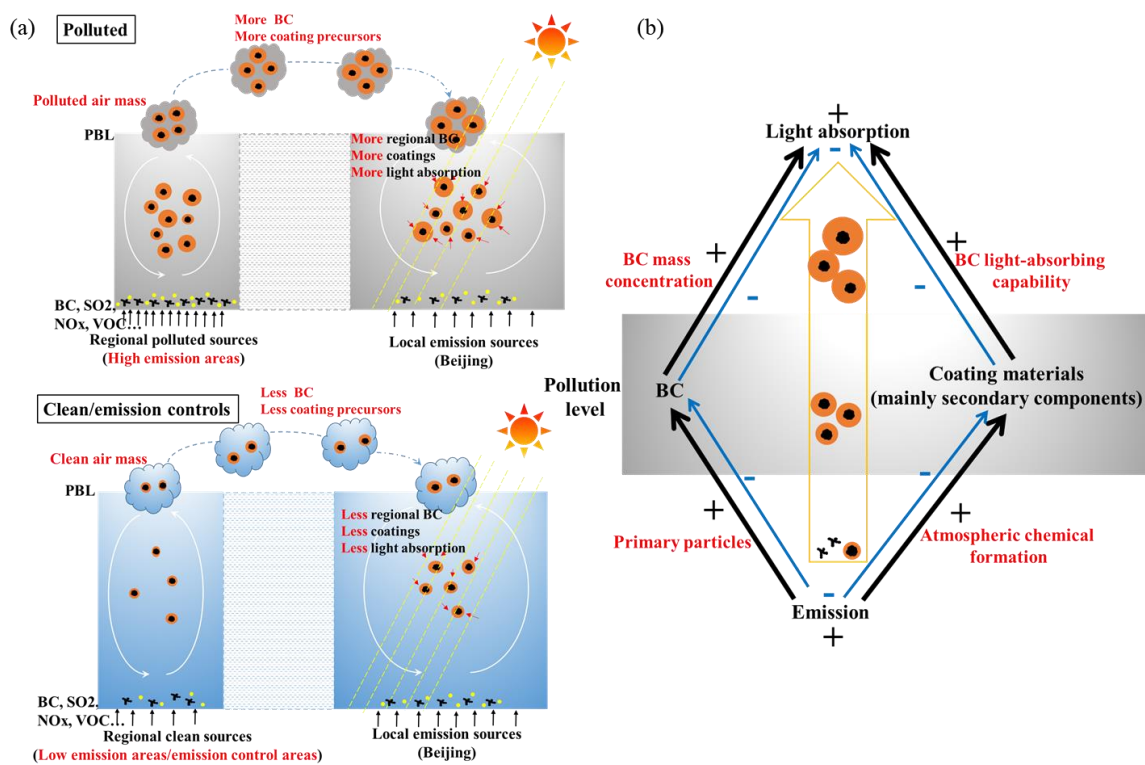


Figure R10 (new Fig. 8 in the revised manuscript). Conceptual scheme of amplification effect on BC light absorption associated with air pollution.

(38) P12, conclusions: The authors should consider reporting mass-weighted averages of D_p/D_c and E_{ab} in addition to the ranges to provide a fuller picture.

Response: Thanks for the comment. Following the reviewer’s suggestion, we have reported the mass-weighted averages of the D_p/D_c ratio and calculated E_{ab} values. Correspondingly, the related statement was added in conclusions section, as “During the campaign period, the hourly values of mass-weighted averages of the D_p/D_c ratio and calculated E_{ab} for BC-containing particles was in the range of 1.5-2.3 and 1.5-2.0, respectively. When PM_1 concentration increased from $\sim 10 \mu g m^{-3}$ to $\sim 230 \mu g m^{-3}$, the mass-weighted averages of the D_p/D_c ratio and calculated E_{ab} values increased by $\sim 33\%$ and $\sim 18\%$, respectively.”

(39) P13/L6: See previous comment regarding the reporting of single points without stated uncertainties. Is the 7.3%/h value believable? It is unclear, since it is a single outlier in the entire plot.

Response: Thanks. As explained in our response to comments (23) and (24), we have removed the statement on the results based on the individual points and have added the statement on some statistical results. In the conclusions section, the revised statement was *“During the campaign period, k_{Eab} values were in the range of -4%-4% h^{-1} , with a peak of frequency distribution around zero, indicating that the BC particles are shrinking as often as they are growing. The frequency distribution of k_{Eab}/k_{PM1} ratio showed that a peak value around 0.05, revealing that the change of calculated E_{ab} was not sensitive to variations in PM_1 concentrations.”*

(40) P13/L10: It is unclear how a 13-44% variation in the E_{ab} s translates to a 28% underestimate in absorption. This appears to simply be an average of 13% and 44%, and not an appropriately mass-weighted average.

Response: Thanks for the reviewer to point this out. As explained in our response to comment (26), we have recalculated the underestimate in absorption based on the changes in the mass-weighted average value of calculated E_{ab} . The related discussion was revised in conclusions section as *“In our case, if we had not considered the increase in the BC light absorption capability with increasing air pollution during the campaign period, the theoretical light absorption of BC-containing particles under polluted conditions would have been underestimated by ~18%.”*

(41) P13/L16: See previous comments about “speeding up”. I do not think the authors have justified this conclusion.

Response: Thanks. As explained in our response to comment (37), the sentence has been revised as *“Not only more BC but also more coatings are carried into Beijing by more polluted regional air mass (Fig. 7 (a)), which can be explained by more coating precursors (e.g. SO_2 , NO_x and VOC) in a more polluted air.”*

(42) P13/L23: It is unclear where the conclusion regarding heterogeneous chemistry comes from. This is pure speculation that is introduced at this point without justification. Why do the authors believe this to be the case? Also, this seems arbitrary. If the authors had defined their periods differently then they could come to a different conclusion.

Response: Thanks for the comment. We have deleted the statement on “heterogeneous chemistry” and the sentence has been revised as “*The further increase of D_p/D_c (~ 2.0 to ~ 2.2) and E_{ab} (~ 1.9 to ~ 2.0) associated with air pollution is harder and is mostly likely attributed to local chemical production.*”

References:

Andreae, M. O., Schmid, O., Yang, H., Chand, D., Zhen Yu, J., Zeng, L.-M., and Zhang, Y.-H.: Optical properties and chemical composition of the atmospheric aerosol in urban Guangzhou, China, *Atmos. Environ.*, 42, 6335-6350, 2008.

Bond, T. C., and Bergstrom, R. W.: Light Absorption by Carbonaceous Particles: An Investigative Review, *Aerosol Sci. Technol.*, 40, 27-67, 2006.

Bond, T. C., Doherty, S. J., Fahey, D. W., Forster, P. M., Berntsen, T., DeAngelo, B. J., Flanner, M. G., Ghan, S., Kärcher, B., Koch, D., Kinne, S., Kondo, Y., Quinn, P. K., Sarofim, M. C., Schultz, M. G., Schulz, M., Venkataraman, C., Zhang, H., Zhang, S., Bellouin, N., Guttikunda, S. K., Hopke, P. K., Jacobson, M. Z., Kaiser, J. W., Klimont, Z., Lohmann, U., Schwarz, J. P., Shindell, D., Storelvmo, T., Warren, S. G., and Zender, C. S.: Bounding the role of black carbon in the climate system: A scientific assessment, *J. Geophys. Res.-Atmos.*, 118, 5380-5552, 10.1002/jgrd.50171, 2013.

Cappa, C. D., Onasch, T. B., Massoli, P., Worsnop, D. R., Bates, T. S., Cross, E. S., Davidovits, P., Hakala, J., Hayden, K. L., Jobson, B. T., Kolesar, K. R., Lack, D. A., Lerner, B. M., Li, S.-M., Mellon, D., Nuaaman, I., Olfert, J. S., Petäjä, T., Quinn, P. K., Song, C., Subramanian, R., Williams, E. J., and Zaveri, R. A.: Radiative Absorption Enhancements Due to the Mixing State of Atmospheric Black Carbon, *Science*, 337, 1078-1081, 2012.

Fuller, K. A., Malm, W. C., and Kreidenweis, S. M.: Effects of mixing on extinction by carbonaceous particles, *J. Geophys. Res.-Atmos.*, 104, 15941-15954, 1999.

Hyvärinen, A.-P., Vakkari, V., Laakso, L., Hooda, R. K., Sharma, V. P., Panwar, T. S., Beukes, J. P., van Zyl, P. G., Josipovic, M., Garland, R. M., Andreae, M. O., Pöschl, U., and Petzold, A.: Correction for a measurement artifact of the Multi-Angle Absorption Photometer (MAAP) at high black carbon mass concentration levels, *Atmos. Meas. Tech.*, 6, 81-90, 2013.

Jacobson, M. Z.: Strong radiative heating due to the mixing state of black carbon in atmospheric aerosols, *Nature*, 409, 695-697, 2001.

Knox, A., Evans, G. J., Brook, J. R., Yao, X., Jeong, C. H., Godri, K. J., Sabaliauskas, K., and Slowik, J. G.: Mass Absorption Cross-Section of Ambient Black Carbon Aerosol in Relation to Chemical Age, *Aerosol Sci. Technol.*, 2009.

Lack, D. A., and Cappa, C. D.: Impact of brown and clear carbon on light absorption enhancement, single scatter albedo and absorption wavelength dependence of black carbon, *Atmos. Chem. Phys.*, 10, 4207-4220, 2010.

McMeeking, G. R., Morgan, W. T., Flynn, M., Highwood, E. J., Turnbull, K., Haywood, J., and Coe, H.: Black carbon aerosol mixing state, organic aerosols and aerosol optical properties over the United Kingdom, *Atmos. Chem. Phys.*, 11, 9037-9052, 2011.

Metcalf, A. R., Loza, C. L., Coggon, M. M., Craven, J. S., Jonsson, H. H., Flagan, R. C., and Seinfeld, J. H.: Secondary Organic Aerosol Coating Formation and Evaporation: Chamber Studies Using Black Carbon Seed Aerosol and the Single-Particle Soot Photometer, *Aerosol Sci. Technol.*, 47, 326-347, 2013.

Moffet, R. C., and Prather, K. A.: In-situ measurements of the mixing state and optical properties of soot with implications for radiative forcing estimates, *Proc. Natl. Acad. Sci. USA*, 106, 11872-11877, 2009.

Peng, J., Hu, M., Guo, S., Du, Z., Zheng, J., Shang, D., Levy Zamora, M., Zeng, L., Shao, M., Wu, Y.-S., Zheng, J., Wang, Y., Glen, C. R., Collins, D. R., Molina, M. J., and Zhang, R.: Markedly enhanced absorption and direct radiative forcing of black carbon under polluted urban environments, *Proc. Natl. Acad. Sci. USA*, 113, 4266-4271, 2016.

Ram, K., and Sarin, M. M.: Absorption Coefficient and Site-Specific Mass Absorption Efficiency of Elemental Carbon in Aerosols over Urban, Rural, and High-Altitude Sites in India, *Environ. Sci. Technol.*, 43, 8233-8239, 2009.

Schnaiter, M., Linke, C., Möhler, O., Naumann, K. H., Saathoff, H., Wagner, R., Schurath, U., and Wehner, B.: Absorption amplification of black carbon internally mixed with secondary organic aerosol, *J. Geophys. Res.-Atmos.*, 110, 2005.

Seinfeld, J. H., and Pandis, S. N.: Atmospheric Chemistry and Physics: From Air Pollution to Climate Change, 2nd ed. *John Wiley & Sons, Inc.*, New York, 2006.

Wang, Q., Huang, R. J., Cao, J., Han, Y., Wang, G., Li, G., Wang, Y., Dai, W., Zhang, R., and Zhou, Y.: Mixing State of Black Carbon Aerosol in a Heavily Polluted Urban Area of China: Implications for Light Absorption Enhancement, *Aerosol Sci. Technol.*, 48, 689-697, 2014b.

Zhang, Y., Zhang, Q., Cheng, Y., Su, H., Kecorius, S., Wang, Z., Wu, Z., Hu, M., Zhu, T., Wiedensohler, A., and He, K.: Measuring the morphology and density of internally mixed black carbon with SP2 and VTDMA: new insight into the absorption enhancement of black carbon in the atmosphere, *Atmos. Meas. Tech.*, 9, 1833-1843, 2016.

Zheng, G. J., Duan, F. K., Su, H., Ma, Y. L., Cheng, Y., Zheng, B., Zhang, Q., Huang, T., Kimoto, T., Chang, D., Pöschl, U., Cheng, Y. F., and He, K. B.: Exploring the severe winter haze in Beijing: the impact of synoptic weather, regional transport and heterogeneous reactions, *Atmos. Chem. Phys.*, 15, 2969-2983, 2015.

Anonymous Referee #3:

The authors investigated the evolution of BC optical properties, and concluded that under more polluted conditions, the aging process will enhance the coating of BC-containing particles and thus contribute to larger enhancement of BC particle light absorption. They further claim that pollution control strategy will have co-benefit effects on both air quality and climate. The content is suitable for publication within the scope of ACP, while some revisions are required. Please see detailed comments below.

We would like to thank the reviewer for the valuable and constructive comments, which helps us to improve the manuscript. Listed below are our responses to the comments point-by-point, as well as the corresponding changes made to the revised manuscript. The reviewer's comments are marked in black and our answers are marked in blue, and the revision in the manuscript is further formatted as *Italics*.

1. Major issues

(1) The manuscript is still in need of a better discussion on uncertainties. Some examples are listed below, while I would suggest the authors do a systematic discussion on all the associated uncertainties, not just here and there.

Response: We thank the reviewer for raising the important issue. Following the reviewer's suggestion, we have systematically discussed all the associated uncertainties. Here, to the uncertainties mentioned by the reviewer is as follows.

(a) Page 4, lines 1-3: The authors mentioned the correction to Aethalometer data in the SI, where there is something confusing to me. First, the authors said they retrieved the correction factor by comparing absorption coefficients measured by AE and MAAP, but since AE was measuring at 660 nm while MAAP at 670 nm, are the

authors just neglecting the difference? Second, the authors used an average value of 2.6 for all their AE measurements while they did determine a pretty wide range of the C , from 1.9 to 4.0, then how did the authors decide the uncertainty of 10% confidently?

Response: We thank the reviewer for raising this question. For the first question, we have discussed the uncertainty from the inconsistency of wavelength for AE and MAAP measurements. Considering that the absorption is inversely proportional to wavelength (Bond and Bergstrom, 2006), the difference of wavelength for AE (at 660 nm) and MAAP (at 670 nm) measurements, would lead to an uncertainty of ~1.5% for the corrected absorption coefficients in AE measurement. The related statement has been added in the revise supplement, as “*Noted that the AE and MAAP measurements used to calculate the factor C were at different wavelengths, namely 660 nm and 670 nm, respectively. Considering that the absorption is inversely proportional to wavelength (Bond and Bergstrom, 2006), the difference in wavelength would lead to an uncertainty of ~1.5% for the corrected absorption coefficients in AE measurement.*”

To the second question, we have reestimated the uncertainty related to the factor C . The uncertainty in the factor C of AE measurements obtained in our study was dominated by the uncertainty in MAAP measurements. In this study, we corrected the MAAP data using the algorithm reported by Hyvärinen et al. (2013). Hyvärinen et al. (2013) compared the results from a PAS against those derived from the MAAP in Beijing, and estimated the uncertainty of ~15% in absorption coefficients derived from MAAP based on the developed algorithm. Therefore, we estimated that the factor C derived by comparing AE and MAAP measurement would exhibit an uncertainty of ~15%. The related statement has been revised as “*In this study, the uncertainty in the factor C was dominated by the uncertainty in MAAP measurements. We corrected the MAAP data using the algorithm reported by Hyvärinen et al. (2013). They estimated that the uncertainty in absorption coefficients derived from MAAP based on the developed algorithm was ~15% by*

comparing the results from a PAS against those derived from the MAAP in Beijing. This indicated that the factor C used in our study (~2.6) would exhibit an uncertainty of ~15% from the uncertainty in MAAP measurements.”

(b) Page 4, line 26: the authors used 1.50-0i as the RIs value, is there any reason why?

Is there some information on, e.g., the chemical compositions of the coating materials, to support that the use of 1.50-0i is reasonable? Otherwise I would suggest the authors consider some sensitivity test on RIs values as well as on RIc.

Response: Thanks for the comment. Following the reviewer’s suggestion, we have demonstrated that the use of 1.50-0i for the refractive index of coating materials based on their chemical compositions during the campaign period (Fig. R1 in the response and new Fig. S4 in the revised manuscript). It is known from the literature (Schkolnik et al., 2007; Mallet et al., 2003; Marley et al., 2001) that major inorganic components of ambient aerosol from urban emission (nitrate, sulfate, mineral dust, sea salt and trace metal) have a refractory of (1.5-1.6)-0i and there is a range of (1.4-1.5)-0i for the refractory of organic components. In this study, we used the values of 1.55-0i and 1.45-0i as refractive indexes of inorganic and organic components of coating materials. The components of coating materials was similar to non-refractory compositions in PM₁ particles (Peng et al., 2016). Figure R1 (new Fig. S4 in the revised manuscript) shows that the fraction of inorganic and organic components in coating materials are ~51% and ~49%, respectively. The refractive index of a mixture particle can be calculated as the volume weighted average of the refractive indices of all components (Hänel, et al. 1968; Marley et al., 2001; Bond and Bergstrom, 2006; Schkolnik et al., 2007), as $\tilde{m} = \sum_i \tilde{m}_i c_i$, where \tilde{m} is the refractive index of a mixture particle; \tilde{m}_i is the refractive index of particle species; c is the volume ratio of particle species. Based on the equation, the refractive index of coating materials of BC-containing particles (RI_s) was ~1.50-0i during the campaign period.

On the other hand, we have considered some sensitivity test on the refractive

index of rBC cores (RI_c), see the statement in page 4 line 26-28 in the manuscript and Fig S3 (new Fig S4 in the revised supplement) in the supplement.

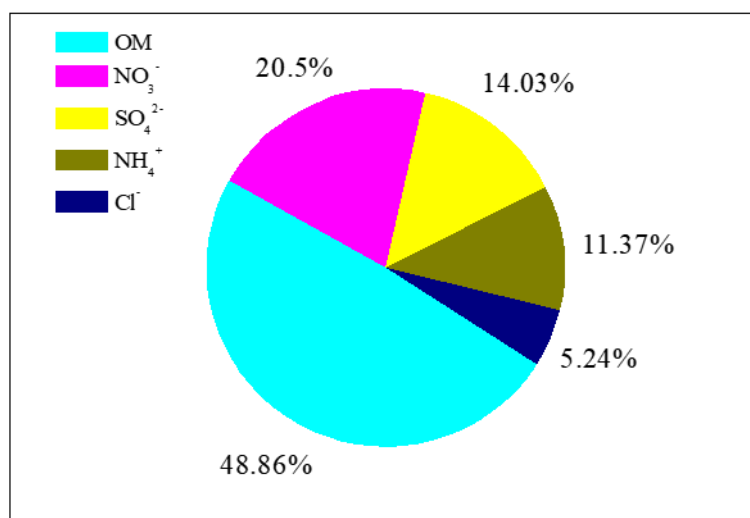


Figure R1 (Fig. S4 in the revised manuscript). Non-refractory compositions of PM_{10} particles during the campaign period.

To make this point clear, we have added Fig. S2 and the related discussion in the revised manuscript, as “*The RI_s value used in this study are 1.50-0i based on the chemical compositions of coating materials during the campaign period. The components of coating materials was similar to non-refractory compositions in PM_{10} particles (Peng et al., 2016). Figure S4 reveals that the fraction of inorganic and organic components in coating materials of BC-containing particles are ~51% and ~49%, respectively. It is known from the literature (Schkolnik et al., 2007; Mallet et al., 2003; Marley et al., 2001) that major inorganic components of ambient aerosol from urban emission (nitrate, sulfate, mineral dust, sea salt and trace metal) have a refractory of (1.5-1.6)-0i and there is a range of (1.4-1.5)-0i for the refractory of organic components. In this study, we used the values of 1.55-0i and 1.45-0i as refractive indexes of inorganic and organic components of coating materials. The refractive index of a mixture particle can be calculated as the volume weighted average of the refractive indices of all components (Hänel, et al. 1968;*

Marley et al., 2001; Bond and Bergstrom, 2006; Schkolnik et al., 2007), as $\tilde{m} = \sum_i \tilde{m}_i c_i$, where \tilde{m} is the refractive index of a mixture particle; \tilde{m}_i is the refractive index of particle species; c is the volume ratio of particle species. Based on the equation, the refractive index of coating materials of BC-containing particles (RI_c) was $\sim 1.50-0i$ during the campaign period.”

- (c) Page 8, line 3: I am not sure how the authors determine that the Mie calculation has an uncertainty “smaller than 7%”. The authors have shown in Figure S3 and the associated discussions that different RI values could result in 3%-10% difference in D_c . Assume it is on average 5%, then the mass concentration of rBC would be different by 16% (1.05^3 , the cubic is converting from diameter to volume), not mentioning the uncertainties on the estimation of e.g., density, mixing, etc. I would suggest the authors do a much more careful job when they are talking about uncertainties.

Response: Thanks for the comments. There might be some misunderstanding on the uncertainty of Mie calculation given here. We would like to kindly clarify that the uncertainty of 3%-10% shown in Fig. S3 from different RI_c values in Mie calculation was for the whole diameter of BC-containing particles (D_p), not for diameter of rBC core (D_c). We did not use Mie calculation to determine the mass concentration of rBC, which was obtained from SP2 measurements. Therefore, the mass concentration of rBC would not be different due to using different RI_c values. We have recalculated the uncertainties on the calculated light absorption. In this study, the MAC for bare BC derived from Mie calculation, using the RI (i.e., $2.26-1.26i$) given here, is $3.5-4.4 \text{ m}^2/\text{g}$ at 880 nm (Fig. R2 in the response). Bond and Bergstrom (2006) suggested a value of $7.5 \text{ m}^2/\text{g}$ for the MAC of bare BC at 550 nm. Considering that the absorption is inversely proportional to wavelength (Bond and Bergstrom, 2006), the MAC of bare BC at 880 nm is estimated to be $\sim 4.7 \text{ m}^2/\text{g}$, which was slightly greater than that ($\sim 4.3 \text{ m}^2/\text{g}$) obtained from Mie calculation in our study. This indicated the uncertainty of MAC for bare BC from Mie calculation was $\sim 8\%$. We estimated that the uncertainties of

calculated BC light absorption related to MAC of bare rBC from Mie calculation was ~8%.

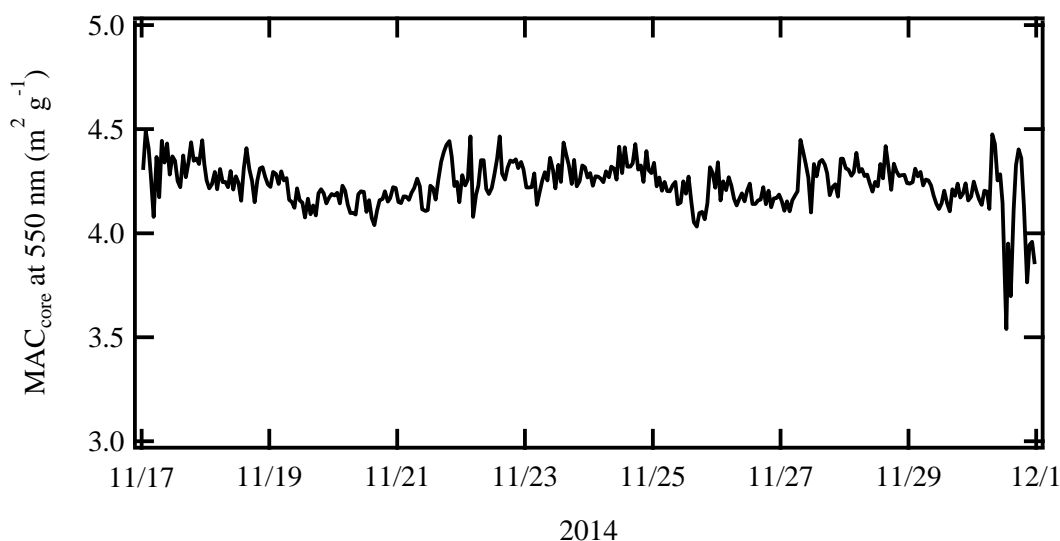


Figure R2 (Fig. S7 in the revised manuscript). The time series of MAC derived from Mie calculation for BC cores (i.e., bare BC) at 880 nm.

Correspondingly, we added the new Fig. S7 and related discussion in the revised supplement, as “Based on Mie calculation, we obtained the MAC of rBC core (MAC_c) at 880 nm in the range of 3.8-4.5 m^2/g with an average of $\sim 4.3 m^2/g$ during the campaign period (Fig. S9). Bond and Bergstrom (2006) suggested a value of 7.5 m^2/g for the MAC of bare BC at 550 nm. Considering that the absorption is inversely proportional to wavelength (Bond and Bergstrom, 2006), the MAC of bare rBC at 880 nm is estimated to be $\sim 4.7 m^2/g$, which was slightly greater than that ($\sim 4.3 m^2/g$) obtained from Mie calculation in our study. This indicated the uncertainty of MAC for bare rBC from Mie calculation was $\sim 8\%$. We estimated that the uncertainties of calculated BC light absorption related to MAC of bare rBC from Mie calculation was $\sim 8\%$.”

- (2) About the processes contributing to the enhancement of BC light absorption. The authors are trying to add some discussions on the causes of BC coating and thus

light absorption enhancement, but these discussions read somewhat weird if there is no sufficient evidence to support. Similarly, a couple of examples below:

Response: Thanks for the comment. Following the reviewer's suggestion, we have modified some discussion on the causes of BC coating and thus light absorption enhancement in the revised manuscript to make them more appropriate. Here, to the discussions/statements mentioned by the reviewer is as follows.

- (a) Page 8, line 18: “due to more secondary component formation”, is it possible that more primary components were also emitted under the more polluted condition and coated onto the BC core during the aging process?

Response: Thanks to the reviewer for raising this concern. We agree with the reviewer. The statement has been revised as “*In terms of BC-containing particles with a certain rBC core size, their D_p/D_c ratio and E_{ab} were greater under higher PM_{10} concentrations, which could be attributed to more coating materials on BC surface under more pollution environment. The increase of both primary and secondary components under more polluted conditions was favorable to BC aging by coagulation and condensation, which happen mostly between BC and non-BC species.*”

- (b) Page 10, lines 19-28: I do not understand why the authors are looking at the temporal trend of O₃ to evaluate local photochemical processes. The trend of O₃ could mean weak production, could mean strong ozonolysis (which could be dark reaction, i.e., nothing with photochemistry), or could just mean cloudy days thus no sunlight. This is not a sound reason for “weak local aging”.

Response: Thanks to the reviewer to point this out. We agree with the reviewer that the decrease in O₃ concentration can not fully support weaken local aging. In this study, we focused on the effect of regional transport on BC aging process. We just roughly discussed the chemical process during BC aging. The chemical process of BC aging under polluted environment in china is complex, which involved photochemical oxidation and heterogeneous chemical production (Zheng et al.

2015). We will investigate the chemical process of BC aging under polluted environment in future.

In the revised manuscript, we have toned down the related discussion on the chemical process of BC aging, as *“When PM_1 concentrations were higher than $\sim 120 \mu\text{g m}^{-3}$, O_3 concentrations decreased to ~ 2 ppb. Zheng et al. (2015) has demonstrated the weakened importance of photochemistry in the production and aging of secondary aerosols in Beijing under polluted conditions due to decrease of oxidant concentrations. This indicated that the photochemical processing in BC aging may be weakened under higher polluted levels (i.e., $PM_1 > 120 \mu\text{g m}^{-3}$). Noted that photochemical processing is not the only possible pathway in BC aging process and other pathways were not discussed in this study. For example, high concentrations of aerosols under polluted environment may compensate the adverse photochemical conditions for BC aging.”*

2. Minor issues

- (1) The authors sometimes used “BC-containing particles” while sometimes “BC particles” and “BC” to name the same term, the BC-cored and other materials coated particles. Please try to be consistent throughout the manuscript, otherwise it will be confusing, e.g., Page 2, the “BC” of line 12, and the first “BC” of line 22, they did not actually have the same meaning.

Response: Thanks for the comment. Throughout the manuscript, we have revised the terms to keep them consistent.

- (2) Page 1, line 14: It “is” well known...

Response: Thanks. We have revised it.

- (3) Page 2, line 5: both emissions of BC and the coating materials -> emissions of both

BC and the coating materials;

Response: Thanks. We have revised it.

- (4) Page 2, line 22: lens effect -> lensing effect. Same problem throughout the paper, e.g., Page 5, line 24, and Page 8, line 10, etc.

Response: Thanks. We have revised them.

- (5) Page 2, line 23: results -> result;

Response: Thanks. We have revised it.

- (6) Page 3, line 25: the particles were not “collected” by the diffusion dryer, please correct;

Response: Thanks for the comment. We have revised the sentence as “*Ambient aerosol particles were collected by a PM₁ cyclone and then passed through a diffusion silica gel dryer.....*”

- (7) Page 4, line 25: not “RIs and RIc”, here it should be RIs only.

Response: Thanks. We have revised it.

- (8) Page 5, line 10: underestimate -> underestimation;

Response: Thanks. We have revised it.

- (9) Page 5, equation (4) and equation (6): what is the difference between m_{rBC} and C_{rBC} ?

Response: Thanks. The m_{rBC} represents the mass of a single rBC core (see the statement in the page 4, line 21 in the manuscript), and the C_{rBC} is the rBC mass concentration (see the statement in the page 6, line 3 in the manuscript).

(10) Page 7, line 21: that -> those;

Response: Thanks. We have revised it.

(11) Page 7, lines 22-24: The logic of this sentence is not 100% correct. D_p increases, which could be the increase of either D_c or coating materials, or both. The authors mentioned “simultaneous increase in the rBC mass concentration” exactly in the following sentence, which makes this sentence reads really weird. Same problem applies to the texts following Figure S8, that the authors only suggested the “18-fold” increase of σ_{ab} , and will need to provide more evidence on the “simultaneous increase” in both rBC and the coating materials.

Response: Thanks. Following the reviewer’s suggestion, we have added the Fig. R3 (new Fig. S8 in the revised manuscript) to support “simultaneous increase in rBC mass concentration and the amount of coating materials”. Correspondingly, the sentences in Page 7, lines 22-24 were revised as “*Moreover, the D_p exhibited sustained growth from ~180 nm to ~400 nm during a pollution episode, which could be a consequence of the increase in either D_c or coating materials, or both. Figure S6a shows a slight change in D_c with pollution development. However, the coating thickness of BC-containing particles increased with PM_1 concentration (Fig. S10a). Therefore, the sustained growth of D_p during a pollution episode was dominated by more coating materials under more polluted conditions. Figure S10 shows the simultaneous increase in the rBC mass concentration and the amount of coating materials on the BC surface, which could significantly enhance the light absorption of BC-containing particles.*”, and the statement following Fig. S8 (new Figure S11 in the revised supplement) in the revised supplement was revised as “*The simultaneous increase in the rBC mass concentration and the amount of coating materials shown in Fig. S10 revealed that the increase of $\sigma_{ab,880nm}$ (~18 fold from ~10 $\mu g m^{-3}$ of PM_1 to ~230 $\mu g m^{-3}$ of PM_1) could be attributed to simultaneous*

increase in the rBC mass concentration and the amount of coating materials on the BC surface.”

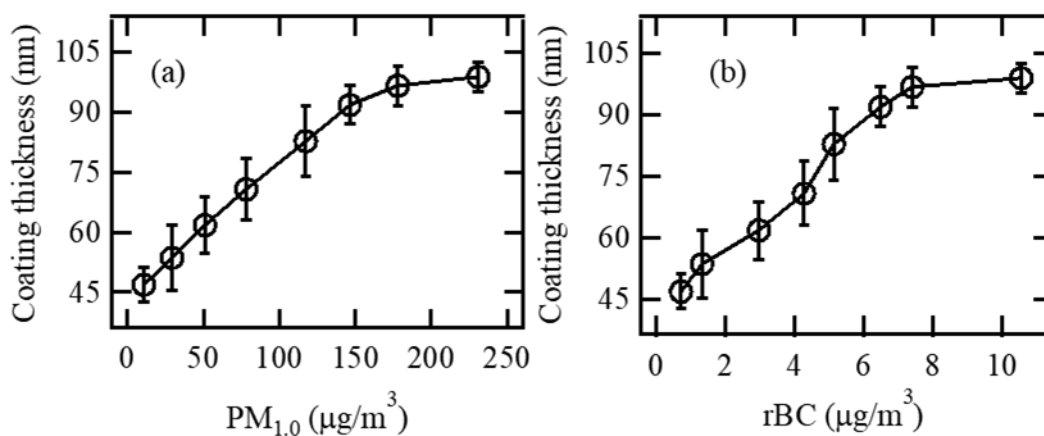


Figure R3 (Fig. S10 in the revised manuscript). Variations in the coating thickness of BC-containing particles with the (a) PM₁ and (b) rBC mass concentrations.

(12) Page 8, line 30: change rates -> changing rates;

Response: Thanks. We have revised it.

(13) Page 9, line 3: at our study -> in our study;

Response: Thanks. We have revised it.

(14) Page 9, line 21: (A) BC aging and (B) BC internally mixed with other components, it is hard to say A is the consequence of B, or vice versa;

Response: Thanks. We have revised the sentence as “BC aging in the atmosphere, namely BC internally mixing with other aerosol components, is associated with atmospheric transport (Gustafsson and Ramanathan, 2016).”

(15) Page 12, line 3: capacity or capability? Please note this is not the only place.

Response: Thanks. Throughout the manuscript, we have changed “capacity” into

“capability”.

(16) Page 12, lines 14-15: decreased by significantly -> decreased significantly;

Response: Thanks. We have revised it.

(17) Table 1, the unit is “ $\mu\text{g m}^{-3}$ ”, not “ $\mu\text{g cm}^{-3}$ ”;

Response: Thanks. We have revised it.

(18) Figure 2: Eab is not light absorption capability, it should be enhancement;

Response: Thanks. We have revised it.

(19) SI: page 4, line 13: what is “larges of coating materials”?

Response: Thanks. We have changed “larges of coating materials” into *“significantly larger in volume of coating materials than that of rBC cores”.*

References:

Bond, T. C., and Bergstrom, R. W.: Light Absorption by Carbonaceous Particles: An Investigative Review, *Aerosol Sci. Technol.*, 40, 27-67, 2006.

Gustafsson, Ö., and Ramanathan, V.: Convergence on climate warming by black carbon aerosols, *Proc. Natl. Acad. Sci. USA*, 113, 4243-4245, 2016.

Hänel, G.: The real part of the mean complex refractive index and the mean density of samples of atmospheric aerosol particles, *Tellus*, 20, 371-379, 1968.

Hyvärinen, A.-P., Vakkari, V., Laakso, L., Hooda, R. K., Sharma, V. P., Panwar, T. S., Beukes, J. P., van Zyl, P. G., Josipovic, M., Garland, R. M., Andreae, M. O., Pöschl, U., and Petzold, A.: Correction for a measurement artifact of the Multi-Angle

Absorption Photometer (MAAP) at high black carbon mass concentration levels, *Atmos. Meas. Tech.*, 6, 81-90, 2013.

Peng, J., Hu, M., Guo, S., Du, Z., Zheng, J., Shang, D., Levy Zamora, M., Zeng, L., Shao, M., Wu, Y.-S., Zheng, J., Wang, Y., Glen, C. R., Collins, D. R., Molina, M. J., and Zhang, R.: Markedly enhanced absorption and direct radiative forcing of black carbon under polluted urban environments, *Proc. Natl. Acad. Sci. USA*, 113, 4266-4271, 2016.

Schkolnik, G., D. Chand, A. Hoffer, M.O. Andreae, C. Erlick, E. Swietlicki and Y. Rudich (2007), Constraining the density and complex refractive index of elemental and organic carbon in biomass burning aerosol using optical and chemical measurements, *Atmos. Environ.*, 41, 1107-1118.

Mallet, M., J.C. Roger, S. Despiiau, O. Dubovik and J.P. Putaud (2003), Microphysical and optical properties of aerosol particles in urban zone during ESCOMPTE. *Atmos. Res.*, 69(1-2), 73-97.

Marley, N.A., J.S. Gaffney, C. Baird, C.A. Blazer, P. J. Drayton and J. E. Frederick (2001), An empirical method for the determination of the complex refractive index of size fractionated atmospheric aerosols for radiative transfer calculations, *Aerospace. Sci. Technol.* 34(6), 535-549.

Zheng, G. J., Duan, F. K., Su, H., Ma, Y. L., Cheng, Y., Zheng, B., Zhang, Q., Huang, T., Kimoto, T., Chang, D., Pöschl, U., Cheng, Y. F., and He, K. B.: Exploring the severe winter haze in Beijing: the impact of synoptic weather, regional transport and heterogeneous reactions, *Atmos. Chem. Phys.*, 15, 2969-2983, 2015.

Amplification of light absorption of black carbon associated with air pollution

Yuxuan Zhang^{1,2}, Qiang Zhang¹, Yafang Cheng^{3,2}, Hang Su^{3,2}, Haiyan Li⁴, Meng Li^{1,2}, Xin Zhang¹, Aijun Ding⁵, and Kebin He⁴

¹Ministry of Education Key Laboratory for Earth System Modeling, Department of Earth System Science, Tsinghua University, Beijing 100084, China

²Multiphase Chemistry Department, Max Planck Institute for Chemistry, Mainz 55020, Germany

³Institute for Environmental and Climate Research, Jinan University, Guangzhou 510630, China

⁴State Key Joint Laboratory of Environment Simulation and Pollution Control, School of Environment, Tsinghua University, Beijing 100084, China

⁵Institute for Climate and Global Change Research, School of Atmospheric Sciences, Nanjing University, Nanjing, China

Correspondence to: Qiang Zhang (qiangzhang@tsinghua.edu.cn)

Abstract. The impacts of black carbon (BC) aerosols on air quality, boundary layer dynamic and climate depend not only on the BC mass concentration but also on the light absorption capability of BC. It is well known that the light absorption capability of BC depends on the amount of coating materials (namely other species on BC by condensation and coagulation). However, the difference of light absorption capability of ambient BC-containing particles under different air pollution conditions (e.g., the air clean and polluted conditions) remains unclear due to the complex aging process of BC in the atmosphere. In this work, we investigated the evolution of light absorption capability for BC-containing particles with changing pollution levels in urban Beijing, China. During the campaign period (17 to 30 November 2014), with the growth of PM₁ concentration from ~10 μg m⁻³ to ~230 μg m⁻³, we found that the mass-weighted averages of the aging degree and theoretical light absorption capability of BC-containing particles with refractory BC cores of ~75–200 nm increased by 28–48% and 13–36% increased by ~33% and ~18%, respectively, indicating stronger light absorption capability of BC-containing particles under more polluted conditions due to more coating materials on the BC surface. By using effective emission intensity (EEI) model, we further found that aging during the regional transport plays an important role in the difference among the light absorption capability of BC-containing particles under different air pollution levels. During the pollution episode, ~63% of the BC over Beijing originated from regional sources outside of Beijing. These regionally sourced BC-containing particles were characterized by more coating materials on BC surface due to accelerated aging process—more coating precursors within more polluted air, which contributed ~78% of the increase in theoretical light absorption capability of BC observed in Beijing during the polluted period (PM₁

1 of $\sim 230 \mu\text{g m}^{-3}$) comparing to that in the clean period (PM_{10} of $\sim 10 \mu\text{g m}^{-3}$). Due to the increase of theoretical light absorption
2 capability of BC associated with air pollution, the direct radiative forcing of BC was estimated to be increased by ~~$\sim 2018\%$~~
3 based on a simple radiation transfer model. Our work identified an amplification of theoretical light absorption and direct
4 radiative forcing under more air polluted environment due to more coating pollutants on BC. The air pollution control measures
5 may, on the other hand, break the amplification effect by reducing ~~both~~ emissions of both BC and the coating materials and
6 achieve co-benefits of both air quality and climate.

7 **1 Introduction**

8 Black carbon (BC) is an important aerosol component that absorbs visible sunlight and contributes to heating of the atmosphere
9 (Bond and Bergstrom, 2006; Gustafsson and Ramanathan, 2016; Menon et al., 2002). Atmospheric BC can impact climate
10 through radiative effects, which are strongly associated with the optical properties of BC, especially the light absorption (Cheng
11 et al., 2006; Jacobson, 2000; Lesins et al., 2002; Ramanathan and Carmichael, 2008). Estimating the climate effects of BC is
12 one of the major challenges in climate change research, partly due to large uncertainties in the light absorption capability of
13 BC-containing particles under ambient conditions (Cappa et al. 2012; Liu et al. 2015; Liu et al. 2017; Gustafsson and
14 Ramanathan, 2016). The light absorption capability of atmospheric BC is complex and poorly quantified, and it changes with
15 the morphology, density and ~~aging degree~~ mixing state of the BC-containing particles (~~Moffet et al., 2009; Knox et al., 2009;~~
16 ~~Peng et al. 2016; Schnaiter et al. 2005; Zhang et al., 2008; Zhang et al., 2016~~). Previous theoretical (Jacobson, 2001; Moffet
17 et al., 2009; Zhang et al., 2016) and observation studies (Cappa et al., 2012; Peng et al., 2016; Knox et al., 2009) studies
18 showed a broad range of absorption ~~enhancements~~ enhancements (1.05-3.05) of BC-containing particles during the
19 atmospheric aging process, ~~ranging from 1.05 to 3.50 (Jacobson, 2001; Peng et al., 2016; Schnaiter et al., 2005)~~. To date,
20 conflicts remain between model- and observation-based studies of the light absorption capability of atmospheric BC-
21 containing particles (Cappa et al., 2012; Jacobson, 2001; Liu et al. 2015; Liu et al. 2017).

22 The light absorption capability of BC-containing particles depends strongly on the particle mixing state (Liu et al. 2015;
23 Liu et al. 2017), i.e., the degree of internal mixing between BC and other particle species (i.e., non-BC components) by the
24 atmospheric aging process (i.e., condensation, coagulation and heterogeneous oxidation). The non-BC species (i.e., coating
25 materials) on the surface of BC cores can enhance BC light absorption via the lensing effect (namely, the coating materials act
26 as a lens to focus more photons on BC, Bond et al., 2006; Fuller et al., 1999; Jacobson, 2001; Lack and Cappa, 2010). In terms
27 of individual BC-containing particle, more ~~More~~ coating materials results in its stronger light absorption capability ~~for the BC-~~
28 ~~containing particles~~. The coating materials on the BC surface are controlled by secondary processes (e.g., photochemical
29 production) (Metcalf et al., 2013).

30 The production of secondary aerosols in the atmosphere varies significantly with pollution levels (Cheng, 2008; Zheng et
31 al., 2016; Yang et al., 2015), indicating that BC-containing particles most likely exert different light absorption capability

1 values under different pollution levels. Compared with air clean conditions, polluted periods feature more secondary aerosols,
2 especially secondary inorganic species such as sulfate (Guo et al., 2014; Sun et al., 2014; Zheng et al., 2015). Whether the
3 changes of secondary aerosols with air pollution will affect the coating materials on the BC is complex, which not only depends
4 on the increase in BC amount versus secondary aerosols but also controlled by secondary material condensation on BC versus
5 non-BC containing particles. The increase in secondary aerosols with increasing air pollution levels affects the amount of
6 coating materials on the BC surface, resulting in changes in the light absorption capability of the ambient BC containing
7 particulates. Recent BC aging measurements in Beijing and Houston using an environmental chamber (flowing ambient air to
8 feed with lab-generated fresh BC) quasi-atmospheric measurements have revealed that a clear distinction in the light absorption
9 capability of BC-containing particles exists between urban cities in developed and developing countries (Peng et al., 2016),
10 and this difference is likely due to the differences in air pollution levels.

11 To date, whether and how the aging degree and light absorption capability of BC-containing particles will change with air
12 pollution development is still unclear. Although the enhancement of BC light absorption due to coating materials on BC
13 surface has already been intensively investigated (Moffet et al., 2009; Schnaiter et al., 2005; Shiraiwa et al., 2010; Zhang et
14 al., 2016), there are few studies on the evolution of the light absorption capability of BC-containing particles with changing
15 air pollution levels. The variation in the light absorption capability of BC-containing particles associated with air pollution can
16 lead to different effects of BC aerosols on air quality and climate under different pollution levels. To improve the evaluation
17 of BC-related effects on air quality and climate, some models have considered BC internally mixed with other species (namely
18 coating materials on BC surface), which can affect the light absorption capability of BC-containing particles. However, the
19 difference of coating materials on BC under different air pollution conditions remains unclear.

20 In this work, we conducted an intensive field measurement campaign in urban Beijing, China, to investigate the difference
21 of the theoretical light absorption capability of atmospheric BC-containing particles under different pollution levels. Firstly,
22 we analyzed the evolution of theoreticalBC light absorption capability of BC with increasing air pollution levels and estimated
23 the relationship between the rates of changes in the theoretical light absorption capability of BC and in the PM₁ or BC mass
24 concentrations. We then explored the cause of the evolution of theoretical light absorption capability of BC with increasing air
25 pollution levels and evaluated the relative importance of regional transport. Finally, we discussed the impact of changes in BC
26 light absorption capability with pollution levels on BC radiative forcing.

27 **2 Methods**

28 **2.1 Sampling site and measurements**

29 The *in-situ* measurements were conducted on the campus of Tsinghua University (Tsinghua site, 40°00'17" N, 116°19'34" E)
30 from November 17-30, 2014. The Tsinghua site (Fig. S1) is located in urban Beijing, China. The megacity Beijing is adjacent

1 to Hebei Province and the megacity Tianjin (Fig. S1), in which considerable industrial manufacturing has led to heavy
2 emissions of air pollution, especially in southern Hebei.

3 Ambient aerosol particles were collected by a PM₁ cyclone and then passed through a diffusion silica gel dryer, and they
4 were then-finally analyzed by an aethalometer (AE33, Magee Scientific Corp.), an Aerosol Chemical Speciation Monitor
5 (ACSM, Aerodyne Research Inc.) and a single particle soot photometer (SP2, Droplet Measurement Technologies Inc.). The
6 AE33 can measure the absorption coefficient (σ_{ab}) of sampled aerosols in seven spectral regions (370, 470, 520, 590, 660, 880
7 and 950 nm). At a wavelength of 880 nm, the absorption of aerosol particles is dominated by BC component because the light
8 absorbed by other aerosol components is significantly less (Drinovec et al., 2015; Sandradewi et al., 2008). In this study, the
9 σ_{ab} at 880 nm measured by the AE33 was used to characterize the theoretical light absorption of the BC-containing particles.
10 More details on the AE33 measurement can be found in the work of Drinovec et al., 2015. Considering the filter-loading effect
11 and multiple-scattering effect (Drinovec et al., 2015; Weingartner et al., 2003; Segura et al., 2014), the aethalometer data was
12 corrected by compensation factors described in the supplementary information (Fig. S2 and the associated discussion). The
13 ACSM and SP2 instruments measured the mass concentrations of non-refractory submicron-scale components (NR-PM₁, i.e.,
14 sulfate, nitrate, ammonium, chloride and organics) and refractory BC (rBC), respectively, and the sum of these two
15 measurements was used to estimate the PM₁ mass concentration. The ACSM instrument used in our study was described by
16 Li et al. (2017).

17 The SP2 instrument measures a single BC-containing particle using a 1064 nm Nd:YAG intra-cavity laser beam. As the
18 light-absorbing rBC passes through the laser beam and is heated to its vaporization temperature (~4000 K), it will emit
19 incandescent light (i.e., visible thermal radiation), which is linearly proportional to the mass of the rBC (Metcalfe et al., 2012;
20 Moteki and Kondo, 2010; Schwarz et al., 2006; Sedlacek et al., 2012). In this study, the calibration curve of rBC mass vs.
21 incandescence signal was obtained from the incandescence signal of size-resolved Aquadag particles (their effective density
22 obtained from Gysel et al., 2011) using a DMA (differential mobility analyzers)-SP2 measurement system. Considering
23 different sensitive of the SP2 to different rBC types (Gysel et al., 2011; Laborde et al., 2012), we corrected SP2 calibration
24 curve by scaling the peak height of incandescence signal for Aquadag particles at each rBC mass based on the relationship
25 between the sensitivity of SP2 to Aquadag and ambient rBC (Laborde et al., 2012). The particle-to-particle mass of ambient
26 rBC can be determined by measuring its incandescence signal and comparing it to the calibration curve. The mass
27 concentration of rBC is calculated from the particle-to-particle mass of rBC and the sampled flow (~0.12 lpm). Note that the
28 SP2 detection efficiency (Fig. S3) have been considered in the calculation of rBC mass concentration. Furthermore, the
29 scattering cross section of a BC-containing particle is obtained from its scattering signal using the leading edge only (LEO)-
30 fit method (Gao et al. 2007). Zhang et al. (2016) has demonstrated the validity of the LEO-fit method for ambient BC-
31 containing particles in China.

1 2.2 SP2 data analysis

2 2.2.1 Aging degree of BC-containing particles

3 Based on the rBC core mass (m_{rBC}) and scattering cross section (C_s) of the BC-containing particle derived from the SP2
4 measurements, the size of the BC-containing particle (D_p), including the rBC core and the coating materials, was calculated
5 by Mie theory with a shell-and-core model (Zhang et al., 2016). ~~In Mie calculation, the D_p is retrieved from C_s , the size of rBC~~
6 ~~core (D_c) and the refractive indices of the non-BC shell (RI_s) and rBC core (RI_c). The D_p is determined by the relationship (1):~~
7 ~~$D_p \sim (C_s, D_c, RI_s, RI_c)$,~~ (1)

8 ~~In the relationship (1), the RI_s and RI_c represent the refractive indices of the non-BC shell, respectively.~~ The RI_s value used
9 in this study are 1.50-0i based on ~~the chemical compositions of coating materials during the campaign period (Fig. S4 and the~~
10 ~~associated discussion in the supplementary information) values in the literature (Cappa et al., 2012).~~ In term of RI_c , we
11 evaluated the sensitivity of D_p values retrieved by Mie mode to the RI_c values (Fig. ~~S3-S5~~ and the associated discussion in the
12 supplementary information). In the following calculation, the RI_c of 2.26-1.26i was used (Taylor et al., 2015).

13 The D_c ~~in the relationship (1) is the size of the rBC core and~~ is calculated using the m_{rBC} and rBC core density (ρ_c , 1.8 g
14 cm^{-3} used in this study (Cappa et al., 2012)) assuming a void-free sphere for rBC core, as given in Eq. (21). The size distribution
15 of rBC cores under different pollution levels during the campaign period ~~was is~~ displayed in Fig. ~~S4S6~~.

$$16 D_c = \left(\frac{6m_{\text{rBC}}}{\pi\rho_c} \right)^{1/3}, \quad (21).$$

17 As in previous studies (Liu et al., 2013; Sedlacek et al., 2012; Zhang et al., 2016), the aging degree of BC-containing
18 particles was characterized by the D_p/D_c ratio ~~in this study~~. Higher D_p/D_c ratios for BC-containing particles indicate higher
19 aging degrees, i.e., more coating materials on the BC surface.

20 In terms of D_p/D_c ratio of BC-containing particles ~~determined by relationship (1) and Eq. (2)~~, we focused on the rBC core
21 size (D_c) above detection limit of SP2 incandescence ($D_c > 75$ nm), while the detection limit of SP2 scattering for the whole
22 particle size (D_p) was not considered in this study. If the BC-containing particles with rBC cores larger than ~75 nm is large
23 enough to be detected by SP2 scattering channel, we would calculated their whole particle size (D_p) using LEO method based
24 on their scattering signal. If not, we would assume that the D_p was equal to the rBC core size (D_c). This assumption might lead
25 to the ~~underestimate-underestimation~~ of ~~aging degree (D_p/D_c)~~ ~~ratio~~ of the BC-containing particles with size above the
26 incandescence limit and blow the scattering limit. To evaluate the uncertainty of D_p/D_c ratio, we calculated the detect efficiency
27 of SP2 scattering (Fig. ~~S5-S7~~ in the supplementary information). In terms of BC-containing particles with rBC core larger than
28 75 nm (SP2 size cut for incandescence) observed in our site during the campaign period, most of them (~90-100%, Fig. ~~S5S7~~)
29 exhibited particle size (180-500 nm shown in Fig. ~~R6R8~~) larger than SP2 size cut for scattering due to large coating materials
30 on rBC cores. This indicated that the uncertainty of D_p/D_c ratio calculated in this study due to mismatch in the SP2 size cut for
31 incandescence vs scattering is no more than 10%. High detection efficiency of SP2 scattering for BC-containing particles
32 observed in our site can be attribute to their large size (180-500 nm, Fig. ~~S6S8~~).

1 2.2.2 BC optical properties

2 Based on the size information on BC-containing particles (i.e., D_c and D_p) obtained from the SP2 measurement (discussed in
3 Sec. 2.2.1), we used Mie theory with a shell-and-core model to retrieve the optical properties of BC-containing particles,
4 including the absorption enhancement (E_{ab}) of rBC, the mass absorption cross-section (MAC) of BC-containing particles and
5 bare rBC cores, the mass scattering cross section of bare BC core (MSC_{core}) and the absorption coefficient (σ_{ab}) of BC-
6 containing particles. The calculation of these parameters is described below.

7 The E_{ab} characterizes the increase in BC light absorption due to the lensing effect of coating materials on the BC surface
8 and is used to quantify the theoretical light absorption capability of BC-containing particles in this study. The E_{ab} is determined
9 by the ratio of the absorption cross section of the entire BC-containing particle ($C_{ab,p}$) to that of bare BC core ($C_{ab,c}$), as
10 expressed in Eq. (32):

$$11 E_{ab} = \frac{C_{ab,p}(D_c, D_p, RI_s, RI_c)}{C_{ab,c}(D_c, RI_c)},$$

12 (32)

13 where $C_{ab,p}$ is determined by the D_c , D_p , RI_s and RI_c using Mie calculation, and $C_{ab,c}$ is determined by the D_c and RI_c .

14 The MAC of BC-containing particles (MAC_p) and bare rBC cores (MAC_c) is defined as the $C_{ab,p}$ and $C_{ab,c}$ per unit rBC mass,
15 as Eqs. (3) and (4), respectively:

$$16 MAC_p = \frac{C_{ab,p}(D_c, D_p, RI_s, RI_c)}{m_{rBC}}, \quad (43)$$

$$17 MAC_c = \frac{C_{ab,c}(D_c, RI_c)}{m_{rBC}}, \quad (4)$$

18 The MSC_{core} is the scattering cross sections of bare rBC cores ($C_{sca,c}$) per unit rBC mass, as calculated by Eq. (5):

$$19 MSC_{core} = \frac{C_{sca,c}(D_c, RI_c)}{m_{rBC}}. \quad (5)$$

20 The σ_{ab} of BC-containing particles is calculated based on the ~~MAC (Eq. (4))~~ and the rBC mass concentration (C_{rBC})
21 measured by the SP2, as expressed in Eq. (6). The uncertainties of σ_{ab} ~~of BC-containing particles from related to MAC of bare~~
22 ~~rBC cores from~~ Mie calculation was evaluated in the supplementary information (Fig. S7-S9 and the associated discussion).

$$23 \sigma_{ab,calculated} = MAC_p \times C_{rBC} = MAC_c \times E_{ab} \times C_{rBC}, \quad (6).$$

24 2.3 BC effective emission intensity

25 To evaluate the impact of regional transport on BC-containing particles, we used a variant of the “effective emission intensity”
26 (EEI) defined by Lu et al. (2012) to quantify the amounts of BC over the observation site from different source regions. In this
27 study, the spatial origin of the BC observed at our site was divided into local sources in Beijing and regional sources in other
28 areas (i.e., Hebei, Tianjin, Shanxi and Inner Mongolia, Fig. S1). The EEI takes into account emission, transport, hydrophilic-
29 to-hydrophobic conversion, and removal processes (i.e., dry and wet deposition) of BC throughout the whole atmospheric

1 transport process from the origin of the BC emission to the receptor site. A novel back-trajectory approach was developed by
2 Lu et al. (2012) to calculate EEI values.

3 In this study, the back-trajectory analysis was performed by the Hybrid Single-Particle Lagrangian Integrated Trajectory
4 (HYSPLIT) model to obtain the transport pathways of BC to the observation site (40°00'17" N, 116°19'34" E) during the
5 campaign period (November 17-30, 2014). The 72-h back-trajectory at 100 m at every hour was calculated with the
6 meteorological fields of NCEP GDAS at a 1°×1° resolution. An anthropogenic BC emission inventory of China in the year
7 2012 at a resolution of 0.25°×0.25° was used to support the back-trajectory analysis. The gridded BC emission data are from
8 the Multi-resolution Emission Inventory for China (MEIC) developed by Tsinghua University (<http://www.meicmodel.org>).

9 We calculated the EEI of BC at a resolution of 0.25°×0.25° based on the algorithm developed by Lu et al. (2012). Following
10 a trajectory l at every hour, the fresh BC ~~particles~~ emitted from a series of spatial grids in sequence (i.e., $l_1, l_2, \dots, l_i, \dots$) are
11 transported to the receptor grid (i.e., l_n). The EEI of trajectory l at the surface grid point i ($EEI_{i,l}$) was determined by Eq. (7):

$$12 \quad EEI_{i,l} = E_i \times TE_{i,l}, \quad (7)$$

13 where E_i is the BC emission at the surface grid point i , and $TE_{i,l}$ represents the BC transport efficiency of trajectory l from the
14 grid point i to the receptor site, as calculated by Eqs. (1)-(4) in Lu et al. (2012).

15 The total EEI of trajectory l characterizes the total amount of BC transported to the observation site at every hour, expressed
16 as Eq. (8):

$$17 \quad EEI_{total} = \sum_{i=1}^n EEI_{i,l}, \quad (8).$$

18 **2.4 BC radiative efficiency**

19 In this study, we use a parameter of the simple forcing efficiency (SFE) to roughly evaluate the radiative forcing of BC-
20 containing particles. The SFE is defined as normalized radiative forcing by BC mass, which is wavelength-dependent (Bond
21 and Bergstrom, 2006; Chen and Bond, 2010; Chylek and Wong, 1995; Saliba et al., 2016). The wavelength-dependent SFE
22 for BC-containing particles is determined by Eq. (9):

$$23 \quad \frac{dSFE}{d\lambda} = -\frac{1}{4} \frac{dS(\lambda)}{d\lambda} \tau_{atm}^2(\lambda) (1 - F_c) \times [2(1 - \alpha_s)^2 \beta(\lambda) \cdot MSC_{core}(\lambda) - 4\alpha_s \times MAC(\lambda)], \quad (9)$$

24 in which a wavelength (λ) of 550 nm is used in this study; $dS(\lambda)/d\lambda$ is the spectral solar irradiance, the value of which is from
25 the ASTM G173-03 Reference Spectra (1.86 W m⁻² nm⁻¹ at 550 nm); and the parameters τ_{atm} , F_c , α_s and β are the atmospheric
26 transmission (0.79), cloud fraction (0.6), urban surface albedo (0.15) and backscatter fraction (0.17), respectively (Jeong et al.,
27 2013; Chen and Bond, 2010; Park et al., 2011; Saliba et al., 2016).

28 **3 Results**

29 **3.1 Light absorption of BC-containing particles during the campaign period**

1 Figure 1 shows the time series of the PM₁ and rBC mass concentration, the diameter of BC-containing particles (D_p) and the
2 measured and calculated light absorption coefficient (σ_{ab}) at 880 nm. During the campaign period, four episodes with different
3 PM₁ evolution processes (Fig. 1a) were observed: November 18-21, November 23-24, November 25-26 and November 28-
4 30. The hourly PM₁ mass concentration ranged from 3.5-275 $\mu\text{g m}^{-3}$, with an average value of 91 $\mu\text{g m}^{-3}$ during the observed
5 period. The rBC mass concentration accounted for ~5% of PM₁. The diameter of BC-containing particles (D_p) including rBC
6 cores and coating materials shown in Figure 1(b) exhibited an excellent temporal coherence with the rBC mass concentration.
7 Figure 1(b) shows that the number distribution of D_p for BC-containing particles exhibited a peak at 180-320 nm, significantly
8 larger than the peak value (D_c of ~95 nm) for number size distribution of bare rBC cores (Fig. ~~S3a~~S5a) due to larges of coating
9 materials on BC surface. The size information (namely entire particle size (D_p) and rBC core size (D_c)) of BC-containing
10 particles observed in our study was consistent with ~~that those~~ (D_p of ~200-300 nm and D_c of ~70-100 nm) in previous studies
11 in China (Gong et al., 2016; Huang et al., 2012; Wang et al., 2014). Moreover, the D_p exhibited sustained growth from ~180
12 nm to ~400 nm during a pollution episode, which could be a consequence of the increase in either D_c or coating materials, or
13 both. Figure S6a shows a slight change in D_c with pollution development. However, the coating thickness of BC-containing
14 particles increased with PM₁ concentration (Fig. S10a). Therefore, the sustained growth of D_p during a pollution episode was
15 dominated by more coating materials under more polluted conditions. Figure S10 shows the simultaneous increase in the rBC
16 mass concentration and the amount of coating materials on the BC surface, which could significantly enhance the light
17 absorption of BC-containing particles, revealing an increase in the amount of coating materials on the BC surface with
18 increasing air pollution levels. With an increase in air pollution, the simultaneous increase in the rBC mass concentration and
19 the amount of coating materials on the BC surface could significantly enhance the light absorption of BC-containing particles.
20 Figure ~~S8-S11~~ shows that the measured absorption coefficient ($\sigma_{ab, \text{measured}}$) at 880 nm (dominated by BC component at this
21 wavelength (Drinovec et al., 2015)) for the aerosol particles measured by the AE33 (~~$\sigma_{ab, \text{measured}}$~~) (dominated by BC component
22 at this wavelength (Drinovec et al., 2015)) exhibited an 18-fold increase in conjunction with an increase in the PM₁
23 concentration from ~10 $\mu\text{g m}^{-3}$ to ~230 $\mu\text{g m}^{-3}$.

24 To valid SP2 measurements and Mie calculation used in this study, we compared the calculated light absorption coefficient
25 ($\sigma_{ab, \text{calculated}}$) of BC-containing particles using Eq. (6) with the measured light absorption coefficient ($\sigma_{ab, \text{measured}}$) from AE33,
26 as shown in Fig. 1c. The $\sigma_{ab, \text{calculated}}$ values for BC-containing particles showed an excellent agreement with the $\sigma_{ab, \text{measured}}$
27 values measured by the AE33, with a difference of ~10% ($R^2=0.98$). The difference was dominated by the uncertainties from
28 compensation algorithm used in the AE33 measurements (~~~10-15%~~, details shown in Fig. S2 and the associated discussion in
29 the supplementary information) and Mie calculation (~~smaller than 10-20%~~, Fig. ~~S7-S4~~, Fig. S5 and Fig. S9 and the associated
30 discussion in the supplementary information). The uncertainty evaluation revealed that the difference between $\sigma_{ab, \text{calculated}}$ and
31 $\sigma_{ab, \text{measured}}$ (~10%) shown in Fig. 1c is reasonable. The comparison between the $\sigma_{ab, \text{calculated}}$ and $\sigma_{ab, \text{measured}}$ values implied that
32 the optical properties (i.e., σ_{ab} , MAC and E_{ab}) of the BC-containing particles derived from Mie calculation combining with
33 SP2 measurement data (i.e., rBC concentrations, D_p and D_c) were reliable in our case.

3.2 Enhancement of the theoretical light absorption capability of black carbon associated with air pollution

3.2.1 The D_p/D_c ratio and calculated E_{ab} under different PM_{10} concentrations

Previous theoretical studies reported that the coating materials on the BC surface can significantly enhance the light absorption of BC via the lensing effect (Fuller et al., 1999; Jacobson, 2001; Lack and Cappa, 2010; Moffet et al., 2009). In other words, the aging degree of BC-containing particles (i.e., characterized by the D_p/D_c ratio in this study) determines their light absorption capability (characterized by i.e., the calculated MAC and E_{ab} in this study). However, whether and how the aging degree and light absorption capability of BC-containing particles will change under different pollution levels remains unclear. During the campaign period, we found that the mass-averaged values of D_p/D_c ratio, aging degree and calculated E_{ab} , light absorption capability of BC-containing particles increased with increasing air pollution levels.

Figure 2a shows the D_p/D_c ratio and calculated E_{ab} of BC-containing particles with rBC cores at 75-300 nm under different PM_{10} concentrations in the range of 1.2-3.5 and 1.3-3.1, respectively. In terms of BC-containing particles with a certain rBC core size, their D_p/D_c ratio and calculated E_{ab} were greater under higher PM_{10} concentrations, which could be attributed to more coating materials on BC surface under more pollution environment due to more. The increase of both primary and secondary components under more polluted conditions was favorable to BC aging by coagulation and condensation, which happen mostly between BC and non-BC species secondary component formation. On average (i.e., mass-weighted mean across rBC core size larger than ~75 nm), the D_p/D_c and calculated E_{ab} for observed BC-containing particles in SP2 under different PM_{10} concentrations during the campaign period varied in the range of 1.6-2.2 and 1.6-2.0, respectively (Fig. 2b). Correspondingly, the mass-averaged values of the D_p/D_c and calculated E_{ab} of BC-containing particles increased by ~33% and ~18%, respectively, with increasing PM_{10} concentrations from ~10 $\mu\text{g m}^{-3}$ to ~230 $\mu\text{g m}^{-3}$.

As shown in Fig. 2, the enhancement of D_p/D_c ratio and E_{ab} associated with air pollution were size-dependent. Smaller rBC cores exhibited more increase in the aging degree and light absorption capability with pollution development. When PM_{10} concentration increasing from ~10 $\mu\text{g m}^{-3}$ to ~230 $\mu\text{g m}^{-3}$ during the campaign period, the D_p/D_c ratio and E_{ab} of BC containing particle with rBC cores at 75-200 nm increased by 28-48% and 13-36%, respectively. The increase of D_p/D_c ratio and E_{ab} associated with air pollution decreased with increasing rBC core size according to an exponential function (Fig. 2b). This revealed that the aging degree and light absorption capability for rBC cores smaller than 75 nm (namely lower detection limit of SP2 incandescence) were most likely more than 48% and 36% respectively, and was about ~28% and ~13% for rBC cores larger than 200 nm. Figure 3 shows the increase of the D_p/D_c ratio and calculated E_{ab} (IR_{D_p/D_c} and $IR_{E_{ab}}$, respectively) for BC-containing particles with increasing PM_{10} concentrations from 10 $\mu\text{g m}^{-3}$ to 230 $\mu\text{g m}^{-3}$ as a function of rBC core size. Based on the D_p/D_c ratio and calculated E_{ab} of BC-containing particles with size-resolved rBC cores in SP2 measurement under different PM_{10} concentration (shown in Fig. 2a), we can obtain the measured IR_{D_p/D_c} and $IR_{E_{ab}}$ as a function of rBC core size. When PM_{10} concentration increasing from ~10 $\mu\text{g m}^{-3}$ to ~230 $\mu\text{g m}^{-3}$ during the campaign period, the D_p/D_c ratio and calculated E_{ab} of BC-containing particle with rBC cores at 75-200 nm increased by 28-48% and 13-36%, respectively. The size-dependent increase of D_p/D_c ratio and calculated E_{ab} associated with air pollution indicated that the aging process of smaller rBC was

1 relatively more sensitive to air pollution levels. This could be attributed to the fact that the condensational growth associated
 2 with air pollution due to the formation of secondary components is more effective for smaller particles in terms of increasing
 3 the diameter (Metcalf et al., 2013). -

4 Meanwhile, following a semiquantitative analysis using in Metcalf et al. (2013), we calculated the IR_{D_p/D_c} and $IR_{E_{ab}}$ based
 5 on diffusion-controlled growth law (Seinfeld and Pandis 2006).

6 According to the diffusion-controlled growth law (Seinfeld and Pandis 2006), the evolution of the size of BC-containing
 7 particles (D_p) is shown:

$$8 \quad \frac{dD_p}{dt} = \frac{A}{D_p} \quad (10)$$

9 in which, $\frac{dD_p}{dt}$ represents the diffusion-controlled growth rate; A is a parameter. Integrating Eq. (10) with $D_p(t=0) = D_c$:

$$10 \quad D_p^2 = D_c^2 + 2At = D_c^2 + B \quad (11)$$

11 in which, D_c is rBC core diameter; B (i.e., $2At$) is a parameter, varying under different PM_{10} concentrations.

12 Following Eq. (11), the D_p/D_c ratio is given:

$$13 \quad \frac{D_p}{D_c} = \left(\frac{B}{D_c^2} + 1\right)^{1/2} \quad (12)$$

14 where the parameter B is determined by the value of the measured D_p/D_c ratio with D_c of 160 nm under different PM_{10}
 15 concentrations.

16 The increase ratio of the D_p/D_c (IR_{D_p/D_c}) for BC-containing particles with PM_{10} concentration increasing from $10 \mu g m^{-3}$ to
 17 $230 \mu g m^{-3}$ can be calculated by Eq. (13):

$$18 \quad IR_{D_p/D_c} = \frac{\left(\frac{D_p}{D_c}\right)_{230} - \left(\frac{D_p}{D_c}\right)_{10}}{\left(\frac{D_p}{D_c}\right)_{10}} = \frac{\left(\frac{B_{230}}{D_c^2} + 1\right)^{1/2} - \left(\frac{B_{10}}{D_c^2} + 1\right)^{1/2}}{\left(\frac{B_{10}}{D_c^2} + 1\right)^{1/2}} \quad (13)$$

19 where $\left(\frac{D_p}{D_c}\right)_{230}$ and $\left(\frac{D_p}{D_c}\right)_{10}$ represent the D_p/D_c ratio when PM_{10} concentrations are $230 \mu g m^{-3}$ and $10 \mu g m^{-3}$, respectively; B_{230}
 20 and B_{10} are parameter B with PM_{10} concentrations of $230 \mu g m^{-3}$ and $10 \mu g m^{-3}$, respectively.

21 The increase ratio of calculated E_{ab} ($IR_{E_{ab}}$) for BC-containing particles with PM_{10} concentration increasing from $10 \mu g m^{-3}$
 22 to $230 \mu g m^{-3}$ can be derived based on $E_{ab}=k \times (D_p/D_c)$, as expressed in Eq. (5):

$$23 \quad IR_{D_p/D_c} = \frac{\left(\frac{D_p}{D_c}\right)_{230} - \left(\frac{D_p}{D_c}\right)_{10}}{\left(\frac{D_p}{D_c}\right)_{10}} = \frac{k_{230} \times \left(\frac{B_{230}}{D_c^2} + 1\right)^{1/2} - k_{10} \times \left(\frac{B_{10}}{D_c^2} + 1\right)^{1/2}}{k_{10} \times \left(\frac{B_{10}}{D_c^2} + 1\right)^{1/2}} \quad (14)$$

24 We compared the calculated IR_{D_p/D_c} and $IR_{E_{ab}}$ based on Eqs. (13) and (14) with those from SP2 measurements, as shown
 25 in Fig.3. The agreement indicated that the increase of the D_p/D_c and E_{ab} for BC-containing particles with increasing PM_{10}
 26 concentrations follow the diffusion-controlled growth law.

3.2.2 Changing rate of the theoretical light absorption capability of black carbon

Figure 3-4a explores the relationship between the ~~change-changing~~ rate of calculated E_{ab} (k_{Eab}) and the ~~change-changing~~ rates of PM_1 and rBC concentrations (k_{PM_1} and k_{rBC} , respectively) with pollution development. Linear relationships were estimated, i.e., $k_{Eab} \approx 4.8\% 0.051 k_{PM_1}$ and $k_{Eab} \approx 2.5\% k_{rBC}$, revealing that rapid increases in air pollution levels lead to rapid increases in BC light absorption capability. When the PM_1 concentration exhibited a sharp increase related to an extreme haze episode (Zheng et al., 2015), the increase in BC light absorption capability was dramatic. ~~During the campaign period, k_{Eab} reached a maximum of $7.3\% h^{-1}$, accompanied by a k_{PM_1} of $107.6\% h^{-1}$ and a k_{rBC} of $130.9\% h^{-1}$. Figure 4b shows frequency distribution of k_{Eab} , k_{PM_1} , and k_{Eab}/k_{PM_1} ratio. During the campaign period, most of k_{Eab} and k_{PM_1} values were in the range of -50% - $50\% h^{-1}$ and -4% - $4\% h^{-1}$, respectively, revealing a lower changing rate for BC aging than that for PM_1 concentration. The peak value of frequency distribution of k_{Eab} was around zero, indicating the BC-containing particles were shrinking as often as they were growing. The k_{Eab}/k_{PM_1} ratio characterized the sensitivity of the change of calculated E_{ab} with changing PM_1 concentrations. The frequency distribution of k_{Eab}/k_{PM_1} ratio showed that $\sim 60\%$ values were in the range of 0-1, with a peak value around 0.05. Smaller values of k_{Eab}/k_{PM_1} ratio indicated that the change of calculated E_{ab} was not sensitive to variations in PM_1 concentrations. The growth rate of E_{ab} (for BC samples with $k_{Eab} > 0$: 0.1 - $7.3\% h^{-1}$) observed at our study was consistent with the BC aging rate (0.2 - $7.8\% h^{-1}$) in previous studies (Cheng et al., 2012; Moteki et al., 2007; Shiraiwa et al., 2007). Moreover, we found that the growth rate of E_{ab} decreased with increasing PM_1 mass concentrations (Fig. S12a9), indicating that the increase in the theoretical light absorption capability of BC-containing particles slowed with further pollution development. This can be explained by larger BC-containing particles when PM_1 concentration is higher (Fig. S12b). The net change in diameter for a given amount of material deposited decreases with increasing particle size due to surface-to-volume scaling, which would expect the growth rate of particles to decrease with increasing PM_1 concentration and thus the k_{Eab} would also decrease (Fig. S12a). On average, the growth rate of BC light absorption capability during the campaign period was $-1.2\% h^{-1}$.~~

~~The evolution of theoretical light absorption of BC with pollution levels depends on the change in both rBC mass concentrations and calculated E_{ab} . Figure S13 shows markedly smaller k_{Eab} than k_{rBC} ($k_{Eab} \approx 0.027 k_{rBC}$), indicating the change of calculated E_{ab} was significantly slower than that of rBC mass concentrations under different pollution levels. Due to less sensitive for calculated E_{ab} to change in air pollution levels compared with that for rBC mass concentrations, some previous measurements (McMeeking et al., 2011; Ram et al., 2009; Wang et al., 2014b; Andreae, et al., 2008) would not have been able to discern a difference of E_{ab} easily among different pollution levels and thus just focus on the change of BC mass concentration. This would lead to uncertainties in estimation of BC light absorption. Compared with the values of k_{PM_1} and k_{rBC} , the significantly smaller k_{Eab} value indicated that the light absorption capability of BC increased more slowly than the PM_1 - or rBC mass concentrations. Smaller growth rate of BC light absorption capability may explain why previous studies (McMeeking et al., 2011; Ram et al., 2009; Wang et al., 2014b; Andreae, et al., 2008) just paid attention to the increase of BC mass concentrations associated with air pollution, but ignored the enhancement of BC light absorption capability. Generally,~~

1 the light absorption capability (i.e., mass absorption cross section) of BC was determined by linear regression of the absorption
2 coefficient against BC (or EC) mass concentrations in previous studies (Wang et al., 2014b; Andreae, et al., 2008). Excellently
3 linear relationship between absorption coefficient and BC mass concentrations can be attributed to that the change of
4 absorption coefficient is dominated by increase or decrease of BC mass concentration due to much rapider change of BC mass
5 concentration compared with that of BC light absorption capability. The linear regression method would cover up the fact that
6 the change of the light absorption capability of BC with their mass concentration under different air pollution levels. In our
7 case, we found the mass-weighted average of calculated E_{ab} increased by ~18% with PM_{10} concentration increasing from ~10
8 $\mu\text{g m}^{-3}$ to ~230 $\mu\text{g m}^{-3}$ (Fig. 2b). ~~if~~ If the increase in calculated E_{ab} , BC light absorption capability of BC due to increasing BC
9 mass concentration with PM_{10} increase was neglected in this study, the theoretical light absorption of BC-containing particles
10 would be underestimated by ~2818% under polluted conditions.

11 3.3 Contribution of regional transport

12 BC aging in the atmosphere, ~~a consequence of~~ ~~namely~~ BC internally ~~mixed-mixing~~ with other aerosol components, is associated
13 with atmospheric transport (Gustafsson and Ramanathan, 2016). In Beijing, the rapid increase in aerosol particle
14 concentrations during pollution episodes is most likely caused by regional transport of polluted air mass (Yang et al., 2015;
15 Zheng et al., 2015). Therefore, regional transport of pollution may play an important role in the enhancement of BC light
16 absorption capability associated with air pollution. In this study, we used the EEI analysis (Lu et al., 2012) to explore the
17 effects of regional transport on the increase in ~~theoretical~~ BC light absorption capability of BC with increasing pollution levels.

18 Figure 5 shows the spatial distribution ($0.25^\circ \times 0.25^\circ$) of the EEI for BC transported to the observation site under different
19 pollution levels (i.e., clear, slightly polluted and polluted periods) during the campaign period. The spatial origin of the BC
20 observed at our site varied significantly among the different pollution periods. In this study, the spatial origin of total BC in
21 the site was classified into local Beijing and other regions (i.e., outside of Beijing, considered as regional origins in this study).
22 Noted that the local region (i.e., Beijing) defined in this study is smaller than areas outside Beijing (e.g., Hebei, Tianjin, Shanxi
23 and Inner Mongolia (Fig. S1)). Table 1 lists the contribution of BC from regional origins (i.e., $EEI_{\text{outside}}/EEI_{\text{total}}$ ratio). During
24 polluted period, the contributions of BC from regional origins was ~63%, larger than that from local Beijing (~37%). This was
25 partly due to comparing the contributions from a small region (Beijing) and a large region (outside of Beijing). In this study,
26 we focus on comparing the contributions of BC from outside of Beijing (considered as regional origins in this study) among
27 different pollution levels (i.e., clean, slight polluted and polluted period). The BC from regional origins (i.e., outside of Beijing)
28 areas adjacent to Beijing (i.e., Hebei, Tianjin, Shanxi and Inner Mongolia (Fig. S1), considered as regional sources in this
29 study) accounted for ~21%, 39% and ~63% of total BC amount in the site during the clean, slightly polluted and polluted
30 periods, respectively. ~~This revealing revealed~~ that the regional contribution to BC over Beijing increased as the air pollution
31 levels increased.

32 Due to the increase of the regional contribution, the total BC amount transported to the observation site, characterized by

1 the EEI (EEI_{total}) in this study, increased under more polluted condition. Table 1 shows that the EEI_{total} was 4.6 times higher
2 during the polluted period than during the clean period, ~~revealed-revealing that-regional transport of~~ polluted air mass brought
3 more BC to Beijing. BC concentration in the site strongly depends on both total BC amount (transported from local Beijing
4 and other regions, characterized by EEI_{total} in this study) and local meteorology. Table 1 shows that the BC concentrations from
5 the clean period to the polluted period increase by ~ 7.4 times. The increase of EEI_{total} (~ 4.6 times) accounted for $\sim 62\%$ the
6 increase in BC mass concentrations (~ 7.4 times). This indicated that the adverse local meteorology contributed $\sim 38\%$ of the
7 increase in BC mass concentration in the site from the clean period to the polluted period. Compared with regional transport,
8 less effect of adverse local meteorology might be attributed to relatively small areas defined as the local region (i.e., Beijing)
9 in this study. Polluted events in China always occur over a large region, e.g., North China Plain (Yang et al., 2017; Zheng et
10 al., 2015). For our case, the adverse meteorology during polluted days in the whole large region including Beijing and other
11 areas can lead to the increase of pollutants and then more transport of pollutants into Beijing. Yang et al. (2017) found that the
12 increases in BC concentration under polluted conditions over the North China Plain (including Beijing and other adjacent
13 areas) is dominated by its local emissions due to adverse meteorology. This ~ 4.6 fold increase in EEI_{total} accounted for 62% of
14 the ~ 7.4 fold increase in BC mass concentrations from the clean period to the polluted period, suggesting that the BC from
15 adjacent areas with regional transport of polluted air mass increased BC mass concentrations in Beijing, rather than merely
16 adverse local meteorology (e.g., lower planetary boundary layer (PBL) and wind speed).

17 Under different pollution levels, regional transport not only influenced the BC mass concentrations but also the BC aging
18 process and timescale. Table 1 shows that the mass-average value of the aging degree (i.e., the D_p/D_c ratio) of BC-containing
19 particles at our site was ~~~ 2.79~~ 04 during the polluted period, significantly higher than that observed during the clean period
20 (~~~ 2.07~~ 1.62) and slightly polluted period (~~~ 2.37~~ 1.81). On one hand, under more polluted conditions, more BC-containing
21 particles in Beijing were from regional sources and thus had undergone a longer aging time during the transport than the BC
22 from local sources in Beijing. On the other hand, compared with the BC carried in the clean air mass from the northwest of
23 Beijing during the clean period (Fig. 4a5a), the BC-containing particles in the polluted air mass undergoing regional transport
24 from the region south of Beijing (i.e., Hebei, one of the most polluted provinces in China with high pollutant emission) during
25 the polluted period ~~exhibited higher aging rates~~ (Fig. 4e5c) ~~(Peng et al., 2015).~~ Peng et al. (2015) pointed out higher BC aging
26 rates under more polluted environments, indicating that BC-containing particles passing through polluted regions would show
27 higher aging rates during atmospheric transport than that from clean regions. The mass-average values of calculated E_{ab} values
28 of the-for BC-containing particles observed at our site were ~~~ 1.90~~ 1.66, ~~~ 2.06~~ 1.81 and ~~~ 2.22~~ 1.91 during the clean, slightly
29 polluted and polluted periods, respectively (Table 1), showing that the theoretical light absorption capability of BC-containing
30 particles observed at our site increased with increasing regional contributions. Our results demonstrated the importance of
31 regional transport in the enhancement of BC light absorption capability associated with air pollution.

32 To further explore the importance of aging during regional transport, its contributions were compared with those of local
33 chemical processes with respect to increases in D_p/D_c ratio~~aging degree~~ and theoretical light absorption capability of BC-

1 containing particles associated with air pollution. Considering the formation of coating materials on BC surface is dominated
2 by photochemical oxidation (Metcalf et al., 2013; Peng et al., 2015), we evaluated the contribution of local photochemical
3 production by the changes of O_3 concentrations in the atmosphere. On the other hand, the changes in the amount of BC from
4 regional transport was characterized by variation of EEI_{total} , which was used to evaluate the contributions of regional transport
5 to BC aging, we used the variation of EEI_{total} per hour to evaluate the contributions of aging during regional transport, taking
6 more EEI_{total} more BC from regional transport into account. Figure 5a shows that the EEI_{total} per hour exhibited a temporal
7 coherence with the mass-averaged values of e-the D_p/D_c ratio and the calculated E_{ab} of BC-containing particles. In contrast,
8 the O_3 concentrations showed a different temporal trend. When PM_{10} concentrations were higher than $\sim 120 \mu g m^{-3}$, O_3
9 concentrations decreased to ~ 2 ppb. Zheng et al. (2015) has demonstrated the weakened importance of photochemistry in the
10 production and aging of secondary aerosols in Beijing under polluted conditions due to decrease of oxidant concentrations.
11 This indicated that the photochemical processing in BC aging may be weakened under higher polluted levels (i.e., $PM_{10} > 120 \mu g$
12 m^{-3}). Noted that photochemical processing is not the only possible pathway in BC aging process and other pathways were not
13 discussed in this study. The local aging process of BC might be enhanced by other pathways. For example, high concentrations
14 of aerosols under polluted environment may compensate the adverse photochemical conditions for BC aging. Therefore
15 In
16 summary, the increases in the aging degree and theoretical light absorption capability of BC-containing particles with
increasing air pollution were more likely caused by aging during regional transport than by local photochemical production.

17 According to the evolution of the EEI_{total} values and O_3 concentrations with increasing air pollution levels (Fig. 5b1 and
18 Fig.5b2), we separated the pollution levels into two periods. When PM_{10} concentrations were lower than $\sim 120 \mu g m^{-3}$ and rBC
19 mass concentrations were lower than $\sim 6 \mu g m^{-3}$, the normalized EEI_{total} increased from ~ 3 to ~ 18 with increasing air pollution
20 levels, and the O_3 concentrations decreased from ~ 20 ppb to ~ 2 ppb, indicating enhanced regional contributions and weakened
21 local photochemical production at observation site. In this period, Fig. 5b3 and Fig. 5b4 show that the mass-averaged values
22 of calculated E_{ab} and the D_p/D_c ratio of BC-containing particles increased from ~ 1.96 to ~ 2.219 and from ~ 2.216 to ~ 2.820 ,
23 respectively, with the increase in the normalized EEI_{total} (from ~ 3 to 18) and the decrease in the O_3 concentrations (from ~ 20
24 to 2 ppb). Therefore, in terms of the increase in the BC light absorption capability with increasing air pollution levels, this
25 period (i.e., conditions of $PM_{10} < 120 \mu g m^{-3}$ and rBC $< 6 \mu g m^{-3}$) represented a regional transport-controlled period. The increase
26 in calculated E_{ab} , BC light absorption capability of BC-containing particles (~ 1.96 - 2.219) during this regional transport-
27 controlled period accounted for $\sim 78.75\%$ of the increase in BC-calculated E_{ab} , light absorption capability (~ 1.96 - 2.30) with
28 increasing air pollution during the whole campaign period. Therefore, the aging process during the regional transport
29 dominated the increase in the theoretical light absorption capability of BC-containing particles in Beijing during the campaign
30 period. Another period is defined by PM_{10} concentrations of more than $\sim 120 \mu g m^{-3}$ and rBC mass concentrations of more than
31 $\sim 6 \mu g m^{-3}$, during which both the EEI_{total} and O_3 concentrations showed slight changes with increasing air pollution levels. In
32 this period, the increase in calculated E_{ab} , BC light absorption capability of BC-containing particles (from ~ 2.219 to ~ 2.30)
33 might be attributed to local heterogeneous chemical production in Beijing.

1 3.4 Implications for BC radiative forcing

2 The increase in BC light absorption capability with increasing air pollution levels suggests that greater solar absorption (i.e.,
3 direct radiative forcing (DRF)) by atmospheric BC occurs under more polluted conditions. The DRF of atmospheric BC-
4 containing particles depends not only on the BC mass concentrations but also on the BC forcing efficiency, which strongly
5 depends on the light absorption capability of BC-containing particles. In this study, the forcing efficiency of BC-containing
6 particles was estimated based on a simple radiation transfer model (Eq. (9)). Figure 6 shows that with increasing pollution
7 levels (i.e., PM_{10} increasing from $\sim 10 \mu g m^{-3}$ to $\sim 230 \mu g m^{-3}$) during the campaign period, the mass-averaged values of
8 calculated MAC at 550 nm for BC-containing particles increased from $\sim 11 m^2 g^{-1}$ to $\sim 14 m^2 g^{-1}$, which resulted in the SFE of
9 BC-containing particles increasing from $\sim 0.7 m^2 g^{-1} nm^{-1}$ to $\sim 0.9 m^2 g^{-1} nm^{-1}$, the SFE of BC-containing particles at 550 nm
10 increased from $\sim 0.8 m^2 g^{-1} nm^{-1}$ to $\sim 1.0 m^2 g^{-1} nm^{-1}$ due to the increase in MAC at 550 nm in the range of $\sim 12-15 m^2 g^{-1}$ with
11 increasing pollution levels (i.e., PM_{10} increasing from $\sim 10 \mu g m^{-3}$ to $\sim 230 \mu g m^{-3}$) during the campaign period. Meanwhile, the
12 DRF of BC-containing particles increased from $\sim 0.51 W m^{-2}$ to $\sim 0.63-61 W m^{-2}$ (Fig. 7c), revealing the importance of BC in
13 terms of solar absorption under more polluted conditions. In this case, the failure to consider the increase in BC light absorption
14 capability with increasing air pollution levels may cause ~~significant~~ underestimation of the radiative forcing of BC-containing
15 particles in Beijing under polluted conditions. Noted that DRF calculation shown in Fig. 7c did not consider the changes of
16 total BC amount -to point out the effect of BC light-absorption capability on DRF under different PM_{10} concentrations.

17 Fig. 7c shows the DRF of BC increased by $\sim 18\%$ during the polluted period compared with that during the clean period.
18 Meanwhile, the BC mass concentration increased by ~ 7 times (Table 1). If assuming the DRF of BC during the clean period
19 to be $\sim 0.5 W m^{-2}$ based on calculation shown in Fig. 7c, it would increase to $\sim 4 W m^{-2}$ under polluted conditions, taking the
20 increase in both of the mass concentration and theoretical absorption capability of BC.

21 The enhanced climate effects of BC aerosols in Beijing could be taken to be representative of polluted regions in China.
22 Previous measurements of BC aerosols in China (Zheng et al., 2015; Wang et al., 2014b; Zhao et al., 2017; Gong et al., 2016;
23 Huang et al., 2013; Andreae et al., 2008; Zhang et al., 2014) showed that the BC mass concentrations in different regions (e.g.,
24 Beijing, Xi'an, Nanjing, Shanghai and Guangzhou) reached values of $\sim 10-50 \mu g m^{-3}$ during polluted periods (Table ~~S1~~S2),
25 similar to our measurements. Therefore, our BC aerosol observations in Beijing were not a special case. In China, high
26 concentrations of BC aerosols under polluted conditions always occur on a regional scale due to intense BC emissions (Zhang
27 et al., 2009; Li et al., 2017) and significant regional transport (Zheng et al., 2015; Wang et al., 2014a; Zhao et al., 2013). Our
28 findings in Beijing can provide some implication in the difference of BC radiative forcing in other regions among different air
29 pollution levels.

30 4 Discussion: breaking the amplification effect by emission control

31 Our results reveal that under more polluted environment, the BC-containing particles are characterized by more BC mass

1 concentrations and more coating materials on BC surface and therefore higher light absorption ~~capacity~~. As shown
2 in Fig. 7, this amplification effect on BC light absorption associated with air pollution is caused by increasing BC
3 concentration and at the same time enhanced light absorption ~~capacity~~ of BC-containing particles by more coating
4 production speeding up the coating processes in the more polluted air. Variation of both the mass concentration and light
5 absorption capability of BC associated with air pollution strongly depend on the air pollutant emission (e.g., BC, SO₂, NO_x
6 and VOC). Under polluted environment, polluted air mass from high emission areas not only brings more BC, but also more
7 coating materials accelerates the production of coating materials on BC surface due to more precursors of secondary
8 components.

9 Air pollution control measures may, on the other hand, break this amplification effect by reducing BC concentration and
10 at the same time lowering the light absorption ~~capacity~~ of BC-containing particles by slowing down the coating
11 processes with a cleaner air (Fig. 7). Take air pollution controls during the 2014 Asia-Pacific Economic Cooperation meeting
12 (APEC) in Beijing, China as an example, we found that as a result of emission controls on local Beijing and areas adjacent to
13 Beijing (i.e., Hebei, Tianjin, Shanxi, Henan, Shandong and Inner Mongolia), light absorption of BC-containing particles
14 decreased by significantly during APEC compared to that of before APEC under ~~similar meteorological~~ polluted conditions
15 (Zhang et al., 2018, ~~in prep~~). This is not only contributed by a reduction of BC mass concentration, but also by lower light
16 absorption ~~capacity~~ of BC-containing particles with less coating materials on BC surface in cleaner atmosphere
17 conditions, indicating that synergetic emission reduction of multi-pollutants could achieve co-benefits of both air quality and
18 climate.

19 5 Conclusions

20 The light absorption of BC-containing particles depends not only on the BC mass concentration but also on their light
21 absorption capability (~~i.e., characterized by the calculated~~ MAC and E_{ab} in this study). In this work, we investigated the
22 difference of theoretical BC light absorption capability of BC under different air pollution conditions. During an intensive field
23 measurement campaign in Beijing, China, we found that with increasing pollution levels, the increase in BC mass
24 concentration was always accompanied by an increase in the theoretical light absorption capability of BC, resulting an
25 amplification effect on the light absorption of the ambient BC-containing particles. During the campaign period, the hourly
26 values of mass-weighted averages of the D_p/D_c ratio and calculated E_{ab} for BC-containing particles was in the range of 1.5-2.3
27 and 1.5-2.0, respectively. When PM₁ concentration increased from $\sim 10 \mu\text{g m}^{-3}$ to $\sim 230 \mu\text{g m}^{-3}$ accompanied with the rBC mass
28 concentration in the range of $\sim 0.37\text{-}12\text{-}11 \mu\text{g m}^{-3}$, the mass-weighted averages of the D_p/D_c ratio and calculated E_{ab} values
29 increased by $\sim 33\%$ and $\sim 18\%$, respectively. ~~the BC-containing particles with $\sim 75\text{-}200$ nm rBC cores measured by SP2~~
30 ~~techniques showed an increase of 28-48% in the BC aging degree (i.e., the D_p/D_c ratio). According to Mie theory with a shell-~~
31 ~~and core model, the 28-48% increase in the BC aging degree associated with air pollution could enhance the BC light~~

1 ~~absorption capability (i.e., MAC and E_{ab}) by 13–36%~~. The increase in BC light absorption capability associated with increasing
2 air pollution can be explained by the increase in coating materials on the BC surface under more polluted conditions. Moreover,
3 the increase of the D_p/D_c ratio and calculated E_{ab} with increasing air pollution levels was size-dependent, namely more increase
4 was exhibited for smaller rBC cores. This indicated that the aging degree and light absorption capability of smaller rBC was
5 more sensitive to air pollution levels. Using a semiquantitative analysis method based on the diffusion-controlled growth law
6 (Seinfeld and Pandis 2006), we also calculated the theoretical increase in the D_p/D_c ratio and calculated E_{ab} with increasing
7 pollution levels for BC-containing particles with size-resolved rBC cores. The agreement between the measured and theoretical
8 increase in the D_p/D_c ratio and E_{ab} indicated the increase of coating materials on BC surface with increasing PM_{10} concentrations
9 following the diffusion-controlled growth law.

10 During the campaign period, ~~the~~ relationships between the growth-changing rate of calculated E_{ab} , ~~the BC light absorption~~
11 ~~capability ($k_{E_{ab}}$)~~ with air pollution development and that of the PM_{10} and rBC concentrations ($k_{PM_{10}}$ and k_{rBC} , respectively) were
12 estimated: $k_{E_{ab}} \approx 4.8\% \cdot 0.051 \cdot k_{PM_{10}}$, and $k_{E_{ab}} \approx 2.5\% \cdot 0.027 \cdot k_{rBC}$. During the campaign period, $k_{E_{ab}}$ values were in the range of -
13 4%–4% h^{-1} , with a peak of frequency distribution around zero, indicating that the BC-containing particles were shrinking as
14 often as they were growing. The frequency distribution of $k_{E_{ab}}/k_{PM_{10}}$ ratio showed that a peak value around 0.05, revealing that
15 the change of calculated E_{ab} was not sensitive to variations in PM_{10} concentrations. When pollution levels sharply increased
16 with a $k_{PM_{10}}$ of 107.6% h^{-1} and a k_{rBC} of 130.9% h^{-1} , the $k_{E_{ab}}$ increased by as much as 7.3% h^{-1} . Although the growth-changing
17 rate of the BC light absorption capability was significantly lower than that of the BC mass concentration, the effect of enhanced
18 BC light absorption capability on the light absorption of ambient BC-containing particles under polluted conditions is not
19 negligible. In our case, if we had not considered the increase in the theoretical BC light absorption capability of BC with
20 increasing air pollution during the campaign period, the theoretical light absorption of BC-containing particles under polluted
21 conditions would have been underestimated by ~~~28~~ 18%.

22 The increase in BC light absorption capability with increasing pollution levels in Beijing was controlled by aging during
23 regional transport. The EEI analysis showed that ~63% of the BC observed at our site was transported from regional sources
24 (i.e., areas adjacent to outside of Beijing) during the polluted period, whereas the regional contributions were significantly
25 lower (~21%) during the clean period. More BC in more polluted air from regional transport could lead to a higher local BC
26 concentration in Beijing. Not only more BC but also more coatings are carried into Beijing by more polluted regional air mass
27 (Fig. 7–8 (a)), which can be explained by more coating precursors (e.g. SO_2 , NO_x and VOC) speeding up coating process (i.e.,
28 the production of coating materials on BC surface by photochemistry and heterogeneous chemistry during regional transport)
29 in a more polluted air. Moreover, we separated the change of the D_p/D_c ratio-aging degree and theoretical light absorption
30 capability of BC associated with air pollution into regional transport-controlled region-period (i.e., $PM_{10} < 120 \mu g m^{-3}$ and BC
31 $< 6 \mu g m^{-3}$) and local chemistry-controlled region-period (i.e., $PM_{10} > 120 \mu g m^{-3}$ and BC $> 6 \mu g m^{-3}$). In the regional transport-
32 controlled region-period, the mass-averaged values of D_p/D_c and calculated E_{ab} of BC-containing particles in Beijing increased
33 from ~~~2.2~~ 1.6 and ~~~1.9~~ to 2.8 and from ~1.6 to ~2.2, respectively, with increasing pollution levels. The further increase ~~of~~

1 in mass-averaged values of D_p/D_c ($\sim 2.82.0$ to $\sim 3.02.2$) and calculated E_{ab} ($\sim 2.21.9$ to $\sim 2.32.0$) associated with air pollution is
2 harder and is mostly likely attributed to local chemical production ~~by heterogeneous chemistry~~. Therefore, we attributed
3 $\sim 7875\%$ of the increase in theoretical BC light absorption capability of BC with increasing air pollution during the campaign
4 period to aging during regional transport, demonstrating the regional transport has an important influence on the variations of
5 light absorption capability of BC-containing particles in Beijing under different pollution levels.

6 Due to the increase in BC light absorption capability with increasing air pollution levels, stronger forcing efficiency of the
7 BC-containing particles was found under more polluted conditions. During the campaign period, the BC forcing efficiency
8 increased by $\sim 2018\%$ with PM_{10} increasing from $10 \mu g m^{-3}$ to $230 \mu g m^{-3}$, ~~while~~ Considering the increasing in both of BC
9 forcing efficiency and BC mass concentration, the DRF values of ambient BC-containing particles could increase from ~ 0.54
10 $W m^{-2}$ during the clean period to ~ 0.634 $W m^{-2}$ under polluted conditions. The results identified that BC in more polluted
11 environment exhibited a larger DRF radiative forcing, which was caused not only by the increase of BC mass concentrations
12 but also by the enhancement of BC light absorption capability.

13 The amplification effect on BC DRF due to the increase of BC light absorption capability introduced in this work not only
14 concerns in Beijing but is also likely to operate in other polluted regions in China. The amplification effect not only could
15 increase the direct contribution of BC to air pollution and climate change due to more light absorption, but also would enhance
16 the indirect contribution by stronger aerosol-meteorology and aerosol-climate feedbacks. Our finds in this work can provide
17 some implication in the difference of BC-related effect on air quality and climate under different air pollution conditions (e.g.,
18 air clean and polluted environment) due to change in BC light absorption capability associated with air pollution.

19 The air pollution control may break the amplification effect by reducing BC concentration and at the same time lower the
20 light absorption ~~capacity~~ capability of BC-containing particles by slowdown the coating processes with a cleaner air. Thereby,
21 breaking the amplification effect by emission control would achieve a co-benefit effect by simultaneous mitigation of air
22 pollution and climate change. Further study will focus on if and how emission reduction of BC and other pollutants in China
23 will break the amplification effect.

24 **Acknowledgments**

25 This work was supported by the National Natural Science Foundation of China (41625020, 41571130032 and 91644218) and
26 the Guangdong “Pearl River Talents Plan” (2016ZT06N263).

27 **References**

28 Andreae, M. O., Schmid, O., Yang, H., Chand, D., Zhen Yu, J., Zeng, L.-M., and Zhang, Y.-H.: Optical properties and chemical
29 composition of the atmospheric aerosol in urban Guangzhou, China, *Atmos. Environ.*, 42, 6335-6350, 2008.

1 Bond, T. C., and Bergstrom, R. W.: Light Absorption by Carbonaceous Particles: An Investigative Review, *Aerosol Sci.*
2 *Technol.*, 40, 27-67, 2006.

3 Bond, T. C., Habib, G., and Bergstrom, R. W.: Limitations in the enhancement of visible light absorption due to mixing state,
4 *J. Geophys. Res.-Atmos.*, 111, 2006.

5 Cappa, C. D., Onasch, T. B., Massoli, P., Worsnop, D. R., Bates, T. S., Cross, E. S., Davidovits, P., Hakala, J., Hayden, K. L.,
6 Jobson, B. T., Kolesar, K. R., Lack, D. A., Lerner, B. M., Li, S.-M., Mellon, D., Nuaaman, I., Olfert, J. S., Petäjä, T., Quinn, P.
7 K., Song, C., Subramanian, R., Williams, E. J., and Zaveri, R. A.: Radiative Absorption Enhancements Due to the Mixing State
8 of Atmospheric Black Carbon, *Science*, 337, 1078-1081, 2012.

9 Chen, Y., and Bond, T. C.: Light absorption by organic carbon from wood combustion, *Atmos. Chem. Phys.*, 10, 1773-1787,
10 2010.

11 Cheng, Y. F., Eichler, H., Wiedensohler, A., Heintzenberg, J., Zhang, Y. H., Hu, M., Herrmann, H., Zeng, L. M., Liu, S., Gnauk,
12 T., Brüggemann, E., and He, L. Y.: Mixing state of elemental carbon and non-light-absorbing aerosol components derived from
13 in situ particle optical properties at Xinken in Pearl River Delta of China, *J. Geophys. Res.-Atmos.*, 111, 2006.

14 Cheng, Y. F., Heintzenberg, J., Wehner, B., Wu, Z. J., Su, H., Hu, M., and Mao, J. T.: Traffic restrictions in Beijing during the
15 Sino-African Summit 2006: aerosol size distribution and visibility compared to long-term in situ observations, *Atmos. Chem.*
16 *Phys.*, 8, 7583-7594, 2008.

17 Cheng, Y. F., Su, H., Rose, D., Gunthe, S. S., Berghof, M., Wehner, B., Achtert, P., Nowak, A., Takegawa, N., Kondo, Y.,
18 Shiraiwa, M., Gong, Y. G., Shao, M., Hu, M., Zhu, T., Zhang, Y. H., Carmichael, G. R., Wiedensohler, A., Andreae, M. O., and
19 Pöschl, U.: Size-resolved measurement of the mixing state of soot in the megacity Beijing, China: diurnal cycle, aging and
20 parameterization, *Atmos. Chem. Phys.*, 12, 4477-4491, 2012.

21 Chylek, P., and Wong, J.: Effect of absorbing aerosols on global radiation budget, *Geophys. Res. Lett.*, 22, 929-931, 1995.

22 Drinovec, L., Močnik, G., Zotter, P., Prévôt, A., Ruckstuhl, C., Coz, E., Rupakheti, M., Sciare, J., Müller, T., and Wiedensohler,
23 A.: The " dual-spot" Aethalometer: an improved measurement of aerosol black carbon with real-time loading compensation,
24 *Atmos. Meas. Tech.*, 8, 1965-1979, 2015.

25 Fuller, K. A., Malm, W. C., and Kreidenweis, S. M.: Effects of mixing on extinction by carbonaceous particles, *J. Geophys.*
26 *Res.-Atmos.*, 104, 15941-15954, 1999.

27 Gao, R. S., Schwarz, J. P., Kelly, K. K., Fahey, D. W., Watts, L. A., Thompson, T. L., Spackman, J. R., Slowik, J. G., Cross, E.
28 S., Han, J. H., Davidovits, P., Onasch, T. B., and Worsnop, D. R.: A Novel Method for Estimating Light-Scattering Properties
29 of Soot Aerosols Using a Modified Single-Particle Soot Photometer, *Aerosol Sci. Technol.*, 41, 125-135, 2007.

30 Gong, X., Zhang, C., Chen, H., Nizkorodov, S. A., Chen, J., and Yang, X.: Size distribution and mixing state of black carbon
31 particles during a heavy air pollution episode in Shanghai, *Atmos. Chem. Phys.*, 16, 5399-5411, 2016.

32 Gustafsson, Ö., and Ramanathan, V.: Convergence on climate warming by black carbon aerosols, *Proc. Natl. Acad. Sci. USA*,
33 113, 4243-4245, 2016.

1 Guo, S., Hu, M., Zamora, M. L., Peng, J., Shang, D., Zheng, J., Du, Z., Wu, Z., Shao, M., Zeng, L., Molina, M. J., and Zhang,
2 R.: Elucidating severe urban haze formation in China, *Proc. Natl. Acad. Sci. USA*, 111, 17373-17378, 2014.

3 Gysel, M., Laborde, M., Olfert, J. S., Subramanian, R., and Gröhn, A. J.: Effective density of Aquadag and fullerene soot black
4 carbon reference materials used for SP2 calibration, *Atmos. Meas. Tech.*, 4, 2851-2858, 2011.

5 Huang, X.-F., Xue, L., Tian, X.-D., Shao, W.-W., Sun, T.-L., Gong, Z.-H., Ju, W.-W., Jiang, B., Hu, M., and He, L.-Y.: Highly
6 time-resolved carbonaceous aerosol characterization in Yangtze River Delta of China: Composition, mixing state and
7 secondary formation, *Atmos. Environ.*, 64, 200-207, 2013.

8 Jacobson, M. Z.: A physically-based treatment of elemental carbon optics: Implications for global direct forcing of aerosols,
9 *Geophys. Res. Lett.*, 27, 217-220, 2000.

10 Jacobson, M. Z.: Strong radiative heating due to the mixing state of black carbon in atmospheric aerosols, *Nature*, 409, 695-
11 697, 2001.

12 Jeong, C.-H., Herod, D., Dabek-Zlotorzynska, E., Ding, L., McGuire, M. L., and Evans, G.: Identification of the Sources and
13 Geographic Origins of Black Carbon using Factor Analysis at Paired Rural and Urban sites, *Environ. Sci. Technol.*, 47, 8462-
14 8470, 2013.

15 [Knox, A., Evans, G. J., Brook, J. R., Yao, X., Jeong, C. H., Godri, K. J., Sabaliauskas, K., and Slowik, J. G.: Mass Absorption](#)
16 [Cross-Section of Ambient Black Carbon Aerosol in Relation to Chemical Age, *Aerosol Sci. Technol.*, 2009.](#)

17 Laborde, M., Mertes, P., Zieger, P., Dommen, J., Baltensperger, U., and Gysel, M.: Sensitivity of the Single Particle Soot
18 Photometer to different black carbon types, *Atmos. Meas. Tech.*, 5, 2012.

19 Lack, D. A., and Cappa, C. D.: Impact of brown and clear carbon on light absorption enhancement, single scatter albedo and
20 absorption wavelength dependence of black carbon, *Atmos. Chem. Phys.*, 10, 4207-4220, 2010.

21 Lesins, G., Chylek, P., and Lohmann, U.: A study of internal and external mixing scenarios and its effect on aerosol optical
22 properties and direct radiative forcing, *J. Geophys. Res.-Atmos.*, 107, 5-12, 2002.

23 Li, H., Zhang, Q., Zhang, Q., Chen, C., Wang, L., Wei, Z., Zhou, S., Parworth, C., Zheng, B., Canonaco, F., Prévôt, A. S. H.,
24 Chen, P., Zhang, H., Wallington, T. J., and He, K.: Wintertime aerosol chemistry and haze evolution in an extremely polluted
25 city of the North China Plain: significant contribution from coal and biomass combustion, *Atmos. Chem. Phys.*, 17, 4751-4768,
26 2017.

27 Li, M., Zhang, Q., Kurokawa, J. I., Woo, J. H., He, K., Lu, Z., Ohara, T., Song, Y., Streets, D. G., Carmichael, G. R., Cheng,
28 Y., Hong, C., Huo, H., Jiang, X., Kang, S., Liu, F., Su, H., and Zheng, B.: MIX: a mosaic Asian anthropogenic emission
29 inventory under the international collaboration framework of the MICS-Asia and HTAP, *Atmos. Chem. Phys.*, 17, 935-963,
30 2017.

31 Liu, D., Allan, J., Whitehead, J., Young, D., Flynn, M., Coe, H., McFiggans, G., Fleming, Z. L., and Bandy, B.: Ambient black
32 carbon particle hygroscopic properties controlled by mixing state and composition, *Atmos. Chem. Phys.*, 13, 2015-2029, 2013.

1 Liu, D., Whitehead, J., Alfara, M. R., Reyes-Villegas, E., Spracklen, D. V., Reddington, C. L., Kong, S., Williams, P. I., Ting,
2 Y.-C., Haslett, S., Taylor, J. W., Flynn, M. J., Morgan, W. T., McFiggans, G., Coe, H., and Allan, J. D.: Black-carbon absorption
3 enhancement in the atmosphere determined by particle mixing state, *Nature Geosci.*, 10, 184-188, 2017.

4 Liu, S., Aiken, A. C., Gorkowski, K., Dubey, M. K., Cappa, C. D., Williams, L. R., Herndon, S. C., Massoli, P., Fortner, E. C.,
5 Chhabra, P. S., Brooks, W. A., Onasch, T. B., Jayne, J. T., Worsnop, D. R., China, S., Sharma, N., Mazzoleni, C., Xu, L., Ng,
6 N. L., Liu, D., Allan, J. D., Lee, J. D., Fleming, Z. L., Mohr, C., Zotter, P., Szidat, S., and Prévôt, A. S. H.: Enhanced light
7 absorption by mixed source black and brown carbon particles in UK winter, *Nat Commun.*, 6, 8435, 2015.

8 Lu, Z., Streets, D. G., Zhang, Q., and Wang, S.: A novel back-trajectory analysis of the origin of black carbon transported to
9 the Himalayas and Tibetan Plateau during 1996–2010, *Geophys. Res. Lett.*, 39, 2012.

10 McMeeking, G. R., Morgan, W. T., Flynn, M., Highwood, E. J., Turnbull, K., Haywood, J., and Coe, H.: Black carbon aerosol
11 mixing state, organic aerosols and aerosol optical properties over the United Kingdom, *Atmos. Chem. Phys.*, 11, 9037-9052,
12 2011.

13 Menon, S., Hansen, J., Nazarenko, L., and Luo, Y.: Climate Effects of Black Carbon Aerosols in China and India, *Science*,
14 297, 2250-2253, 2002.

15 [Metcalf, A. R., Craven, J. S., Ensberg, J. J., Brioude, J., Angevine, W., Sorooshian, A., Duong, H. T., Jonsson, H. H., Flagan,
16 R. C., and Seinfeld, J. H.: Black carbon aerosol over the Los Angeles Basin during CalNex, *J. Geophys. Res.-Atmos.*, 117,
17 \[10.1029/2011JD017255\]\(#\), 2012.](#)

18 Metcalf, A. R., Loza, C. L., Coggon, M. M., Craven, J. S., Jonsson, H. H., Flagan, R. C., and Seinfeld, J. H.: Secondary Organic
19 Aerosol Coating Formation and Evaporation: Chamber Studies Using Black Carbon Seed Aerosol and the Single-Particle Soot
20 Photometer, *Aerosol Sci. Technol.*, 47, 326-347, 2013.

21 Moffet, R. C., and Prather, K. A.: In-situ measurements of the mixing state and optical properties of soot with implications for
22 radiative forcing estimates, *Proc. Natl. Acad. Sci. USA*, 106, 11872-11877, 2009.

23 Moteki, N., and Kondo, Y.: Dependence of Laser-Induced Incandescence on Physical Properties of Black Carbon Aerosols:
24 Measurements and Theoretical Interpretation, *Aerosol Sci. Technol.*, 44, 663-675, 2010.

25 Moteki, N., Kondo, Y., Miyazaki, Y., Takegawa, N., Komazaki, Y., Kurata, G., Shirai, T., Blake, D. R., Miyakawa, T., and
26 Koike, M.: Evolution of mixing state of black carbon particles: Aircraft measurements over the western Pacific in March 2004,
27 *Geophys. Res. Lett.*, 34, 2007.

28 Park, S. H., Gong, S. L., Bouchet, V. S., Gong, W., Makar, P. A., Moran, M. D., Stroud, C. A., and Zhang, J.: Effects of black
29 carbon aging on air quality predictions and direct radiative forcing estimation, *Tellus B*, 63, 1026-1039, 2011.

30 Peng, J., Hu, M., Guo, S., Du, Z., Zheng, J., Shang, D., Levy Zamora, M., Zeng, L., Shao, M., Wu, Y.-S., Zheng, J., Wang, Y.,
31 Glen, C. R., Collins, D. R., Molina, M. J., and Zhang, R.: Markedly enhanced absorption and direct radiative forcing of black
32 carbon under polluted urban environments, *Proc. Natl. Acad. Sci. USA*, 113, 4266-4271, 2016.

1 Ram, K., and Sarin, M. M.: Absorption Coefficient and Site-Specific Mass Absorption Efficiency of Elemental Carbon in
2 Aerosols over Urban, Rural, and High-Altitude Sites in India, *Environ. Sci. Technol.*, 43, 8233-8239, 2009.

3 Ramanathan, V., and Carmichael, G.: Global and regional climate changes due to black carbon, *Nature Geosci.*, 1, 221-227,
4 2008.

5 Saliba, G., Subramanian, R., Saleh, R., Ahern, A. T., Lipsky, E. M., Tasoglou, A., Sullivan, R. C., Bhandari, J., Mazzoleni, C.,
6 and Robinson, A. L.: Optical properties of black carbon in cookstove emissions coated with secondary organic aerosols:
7 Measurements and modeling, *Aerosol Sci. Technol.*, 50, 1264-1276, 2016.

8 Sandradewi, J., Prévôt, A. S., Szidat, S., Perron, N., Alfarra, M. R., Lanz, V. A., Weingartner, E., and Baltensperger, U.: Using
9 aerosol light absorption measurements for the quantitative determination of wood burning and traffic emission contributions
10 to particulate matter, *Environ. Sci. Technol.*, 42, 3316-3323, 2008.

11 Schnaiter, M., Linke, C., Möhler, O., Naumann, K. H., Saathoff, H., Wagner, R., Schurath, U., and Wehner, B.: Absorption
12 amplification of black carbon internally mixed with secondary organic aerosol, *J. Geophys. Res.-Atmos.*, 110, 2005.

13 Schwarz, J. P., Gao, R. S., Fahey, D. W., Thomson, D. S., Watts, L. A., Wilson, J. C., Reeves, J. M., Darbeheshti, M.,
14 Baumgardner, D. G., Kok, G. L., Chung, S. H., Schulz, M., Hendricks, J., Lauer, A., Kärcher, B., Slowik, J. G., Rosenlof, K.
15 H., Thompson, T. L., Langford, A. O., Loewenstein, M., and Aikin, K. C.: Single-particle measurements of midlatitude black
16 carbon and light-scattering aerosols from the boundary layer to the lower stratosphere, *J. Geophys. Res.-Atmos.*, 111, 2006.

17 Sedlacek, A. J., Lewis, E. R., Kleinman, L., Xu, J., and Zhang, Q.: Determination of and evidence for non-core-shell structure
18 of particles containing black carbon using the Single-Particle Soot Photometer (SP2), *Geophys. Res. Lett.*, 39, 2012.

19 Segura, S., Estellés, V., Titos, G., Lyamani, H., Utrillas, M. P., Zotter, P., Prévôt, A. S. H., Močnik, G., Alados-Arboledas, L.,
20 and Martínez-Lozano, J. A.: Determination and analysis of in situ spectral aerosol optical properties by a multi-instrumental
21 approach, *Atmos. Meas. Tech.*, 7, 2373-2387, 2014.

22 [Seinfeld, J. H., and Pandis, S. N.: Atmospheric Chemistry and Physics: From Air Pollution to Climate Change, 2nd ed. John](#)
23 [Wiley & Sons, Inc., New York, 2006.](#)

24 Shiraiwa, M., Kondo, Y., Iwamoto, T., and Kita, K.: Amplification of Light Absorption of Black Carbon by Organic Coating,
25 *Aerosol Sci. Technol.*, 44, 46-54, 2010.

26 Shiraiwa, M., Kondo, Y., Moteki, N., Takegawa, N., Miyazaki, Y., and Blake, D. R.: Evolution of mixing state of black carbon
27 in polluted air from Tokyo, *Geophys. Res. Lett.*, 34, 2007.

28 Sun, Y., Jiang, Q., Wang, Z., Fu, P., Li, J., Yang, T., and Yin, Y.: Investigation of the sources and evolution processes of severe
29 haze pollution in Beijing in January 2013, *J. Geophys. Res.-Atmos.*, 119, 4380-4398, 2014.

30 Taylor, J. W., Allan, J. D., Liu, D., Flynn, M., Weber, R., Zhang, X., Lefer, B. L., Grossberg, N., Flynn, J., and Coe, H.:
31 Assessment of the sensitivity of core / shell parameters derived using the single-particle soot photometer to density and
32 refractive index, *Atmos. Meas. Tech.*, 8, 1701-1718, 2015.

1 Wang, L. T., Wei, Z., Yang, J., Zhang, Y., Zhang, F. F., Su, J., Meng, C. C., and Zhang, Q.: The 2013 severe haze over southern
2 Hebei, China: model evaluation, source apportionment, and policy implications, *Atmos. Chem. Phys.*, 14, 3151-3173, 2014a.

3 Wang, Q., Huang, R. J., Cao, J., Han, Y., Wang, G., Li, G., Wang, Y., Dai, W., Zhang, R., and Zhou, Y.: Mixing State of Black
4 Carbon Aerosol in a Heavily Polluted Urban Area of China: Implications for Light Absorption Enhancement, *Aerosol Sci.*
5 *Technol.*, 48, 689-697, 2014b.

6 Weingartner, E., Saathoff, H., Schnaiter, M., Streit, N., Bitnar, B., and Baltensperger, U.: Absorption of light by soot particles:
7 determination of the absorption coefficient by means of aethalometers, *J. Aerosol Sci.*, 34, 1445-1463, 2003

8 Yang, Y. R., Liu, X. G., Qu, Y., An, J. L., Jiang, R., Zhang, Y. H., Sun, Y. L., Wu, Z. J., Zhang, F., Xu, W. Q., and Ma, Q. X.:
9 Characteristics and formation mechanism of continuous hazes in China: a case study during the autumn of 2014 in the North
10 China Plain, *Atmos. Chem. Phys.*, 15, 8165-8178, 2015.

11 [Yang, Y., Wang, H., Smith, S. J., Ma, P.-L., and Rasch, P. J.: Source attribution of black carbon and its direct radiative forcing
12 in China, *Atmos. Chem. Phys.*, 17, 4319-4336, 2017.](#)

13 Zhang, G., Bi, X., He, J., Chen, D., Chan, L. Y., Xie, G., Wang, X., Sheng, G., Fu, J., and Zhou, Z.: Variation of secondary
14 coatings associated with elemental carbon by single particle analysis, *Atmos. Environ.*, 92, 162-170, 2014.

15 Zhang, Q., Streets, D. G., Carmichael, G. R., He, K. B., Huo, H., Kannari, A., Klimont, Z., Park, I. S., Reddy, S., Fu, J. S.,
16 Chen, D., Duan, L., Lei, Y., Wang, L. T., and Yao, Z. L.: Asian emissions in 2006 for the NASA INTEX-B mission, *Atmos.*
17 *Chem. Phys.*, 9, 5131-5153, 2009.

18 Zhang, R., Khalizov, A. F., Pagels, J., Zhang, D., Xue, H., and McMurry, P. H.: Variability in morphology, hygroscopicity, and
19 optical properties of soot aerosols during atmospheric processing, *Proc. Natl. Acad. Sci. USA*, 105, 10291-10296, 2008.

20 [Zhang, Y., Li, X., Li, M., Zheng, Y., Geng, G., Hong, C., Li, H., Tong, D., Zhang, X., Cheng, Y., Su, H., He, K., and Zhang,
21 Q.: Reduction in black carbon light absorption due to multi-pollutant emission control during APEC China 2014, *Atmos. Chem.*
22 *Phys. Discuss.*, <https://doi.org/10.5194/acp-2018-274>, in review, 2018.](#)

23 Zhang, Y., Zhang, Q., Cheng, Y., Su, H., Kecorius, S., Wang, Z., Wu, Z., Hu, M., Zhu, T., Wiedensohler, A., and He, K.:
24 Measuring the morphology and density of internally mixed black carbon with SP2 and VTDMA: new insight into the
25 absorption enhancement of black carbon in the atmosphere, *Atmos. Meas. Tech.*, 9, 1833-1843, 2016.

26 Zhao, Q., Shen, G., Li, L., Chen, F., Qiao, Y., Li, C., Liu, Q., and Han, J.: Ambient Particles (PM10, PM2.5 and PM1.0) and
27 PM2.5 Chemical Components in Western Yangtze River Delta (YRD): An Overview of Data from 1-year Online Continuous
28 Monitoring at Nanjing, *Aerosol Sci. Eng.*, 2017.

29 Zhao, X. J., Zhao, P. S., Xu, J., Meng, W., Pu, W. W., Dong, F., He, D., and Shi, Q. F.: Analysis of a winter regional haze event
30 and its formation mechanism in the North China Plain, *Atmos. Chem. Phys.*, 13, 5685-5696, 2013.

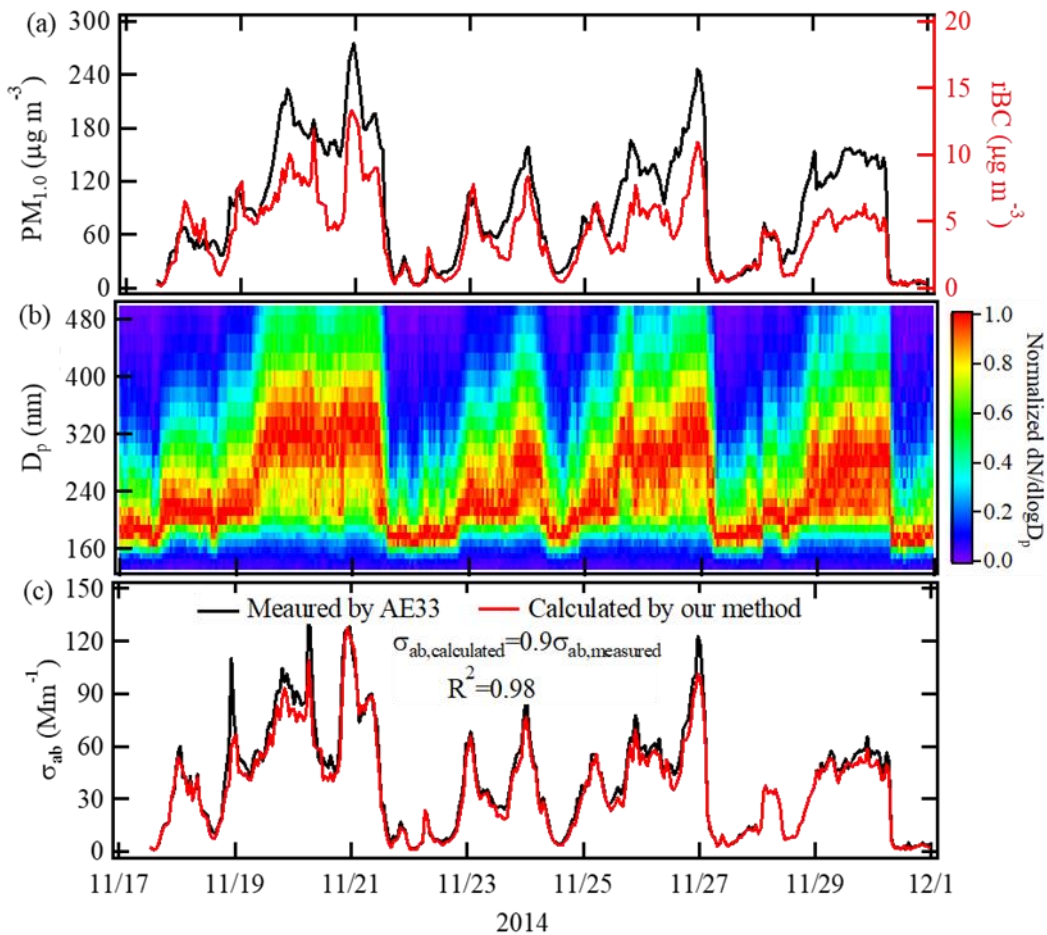
31 Zheng, G., Duan, F., Ma, Y., Zhang, Q., Huang, T., Kimoto, T., Cheng, Y., Su, H., and He, K.: Episode-Based Evolution Pattern
32 Analysis of Haze Pollution: Method Development and Results from Beijing, China, *Environ. Sci. Technol.*, 50, 4632-4641,
33 2016.

- 1 Zheng, G. J., Duan, F. K., Su, H., Ma, Y. L., Cheng, Y., Zheng, B., Zhang, Q., Huang, T., Kimoto, T., Chang, D., Pöschl, U.,
- 2 Cheng, Y. F., and He, K. B.: Exploring the severe winter haze in Beijing: the impact of synoptic weather, regional transport
- 3 and heterogeneous reactions, *Atmos. Chem. Phys.*, 15, 2969-2983, 2015.

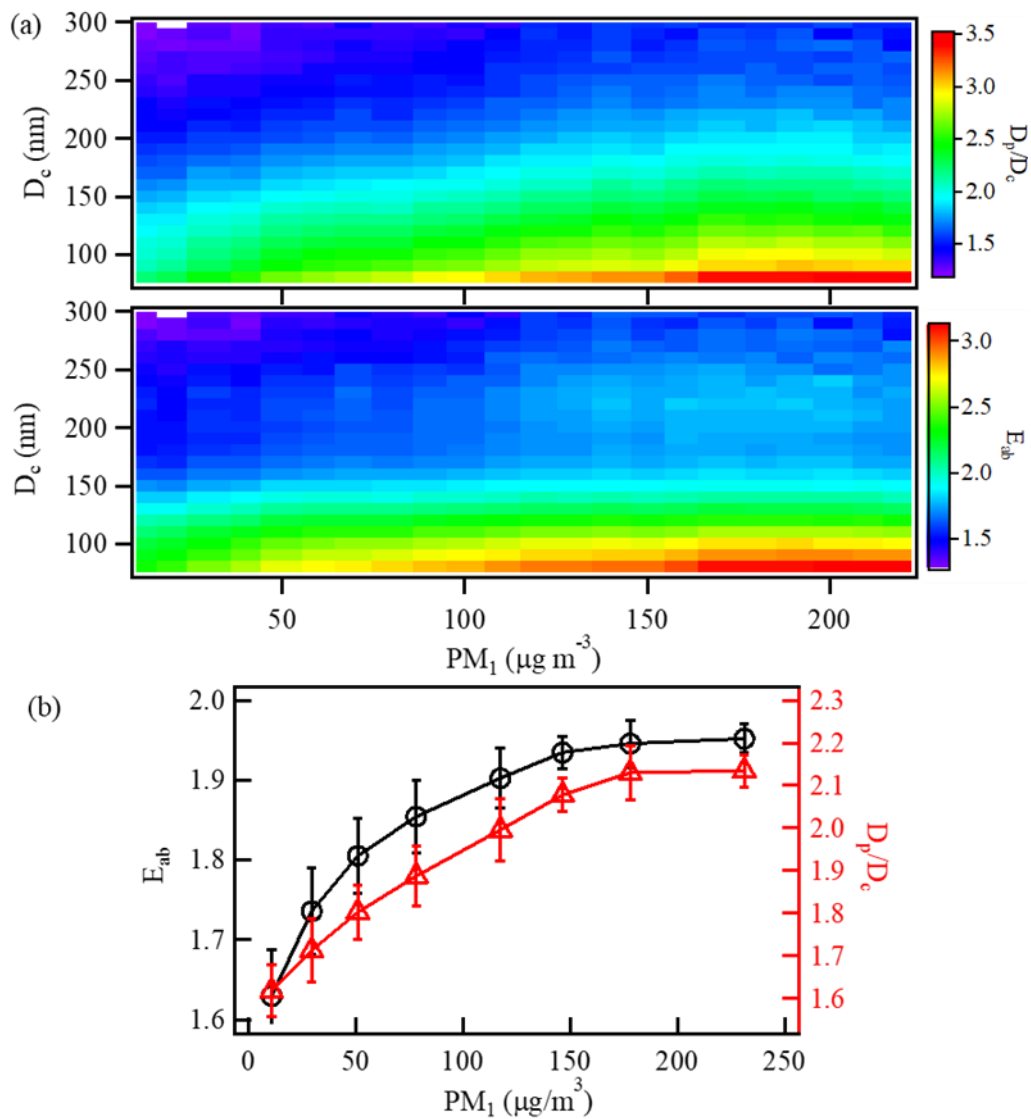
1 **Table 1.** The average PM₁ mass concentration, rBC mass concentration, normalized EEI_{total} , $EEI_{adjacent}/EEI_{total}$ ratio, the mass-
2 averaged values of the D_p/D_c ratio and calculated E_{ab} during clean, slightly polluted and polluted periods. $EEI_{adjacent}$ is the EEI
3 of BC from areas ~~adjacent to~~ outside Beijing; the ~~$EEI_{adjacent}$~~ $EEI_{outside}/EEI_{total}$ ratio reflects the amount of BC contributed by
4 regional transport to the total amount of BC observed at our site. The clean ($PM_{2.5} \leq 35 \mu g m^{-3}$), slightly polluted ($35 \mu g m^{-3} <$
5 $PM_{2.5} \leq 115 \mu g m^{-3}$) and polluted ($PM_{2.5} > 115 \mu g m^{-3}$) periods were classified according to the Air Quality Index (Zheng et al.
6 2015).

	Clean	Slightly polluted	Polluted
PM ₁ ($\mu g m^{-3}$)	12.57	54.26	141.93
rBC ($\mu g m^{-3}$)	0.82	2.89	6.07
Normalized EEI_{total}	3.68	9.19	16.87
$EEI_{adjacent}$ $EEI_{outside}/EEI_{total}$	0.21	0.39	0.63
D_p/D_c	<u>2.071.62</u>	<u>2.371.81</u>	<u>2.792.04</u>
<u>Calculated</u> E_{ab}	<u>1.901.66</u>	<u>2.061.81</u>	<u>2.221.91</u>

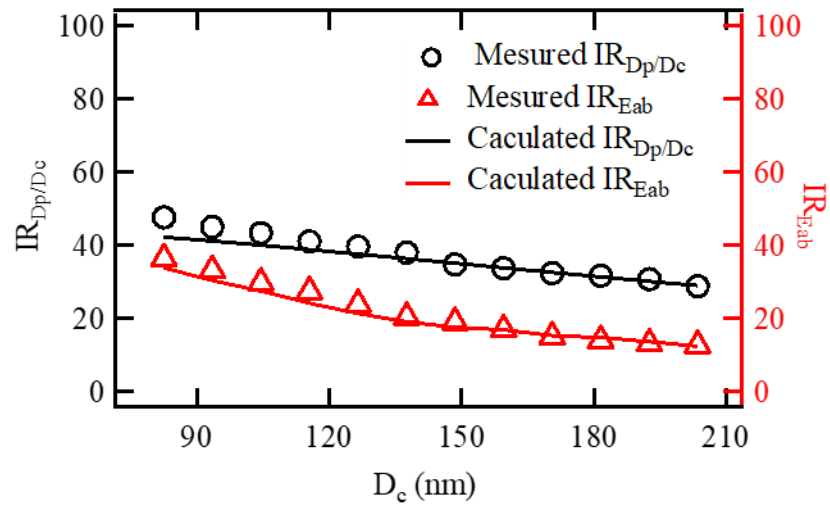
7



1
2 **Figure 1.** Time series of (a) the $PM_{1.0}$ and rBC mass concentrations, (b) the diameter of BC-containing particles (D_p) and (c)
3 the light absorption coefficient (σ_{ab}) at 880 nm. The correlation between the calculated σ_{ab} ($\sigma_{ab, \text{calculated}}$) using Mie theory
4 combined with SP2 measurements and the measured σ_{ab} ($\sigma_{ab, \text{measured}}$) by the AE33 is also shown in (c).

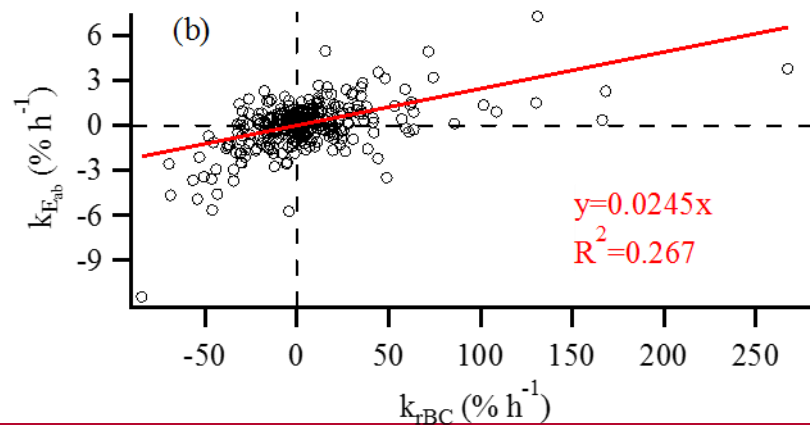
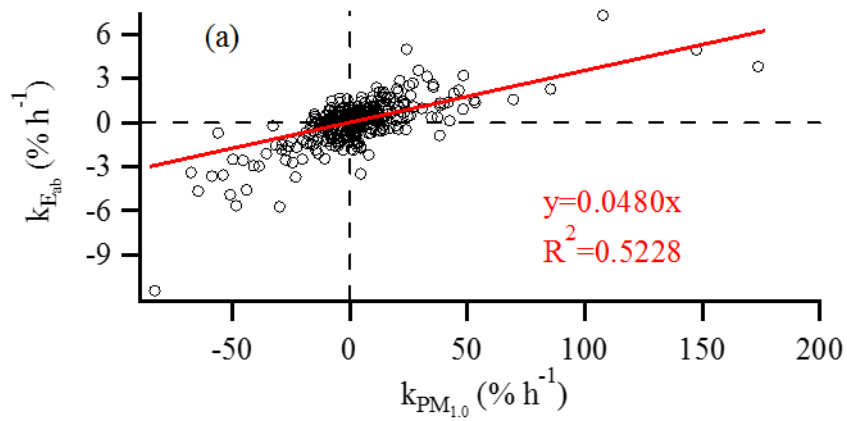


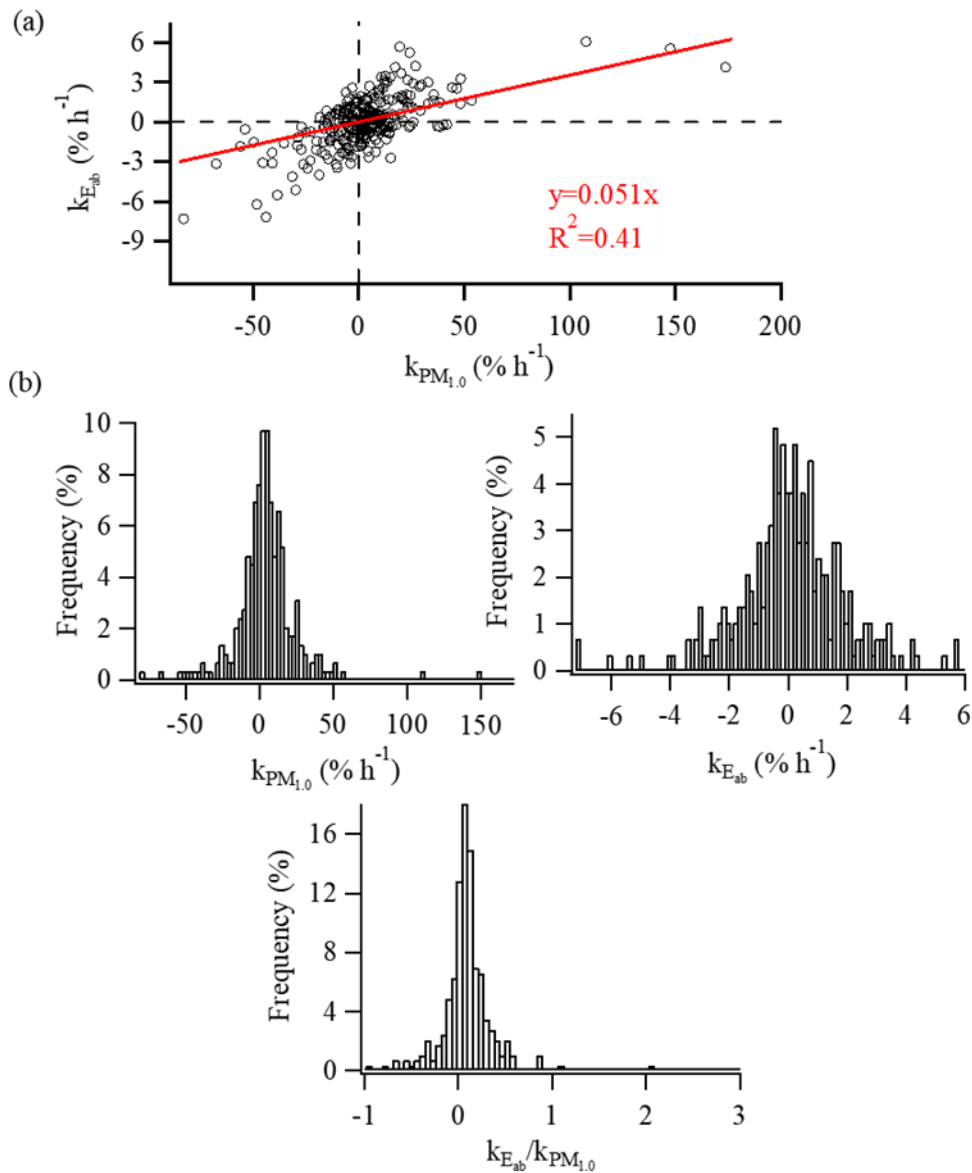
1
 2 **Figure 2.** (a) The aging degree (D_p/D_c ratio) and light absorption ~~capability-enhancement~~ (calculated E_{ab}) of BC-containing particles with
 3 size-resolved rBC cores (D_c) under different PM_1 concentration (28 samples); (b) Variations in the mass-averaged values of the D_p/D_c ratio
 4 and calculated E_{ab} of BC-containing particles with PM_1 concentration.
 5



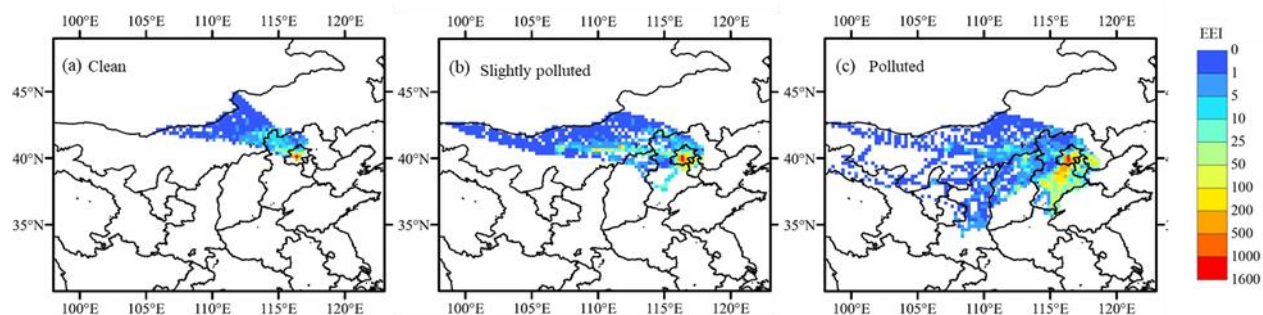
1

2 **Figure 3.** The increase ratio of the D_p/D_c and calculated E_{ab} (IR_{D_p/D_c} and $IR_{E_{ab}}$) for BC-containing particles with PM_{10}
 3 concentration increasing from $10 \mu\text{g m}^{-3}$ to $230 \mu\text{g m}^{-3}$. The calculated IR_{D_p/D_c} and $IR_{E_{ab}}$ was determined based on Eqs. (13)
 4 and (14). The measured IR_{D_p/D_c} and $IR_{E_{ab}}$ was obtained from SP2 measurements.

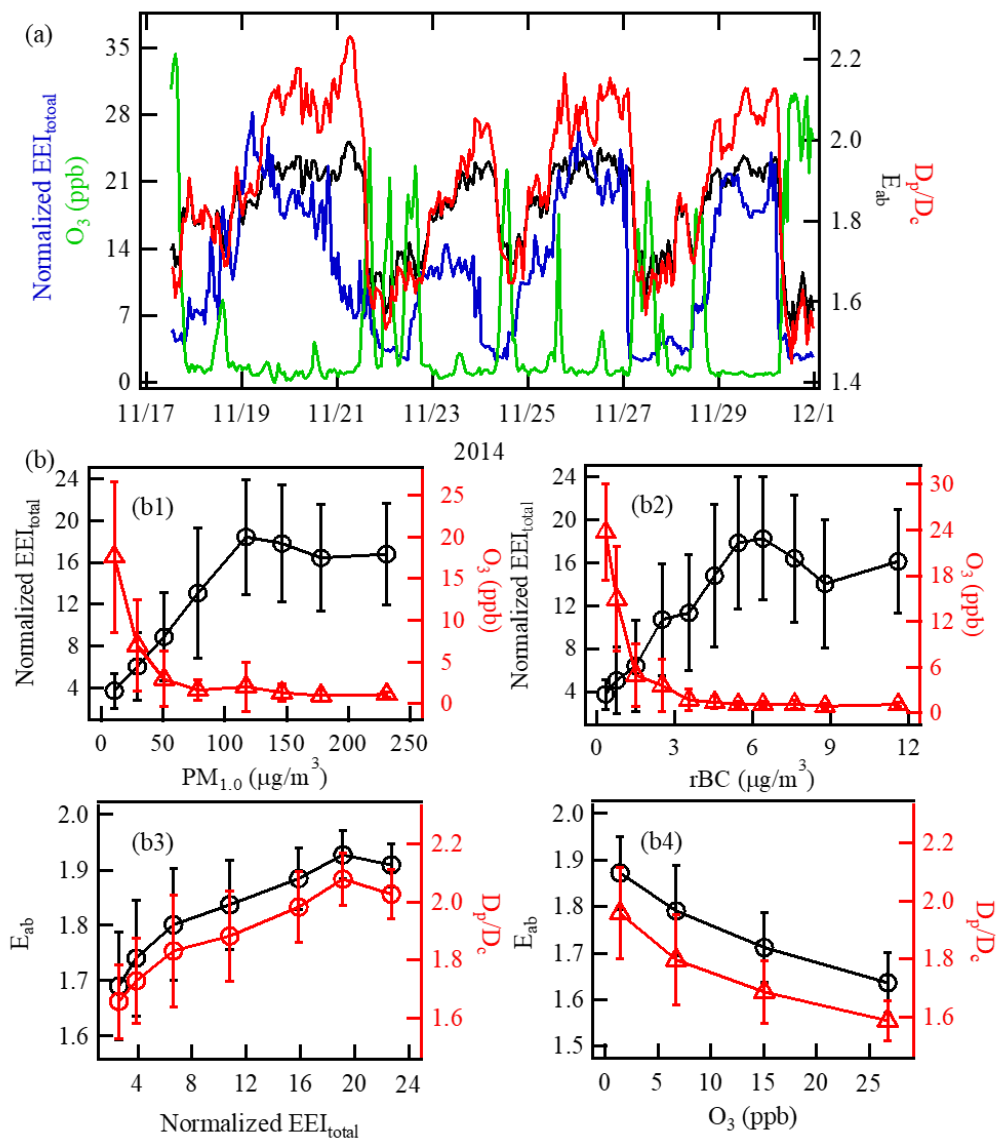




1
2 **Figure 34.** (a) Correlation between the **changing** rate of calculated E_{ab} ($k_{E_{ab}}$) and the **changing** rates of PM_1 concentrations
3 (k_{PM_1}) during the campaign period. (b) Frequency distribution of $k_{E_{ab}}$, k_{PM_1} , and $k_{E_{ab}}/k_{PM_1}$. The $k_{E_{ab}}$ and k_{PM_1} values represent
4 an apparent changing rate of calculated E_{ab} , PM_1 concentration and rBC mass concentration, respectively, and are from point-
5 by-point differences of hourly E_{ab} , namely $k_{E_{ab}} = (E_{ab,t2} - E_{ab,t1}) / (E_{ab,t1} * (t_2 - t_1))$ and $k_{PM_1} = (PM_{1,t2} - PM_{1,t1}) / (PM_{1,t1} * (t_2 - t_1))$. The
6 sensitivity of the change of calculated E_{ab} with changing PM_1 concentrations was obtained by plotting $k_{E_{ab}}$ vs. k_{PM_1} (i.e.,
7 $k_{E_{ab}}/k_{PM_1}$, the slope shown in (a)). Correlation between the growth rate of E_{ab} ($k_{E_{ab}}$) and the growth rates of PM_1 - and rBC mass
8 concentrations (k_{PM_1} and k_{rBC} , respectively) during the campaign period.

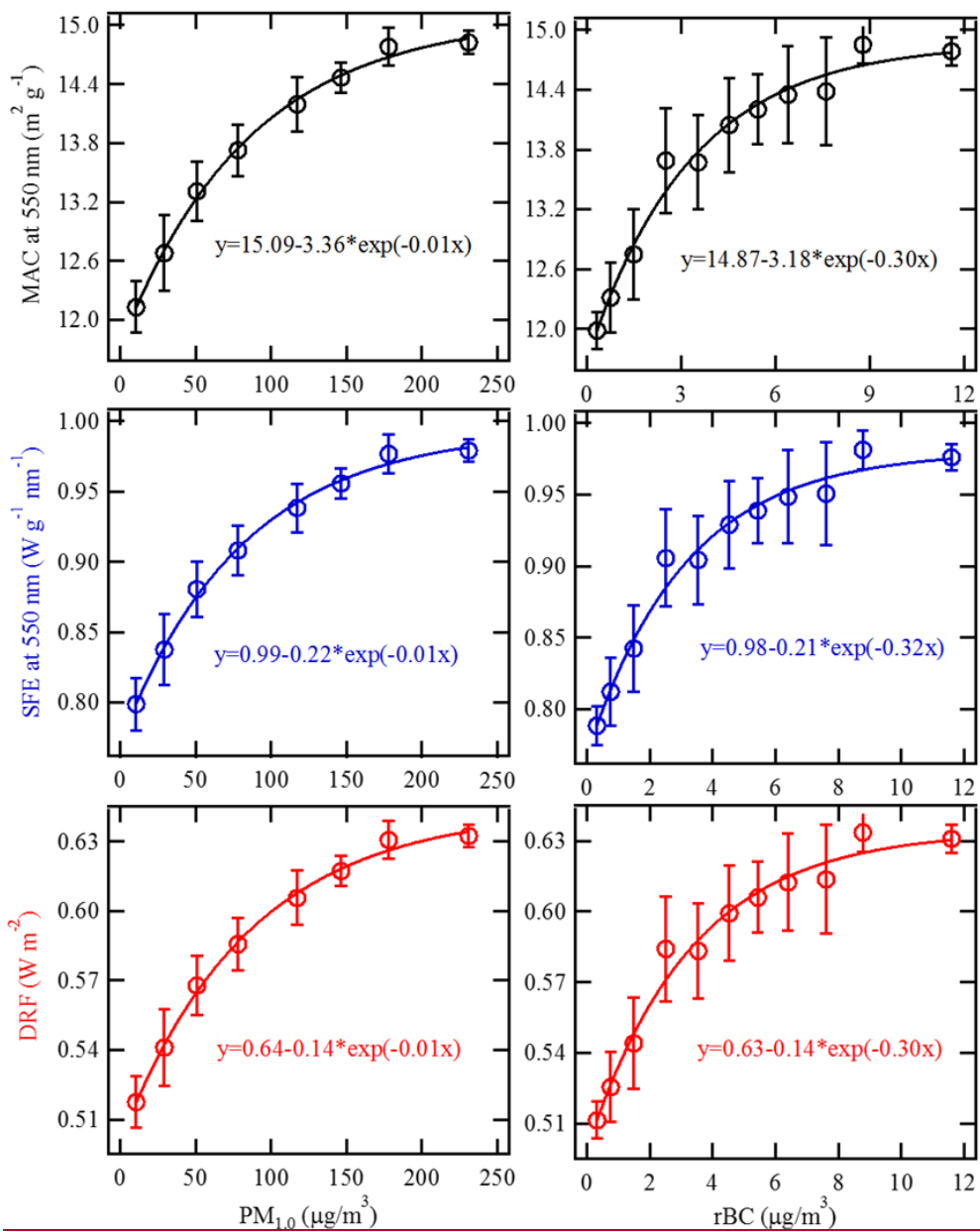


1
 2 **Figure 45.** Spatial distribution ($0.25^\circ \times 0.25^\circ$) of the effective emission intensity (EEI, unit of ton/grid/year) for BC transported
 3 to the observation site ($40^\circ 00' 17''$ N, $116^\circ 19' 34''$ E) during clean, slightly polluted and polluted periods. The clean ($PM_{2.5} \leq$
 4 $35 \mu\text{g m}^{-3}$), slightly polluted ($35 \mu\text{g m}^{-3} < PM_{2.5} \leq 115 \mu\text{g m}^{-3}$) and polluted ($PM_{2.5} > 115 \mu\text{g m}^{-3}$) periods were classified
 5 according to the Air Quality Index (Zheng et al. 2015). The site location and the boundaries of the in-region (i.e., Beijing) vs.
 6 outside of region (i.e., other areas such as Tianjin, Hebei, Inner Mongolia, Shanxi, Shandong), shown in Fig. S1. Noted that
 7 these regions are defined based on political boundaries.

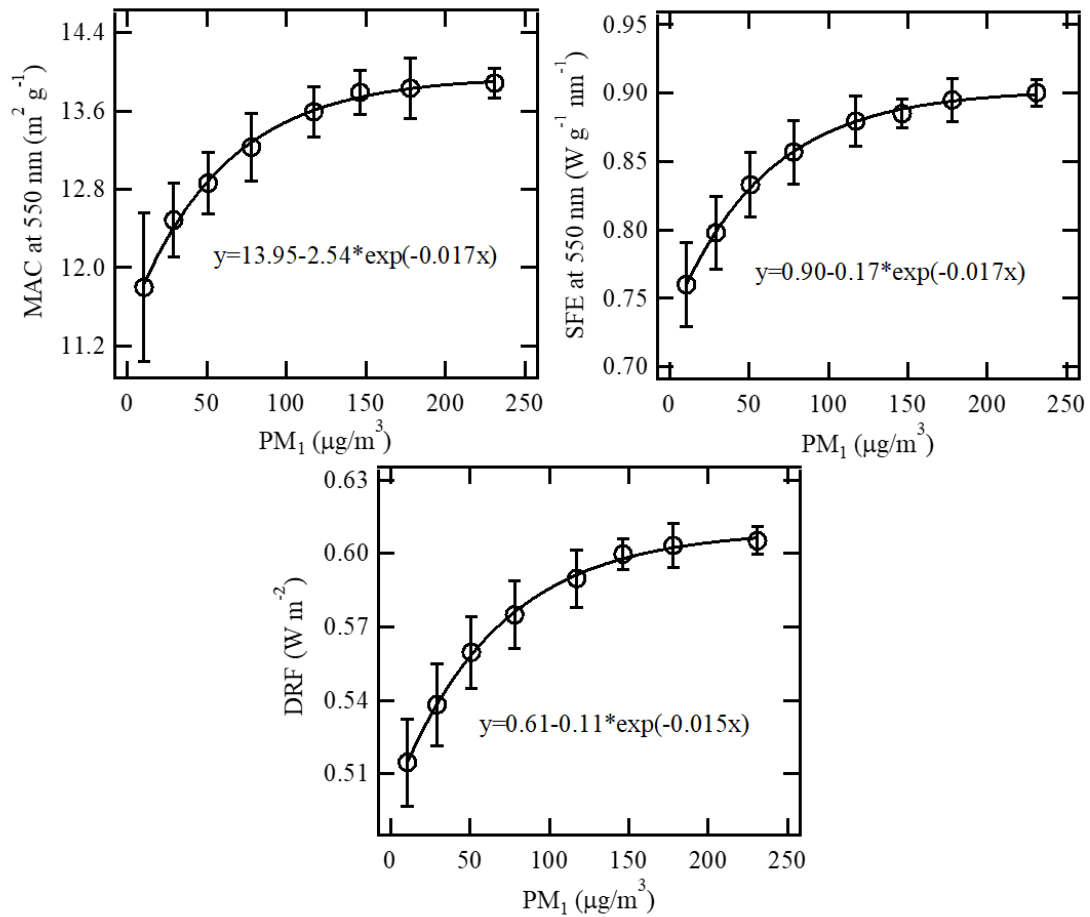


1

2 **Figure 56.** (a) Time series of the normalized EEI_{total} , D_p/D_c ratios and E_{ab} of BC-containing particles and the O_3 concentration
 3 during the campaign period. (b) Variations in the D_p/D_c and E_{ab} of BC-containing particles with the normalized EEI_{total} and O_3
 4 concentration. Normalized EEI_{total} ($EEI_{total-normalized}$) was calculated by scaling by a factor of 10^{-3} , namely $EEI_{total-normalized} \equiv$
 5 $EEI_{total}/1000$.

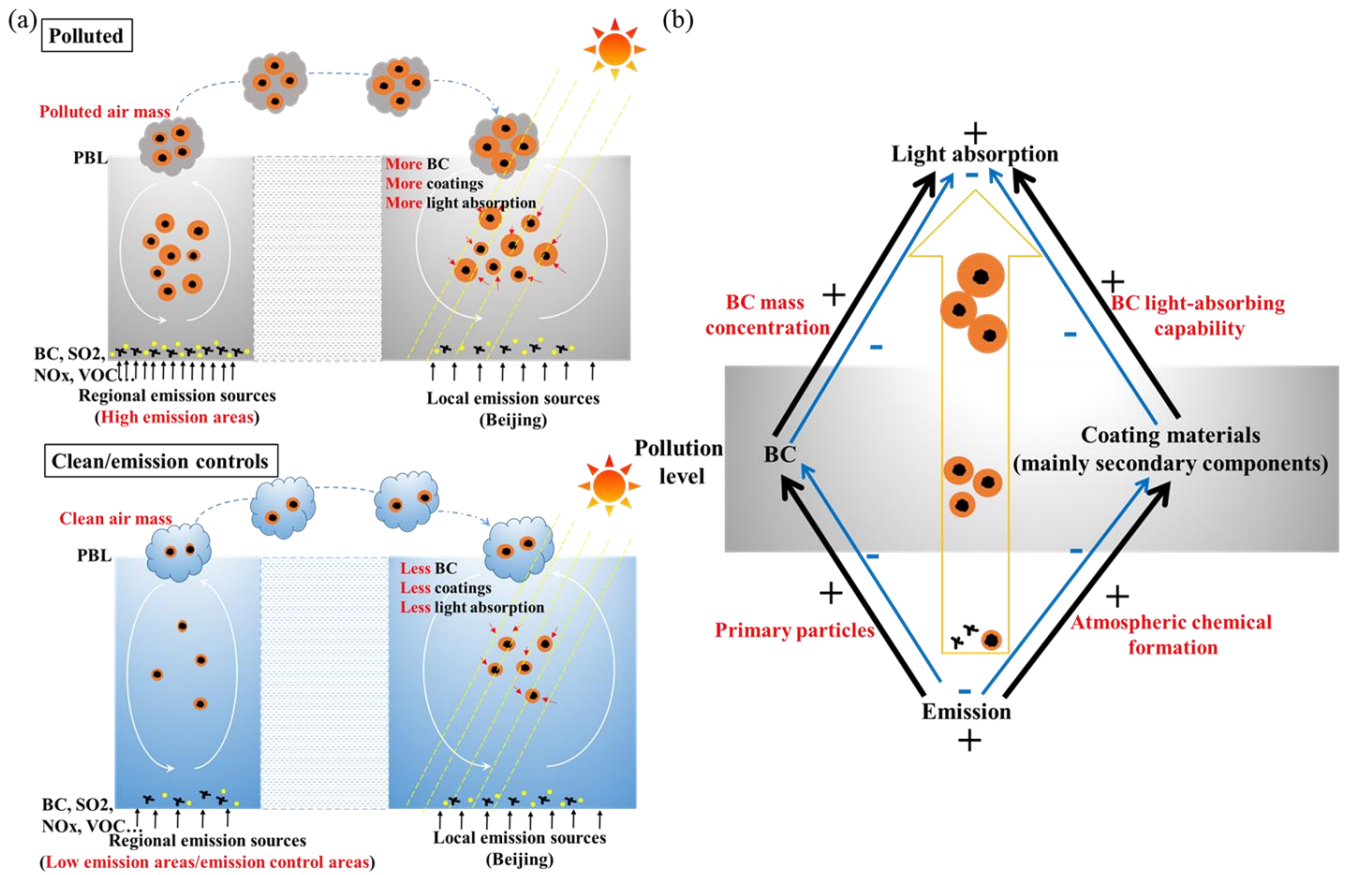


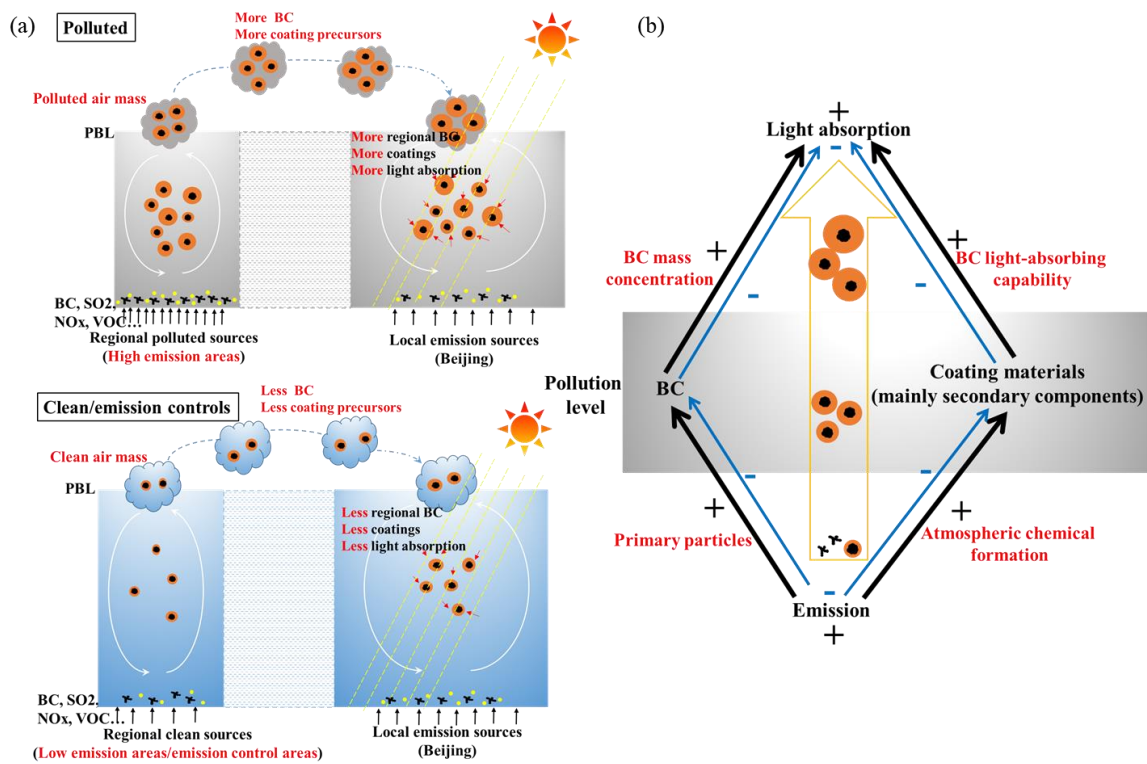
1



1

2 **Figure 67.** Variations in the *MAC*, *SFE* and *DRF* of BC-containing particles with the PM₁ and BC mass concentrations. The
 3 *DRF* values for BC-containing particles at different pollution levels were obtained by scaling the average *DRF* (0.32-31 W m⁻²,
 4 Table S1) of externally mixed BC with an average *MAC* of 7.5 m² g⁻¹ from various climate models (Bond et al., 2013) with
 5 a scaling factor of E_{ab} under different PM₁ concentrations. In order to point out the effect of BC light-absorption capability on
 6 *DRF* under different PM₁ concentrations, we did not consider the changes of total BC amount for *DRF* calculation in (c).





1

2 **Figure 78.** Conceptual scheme of amplification effect on BC light absorption associated with air pollution.

1 *Supplement of*

2 **Amplification of light absorption of black carbon**
3 **associated with air pollution**

4 Yuxuan Zhang^{1,2}, Qiang Zhang¹, Yafang Cheng^{3,2}, Hang Su^{3,2}, Haiyan Li⁴, Meng Li^{1,2},
5 Xin Zhang¹, Aijun Ding⁵, and Kebin He⁴

6 ¹Ministry of Education Key Laboratory for Earth System Modeling, Department of Earth System
7 Science, Tsinghua University, Beijing 100084, China

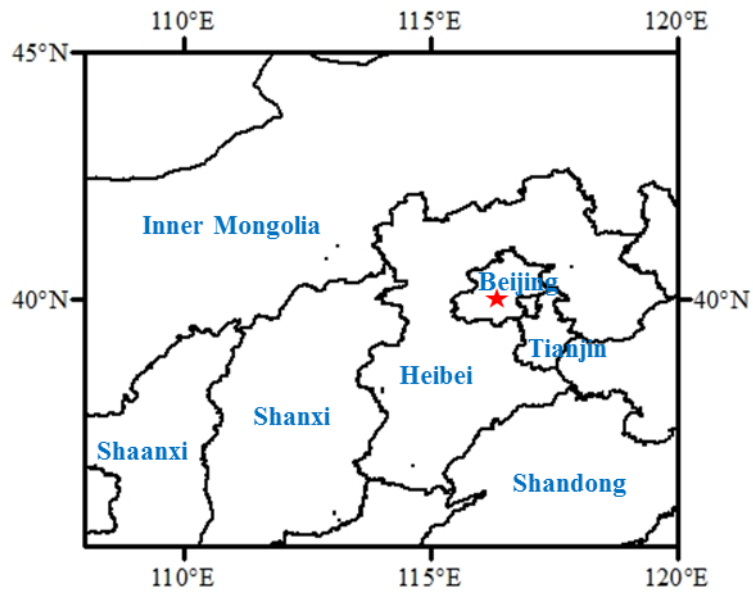
8 ²Multiphase Chemistry Department, Max Planck Institute for Chemistry, Mainz 55020, Germany

9 ³Institute for Environmental and Climate Research, Jinan University, Guangzhou 510630, China

10 ⁴State Key Joint Laboratory of Environment Simulation and Pollution Control, School of Environment,
11 Tsinghua University, Beijing 100084, China

12 ⁵Institute for Climate and Global Change Research, School of Atmospheric Sciences, Nanjing University,
13 Nanjing, China

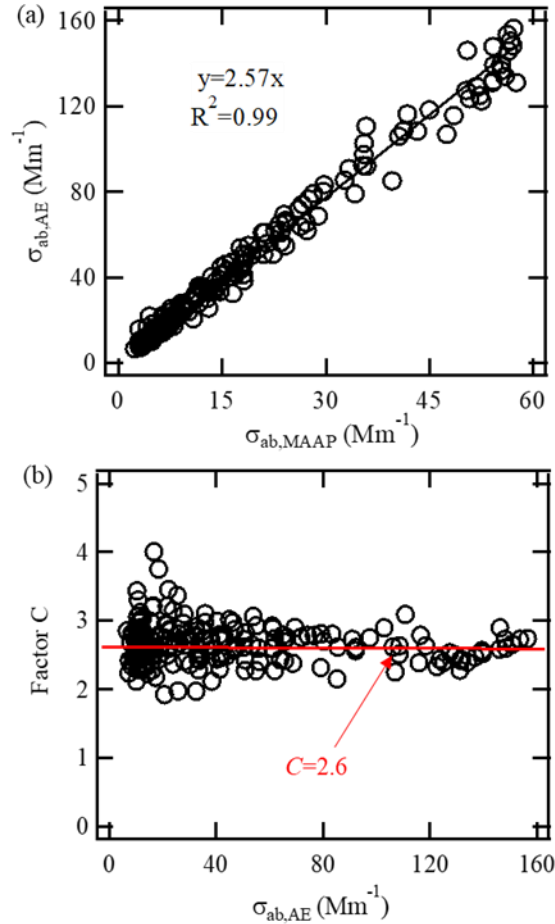
14 *Correspondence to:* Qiang Zhang (qiangzhang@tsinghua.edu.cn)



1

2 Figure S1. Location of the observation site (red star).

3 Figure S1 shows the geographic location of our observation site (namely red star
 4 marked in the Fig. S4). The site ($40^{\circ}00'17''$ N, $116^{\circ}19'34''$ E) is located in megacity
 5 Beijing, the capital of China. The air pollution levels in our site can be influence by the
 6 air mass from adjacent regions (i.e., Tianjin, Hebei, Inner Mongolia, Shanxi,
 7 Shandong).

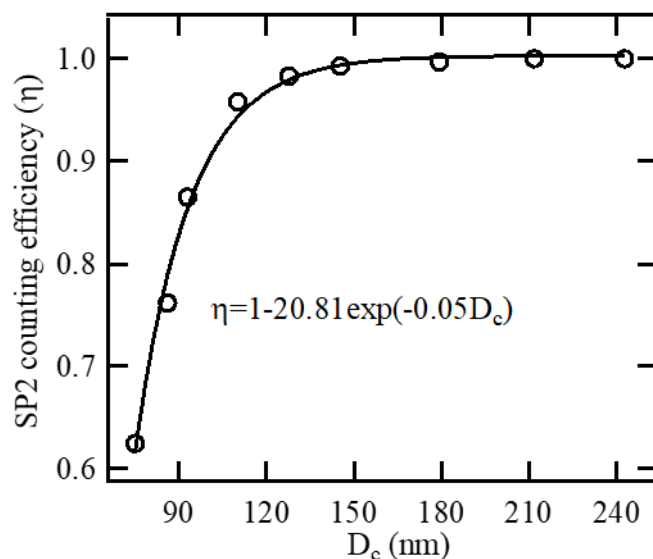


1

2 Figure S2. (a) The correlation between the absorption coefficient from AE33 at 660 nm
 3 ($\sigma_{ab,AE}$) and MAAP at 670 nm ($\sigma_{ab,MAAP}$). (b) Variety of multiple-scattering
 4 compensation factor C with different Aethalometer measurements.

5 Aethalometer artefacts are mainly from the loading effect and multiple-scattering
 6 effect (Weingartner et al., 2003; Segura et al., 2014). In terms of the loading effect, the
 7 compensation algorithm has been incorporated into Aethalometer model AE33
 8 (Drinovec et al., 2015). In this study, we focused on the multiple-scattering
 9 compensation, which was characterized by enhancement parameter C . The factor C for
 10 our sites was determined by comparing the absorption coefficient derived from AE33
 11 ($\sigma_{ab,AE}$) with the ones from MAAP ($\sigma_{ab,MAAP}$). Noted that the AE and MAAP
 12 measurements used to calculate the factor C were at different wavelengths, namely 660
 13 nm and 670 nm, respectively. Considering that the absorption is inversely proportional
 14 to wavelength (Bond and Bergstrom, 2006), the difference in wavelength would lead to
 15 an uncertainty of $\sim 1.5\%$ for the corrected absorption coefficients in AE measurement.

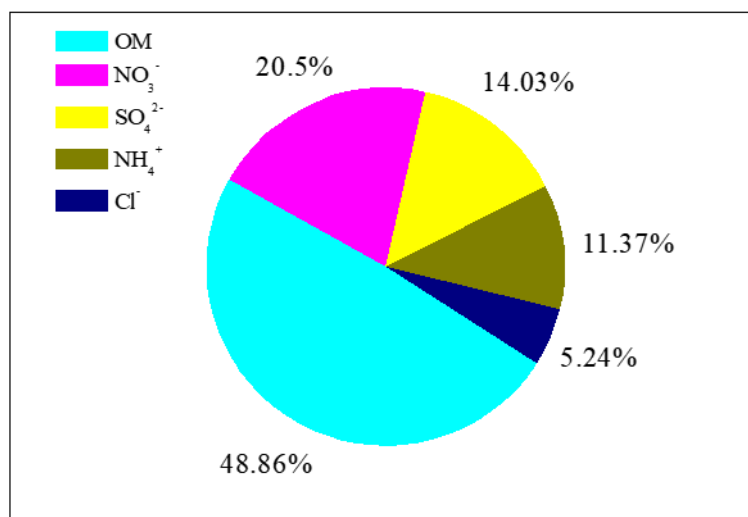
1 As shown in Fig. S2a, the slope 2.6 was taken as the value of factor C to compensate
 2 the Aethalometer data. The specifically site-calculated values of the factor C varies in
 3 the range of 1.9-4 in this work (Fig. S2b), consistent with previous studies (Drinovec et
 4 al., 2015; Weingartner et al., 2003; Segura et al., 2014). In this study, the uncertainty in
 5 the factor C was dominated by the uncertainty in MAAP measurements. We corrected
 6 the MAAP data using the algorithm reported by Hyvärinen et al. (2013). They estimated
 7 that the uncertainty in absorption coefficients derived from MAAP based on the
 8 developed algorithm was ~15% by comparing the results from a PAS against those
 9 derived from the MAAP in Beijing. This indicated that the factor C used in our study
 10 (~2.6) would exhibit an uncertainty of ~15% from the uncertainty in MAAP
 11 measurements. Considering the uncertainty on the AE33 measurements was mainly
 12 from the factor C , the absorption coefficient from AE33 was estimated to have an
 13 uncertainty of ~15%. Considering using a constant of 2.6 to simplify calculation, the
 14 uncertainty of the factor C is about ~10%, which would lead to an uncertainty of ~10%
 15 in absorption coefficient derived from Aethalometer measurements.



16
 17 Figure S3. SP2 detection efficiency of particle (η) in each rBC size-bin.

18 Figure S3 shows the SP2 detection efficiency concentration (η) in each rBC size-
 19 bin. In our study, the SP2 detection efficiency was determined with a DMA-SP2/CPC
 20 system. Monodispersed Aquadag particles generated by DMA were simultaneously

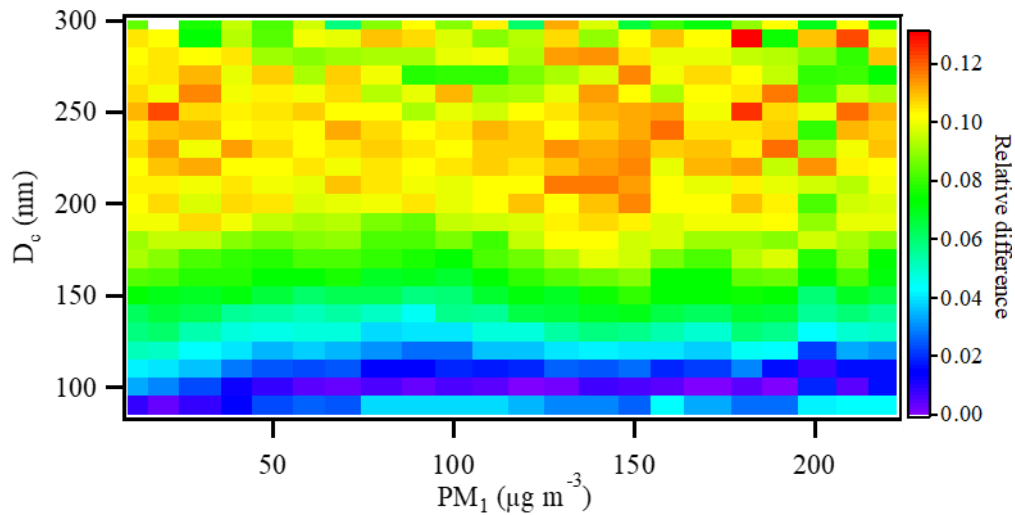
1 measured by SP2 and CPC. The size-resolved η was calculated by dividing the particle
2 number concentration from SP2 measurement by that from CPC measurement. The SP2
3 detection efficiency (Fig. S3) have been considered in the calculation of rBC mass
4 concentration.



6
7 Figure. S4. Non-refractory compositions of PM₁ particles during the campaign period.

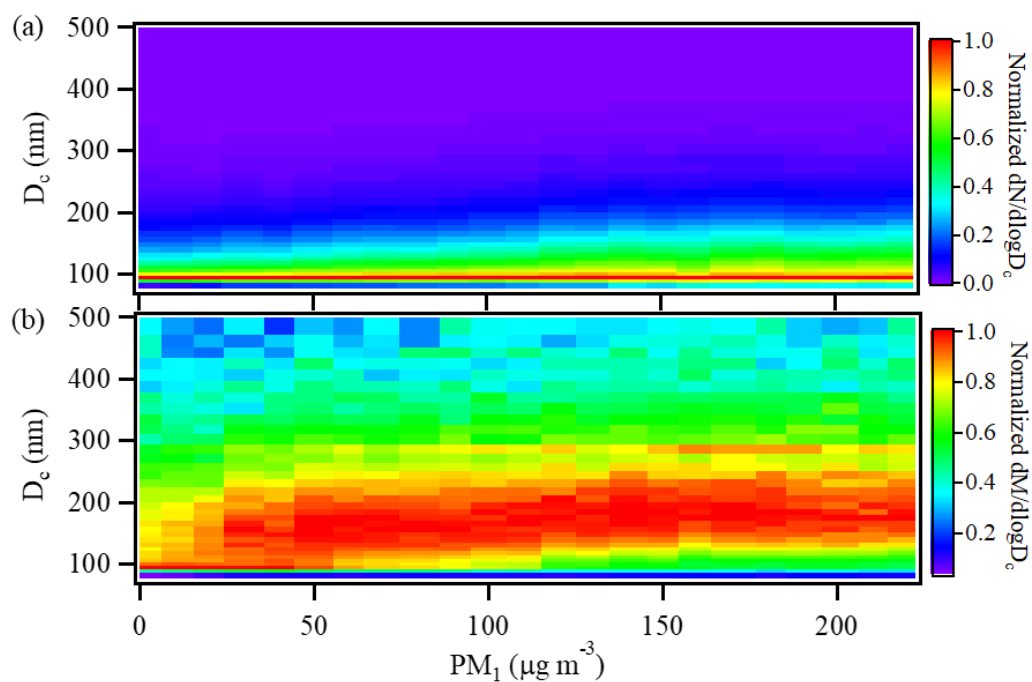
8 The R_{I_s} value used in this study are 1.50-0i based on the chemical compositions of
9 coating materials during the campaign period. The components of coating materials was
10 similar to non-refractory compositions in PM₁ particles (Peng et al., 2016). Figure S4
11 reveals that the fraction of inorganic and organic components in coating materials of
12 BC-containing particles are ~51% and ~49%, respectively. It is known from the
13 literature (Schkolnik et al., 2007; Mallet et al., 2003; Marley et al., 2001) that major
14 inorganic components of ambient aerosol from urban emission (nitrate, sulfate, mineral
15 dust, sea salt and trace metal) have a refractory of (1.5-1.6)-0i and there is a range of
16 (1.4-1.5)-0i for the refractory of organic components. In this study, we used the values
17 of 1.55-0i and 1.45-0i as refractive indexes of inorganic and organic components of
18 coating materials. The refractive index of a mixture particle can be calculated as the
19 volume weighted average of the refractive indices of all components (Hänel, et al. 1968;
20 Marley et al., 2001; Bond and Bergstrom, 2006; Schkolnik et al., 2007), as $\tilde{m} =$

1 $\sum_i \tilde{m}_i c_i$, where \tilde{m} is the refractive index of a mixture particle; \tilde{m}_i is the refractive index
2 of particle species; c is the volume ratio of particle species. Based on the equation, the
3 refractive index of coating materials of BC-containing particles (RI_s) was $\sim 1.50-0i$
4 during the campaign period.



5
6 Figure S3S5. The relative difference between the sizes of BC-containing particles (D_p)
7 derived from Mie calculation with RI_c of 2.26-1.26i and 1.95-0.79i.

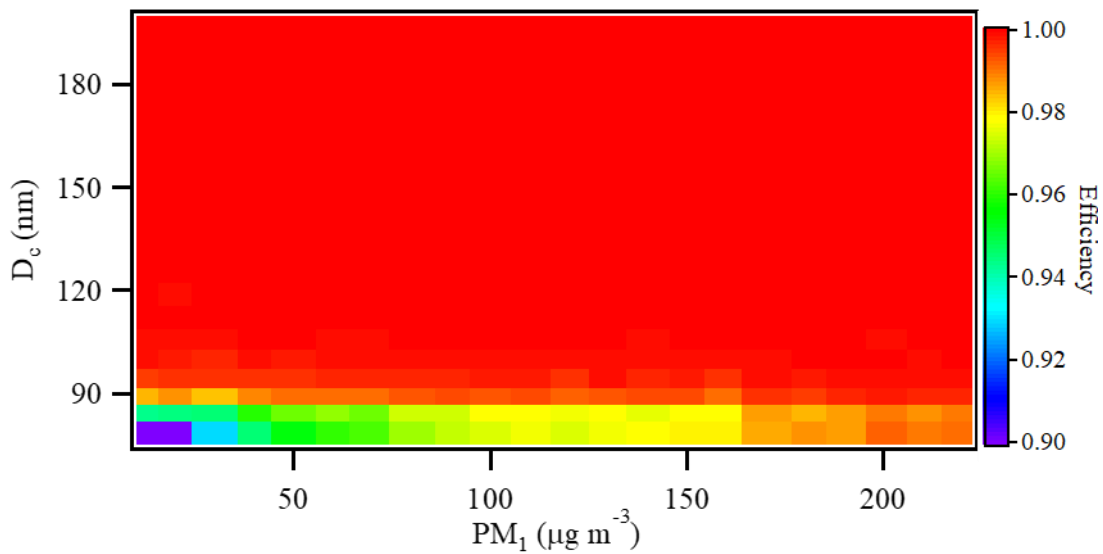
8 Various values (e.g., 2.26-1.26i, 1.95-0.79i) of refractive index of BC core (RI_c)
9 have been used in literature (Bond and Bergstrom, 2006; Cappa et al., 2012; Taylor et al.,
10 2015). Figure S3-S5 shows the relative difference between the sizes of BC-containing
11 particles (D_p) derived from Mie calculation with RI_c of 2.26-1.26i and 1.95-0.79i. For
12 BC-containing particles with 75-300 nm rBC cores, the relative difference is 3-10%,
13 indicating that the D_p values were not sensitive to RI_c values in our study. This could
14 be attributed to significantly larger in volume of coating materials than that of rBC
15 cores/larges of coating materials on BC surface in our site.



1

2 Figure S4-S6. Size distribution of refractory BC (rBC) as a function of the PM₁
 3 concentration: (a) number size distribution and (b) mass size distribution.

4 Figure S4-S6 shows the size distribution of rBC as a function of the PM₁
 5 concentration. Above the detection limit of SP2 incandescence (rBC with size larger
 6 than ~75 nm), the number size distribution of rBC cores shows a peak at ~95 nm under
 7 different PM₁ concentration (Fig. S4-S6 (a)), and there are about 95% of rBC particles
 8 in number concentration lower than 200 nm. As shown in Fig. S4-S6 (b), the mass size
 9 distribution of rBC cores shows a wide mode at ~95-200 nm under different PM
 10 concentration.

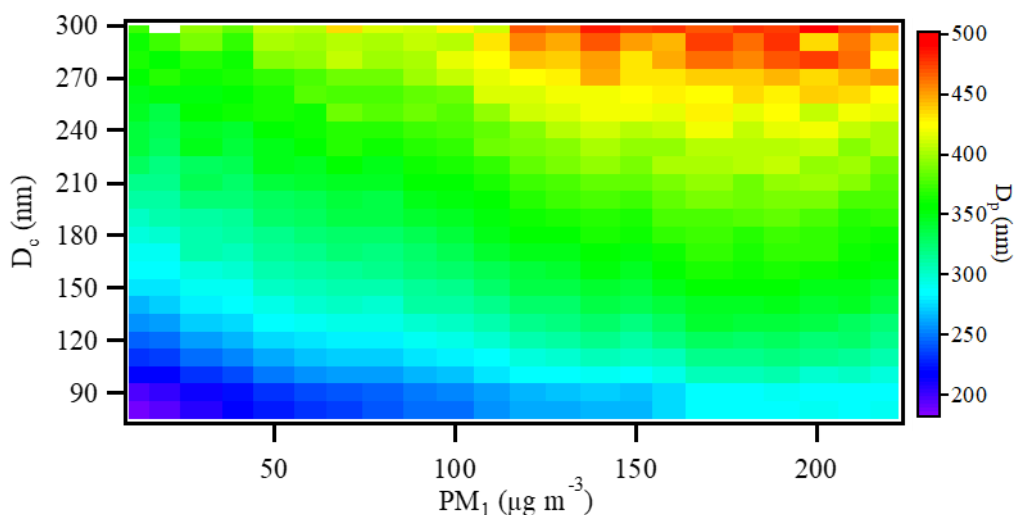


1

2 Figure [S5S7](#). The detect efficiency of SP2 scattering for BC-containing particles with
 3 size-resolved rBC cores (75-200 nm) under different PM_{10} concentration. In this study,
 4 the detect efficiency of SP2 scattering in terms of BC-containing particles at a certain
 5 rBC core size is defined as the ratio of the number concentration of particles above the
 6 detection limit of SP2 scattering and total particles.

7

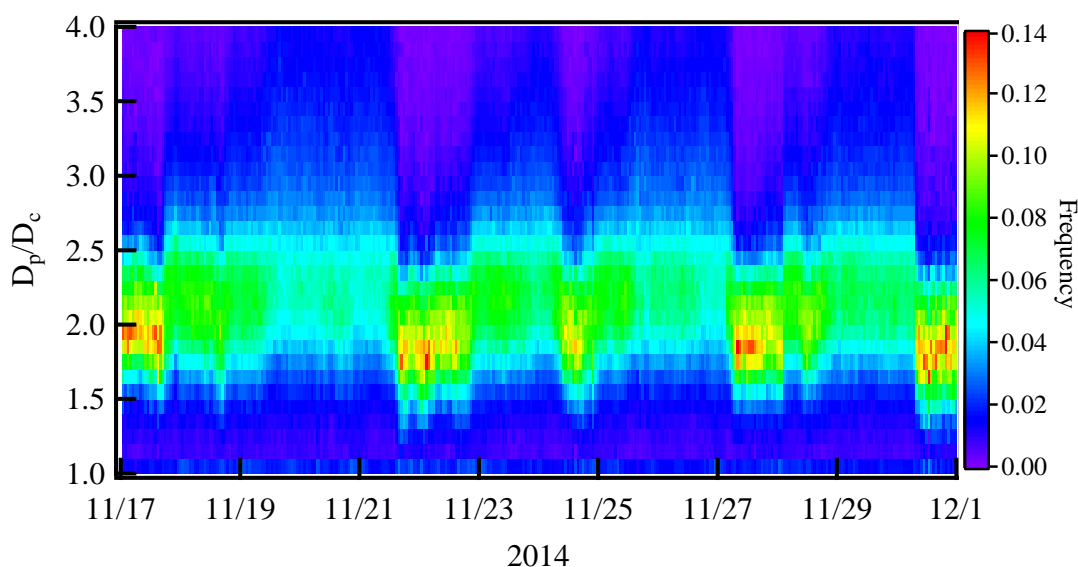
8 Figure [S5-S7](#) shows the detect efficiency of SP2 scattering for BC-containing
 9 particles with size-resolved rBC cores (75-200 nm) under different PM_{10} concentration.
 10 For BC-containing particles above the detection limit of our SP2 incandescence (rBC
 11 cores larger than ~ 75 nm), the detect efficiency of SP2 scattering is defined as the ratio
 12 of the number concentration of particles above the detection limit of SP2 scattering and
 13 total particles. The SP2 scattering exhibited a high detection efficiency (90-100%) for
 14 observed BC-containing particles with rBC cores more than 75 nm, which could be
 15 attributed to large BC-containing particles (~ 180 -500 nm shown in Fig. [S6S8](#)) in our
 16 site due to atmospheric aging. High detection efficiency of SP2 scattering is favor to
 17 retrieve the thickness of coating materials on rBC cores (>75 nm size studied in this
 work) based on scattering signal.



1

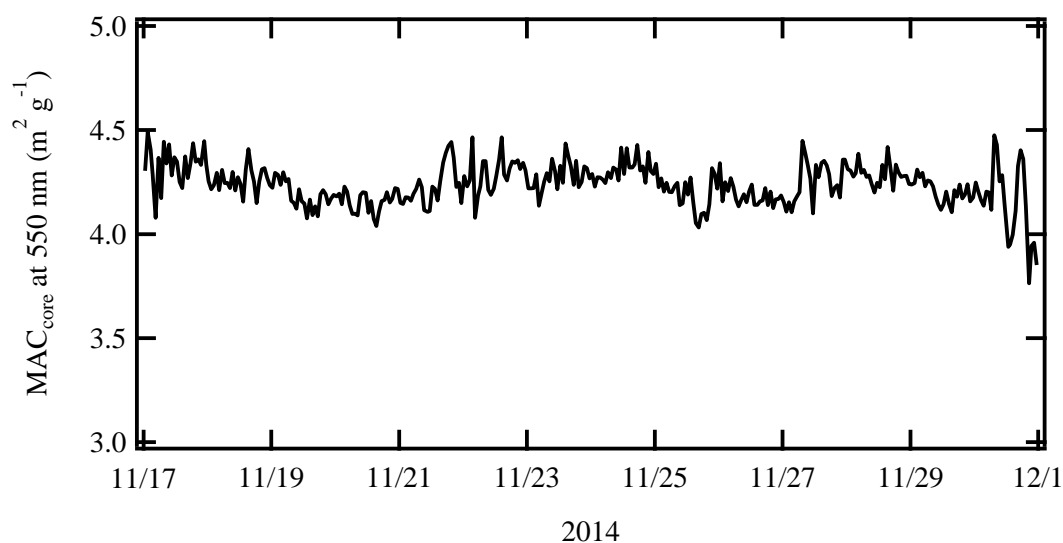
2 Figure S6S8. Frequency of the D_p/D_c ratio of BC-containing particles with size-
 3 resolved rBC cores as a function of PM_1 concentrations.

4 Figure S6-S8 shows frequency distribution of the D_p/D_c ratio of BC-containing
 5 particles with size-resolved rBC cores under different PM_1 concentrations. For BC-
 6 containing particles with 75-300 nm rBC cores, their particle size was in the range of
 7 180-500 nm. The particle size (D_p) of BC-containing particles with rBC cores at a
 8 certain size significantly increased with increasing PM_1 concentration, revealing more
 9 coating materials on BC surface under more polluted environment.



10

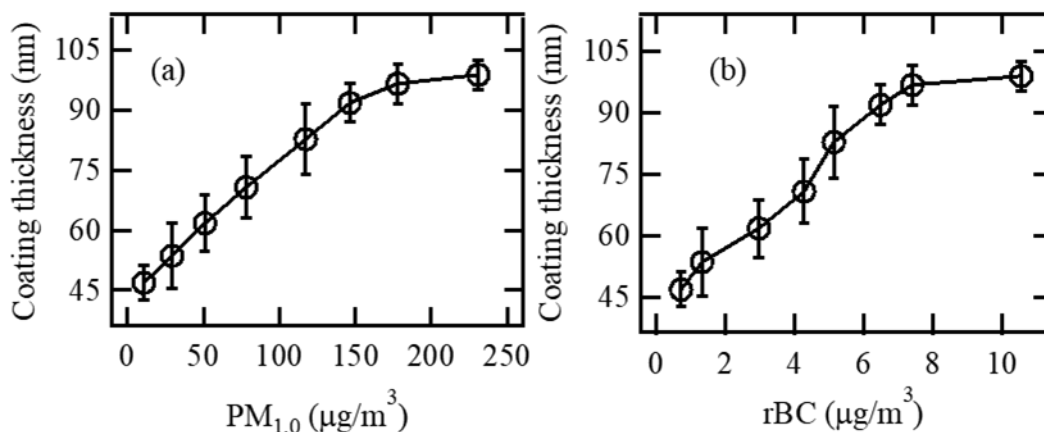
11 Figure S7. Frequency of the D_p/D_c ratio of BC-containing particles during the campaign
 12 period.



1 _____
 2 Figure. S9. The time series of MAC derived from Mie calculation for BC cores (i.e.,
 3 bare BC) at 880 nm.

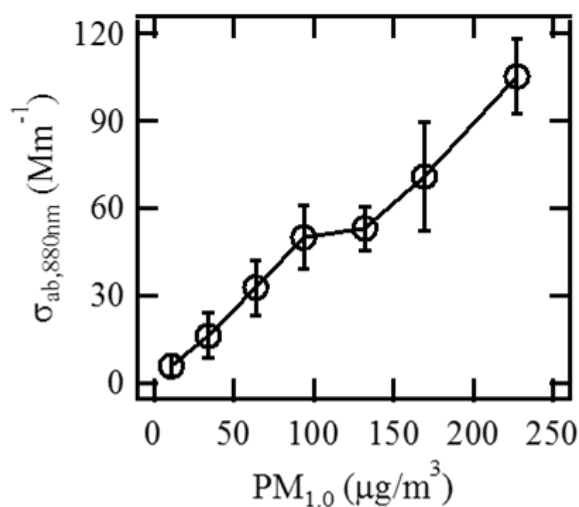
4 In this study, we used Mie mode to calculate optical properties of all BC-containing
 5 particles including bare BC and aged BC. Note that Mie theory is fundamentally ill-
 6 suited to calculation of optical properties for bare BC particles, which would lead to an
 7 uncertainty underestimate of their light absorption. Based on Mie calculation, we
 8 obtained the MAC of rBC core (MAC_c) at 880 nm in the range of 3.8-4.5 m²/g with an
 9 average of ~4.3 m²/g during the campaign period (Fig. S9). Bond and Bergstrom (2006)
 10 suggested a value of 7.5 m²/g for the MAC of bare BC at 550 nm. Considering that the
 11 absorption is inversely proportional to wavelength (Bond and Bergstrom, 2006), the
 12 MAC of bare rBC at 880 nm is estimated to be ~4.7 m²/g, which was slightly greater
 13 than that (~4.3 m²/g) obtained from Mie calculation in our study. This indicated the
 14 uncertainty of MAC for bare rBC from Mie calculation was ~8%. We estimated that
 15 the uncertainties of calculated BC light absorption related to MAC of bare rBC from
 16 Mie calculation was ~8%.Based on the ratio between absorption predictions of
 17 Rayleigh-Debye-Gans (RDG) theory and Mie theory for size-resolved bare BC
 18 particles shown by Bond and Bergstrom (2006), we estimated that the absorption of
 19 bare BC observed in our site (most of rBC particles with size in the range of 90-200
 20 nm, Fig. S4) using Mie theory with refractory index of 2.26-1.26i was underestimated
 21 by no more than 50%. Figure S7 shows that the bare BC particles (namely D_p/D_c smaller

1 than 1.1) only accounted for ~3% of total BC particles during the campaign period.
2 Therefore, the uncertainty of BC light absorption from the calculation of bare BC
3 properties using Mie theory is no more than 2%.



4
5 Figure S10. Variations in the coating thickness of BC-containing particles with the
6 (a) PM_1 and (b) rBC mass concentrations.

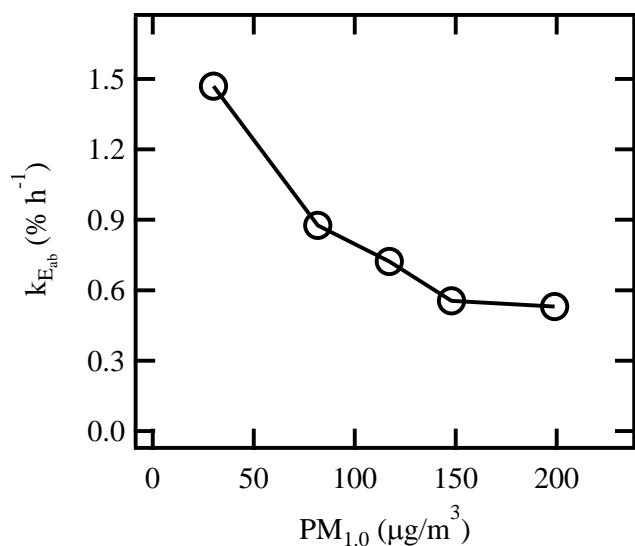
7 Figure S10 shows the coating thickness of BC-containing particles increased
8 with PM_1 and rBC concentration. The simultaneous increase in the rBC mass
9 concentration and the amount of coating materials on the BC surface could
10 significantly enhance the light absorption of BC-containing particles.



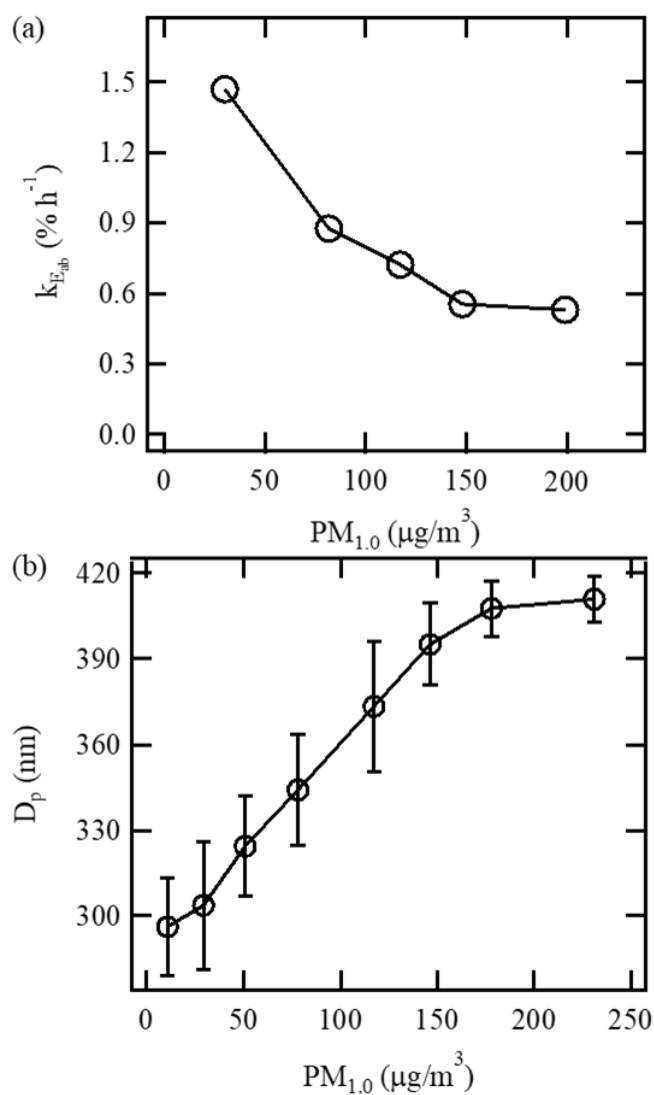
12

1 Figure ~~S8~~S11. Changes of the light absorption coefficient at 880 nm ($\sigma_{ab,880nm}$) with
2 PM₁ mass concentrations.

3 Figure ~~S8~~S11 shows the changes of the light absorption coefficient at 880 nm
4 ($\sigma_{ab,880nm}$) with PM₁ mass concentrations. The simultaneous increase in the rBC mass
5 concentration and the amount of coating materials shown in Fig. S10 revealed that the
6 increase of $\sigma_{ab,880nm}$ (~18 fold from ~10 $\mu\text{g m}^{-3}$ of PM₁ to ~230 $\mu\text{g m}^{-3}$ of PM₁) could be
7 attributed to simultaneous increase in the rBC mass concentration and the amount of
8 coating materials on the BC surface.~~The $\sigma_{ab,880nm}$ and rBC mass concentrations~~
9 ~~increased with increasing PM₁ mass concentrations. The increase of $\sigma_{ab,880nm}$ (~18 fold~~
10 ~~from ~10 $\mu\text{g m}^{-3}$ of PM₁ to ~230 $\mu\text{g m}^{-3}$ of PM₁) could be attributed to simultaneous~~
11 ~~increase in the rBC mass concentration and the amount of coating materials on the BC~~
12 ~~surface.~~



1

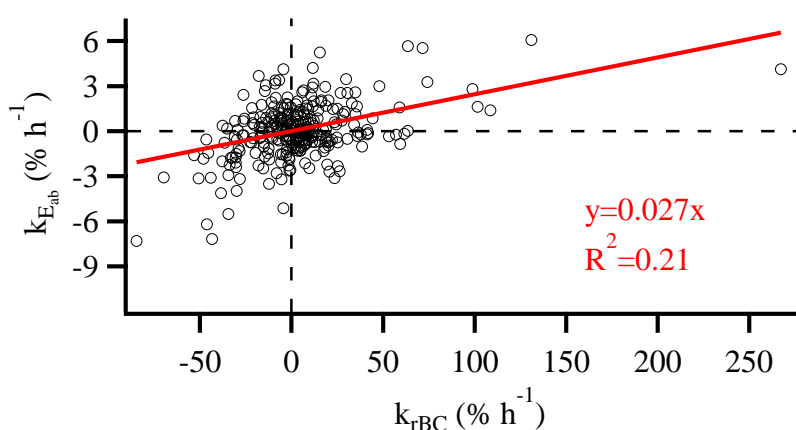


2

3 Figure S9S12. (a) Changes of growth rate of calculated E_{ab} ($k_{E_{ab}}$) with PM1 mass
 4 concentration. (b) Variations in the diameter of BC-containing particles (D_p) with the

1 normalized PM₁ concentrations.

2 As shown in Figure S9S12, the changes of growth rate of E_{ab} (k_{Eab}) decreased with
3 increasing PM₁ mass concentration. During the campaign period, the k_{Eab} of BC-
4 containing particles was in the 0.5-1.5% h⁻¹. The decrease of k_{Eab} associated with air
5 pollution indicated the enhancement of light absorption capability of BC-containing
6 particles slowed with further air pollution, because BC aging process by condensational
7 growth was less effective for more-aged BC particles with larger size under more
8 pollution environment (Fig. S6S12b). The net change in diameter for a given amount
9 of material deposited decreases with increasing particle size due to surface-to-volume
10 scaling, which would expect the growth rate of particles to decrease with increasing
11 PM₁ concentration and thus the k_{Eab} would also decrease.



12
13 Figure S13. Correlation between the growth rate of E_{ab} (k_{Eab}) and the growth rates of
14 rBC mass concentrations (k_{rBC}) during the campaign period.

15 Figure S13 shows the the relationship between the change rate of calculated E_{ab}
16 (k_{Eab}) and the change rates of rBC mass concentrations (k_{rBC}) with pollution
17 development. Linear relationships were estimated, i.e., $k_{Eab} \approx 0.027 k_{rBC}$. Compared
18 with the values of k_{rBC} , the significantly smaller k_{Eab} value indicated that the light
19 absorption capability of BC increased more slowly than rBC mass concentrations.

20
21 Table S1 The DRF of externally mixed BC from global climate models. The modeled
22 values were taken from Bond et al. (2013).

<u>Global climate</u> <u>Model</u>	<u>Mixing</u> <u>state</u>	<u>Modeled MAC</u> <u>(m² g⁻¹)</u>	<u>Modeled DRF</u> <u>(W m⁻²)</u>	<u>Reference</u>
<u>AeroCom models</u>				
<u>GISS</u>	<u>External</u>	<u>8.4</u>	<u>0.22</u>	<u>Schulz et al. (2006)</u>
<u>LOA</u>	<u>External</u>	<u>8.0</u>	<u>0.32</u>	<u>Schulz et al. (2006)</u>
<u>LSCE</u>	<u>External</u>	<u>4.4</u>	<u>0.30</u>	<u>Schulz et al. (2006)</u>
<u>SPRINTARS</u>	<u>External</u>	<u>9.8</u>	<u>0.32</u>	<u>Schulz et al. (2006)</u>
<u>UIO-CTM</u>	<u>External</u>	<u>7.2</u>	<u>0.22</u>	<u>Schulz et al. (2006)</u>
<u>UMI</u>	<u>External</u>	<u>6.8</u>	<u>0.25</u>	<u>Schulz et al. (2006)</u>
<u>Other models</u>				
<u>BCC_AGCM</u>	<u>External</u>	<u>4.3</u>	<u>0.10</u>	<u>Zhang et al. (2012)</u>
<u>CAM3 ECA</u>	<u>External</u>	<u>10.6</u>	<u>0.57</u>	<u>Kim et al. (2008)</u>
<u>GISS-GCM II</u>	<u>External</u>	<u>7.8</u>	<u>0.51</u>	<u>Chung and Seinfeld (2002)</u>
<u>Average values</u>		<u>7.5</u>	<u>0.31</u>	

1 The DRF values for BC-containing particles at different pollution levels were
2 obtained by scaling the average DRF (0.31 W m⁻²) of externally mixed BC from various
3 climate models (Bond et al. 2013) with a scaling factor of the calculated E_{ab} under
4 different PM₁ concentrations (Fig. 2b). The DRF (0.31 W m⁻²) of externally mixed BC
5 was the global averages from the global climate models listed in Table S1. In order to
6 point out the effect of BC light-absorption capability on DRF under different PM₁
7 concentrations, we did not consider the changes of BC amount for DRF calculation.

1 Table S4S2. Previous studies on the BC and PM (PM₁ or PM_{2.5}) mass concentrations in China.

Site	Measurement Period	PM ($\mu\text{g m}^{-3}$)	BC ($\mu\text{g m}^{-3}$)	Reference
Beijing (urban site)	1 to 31 January 2013	PM _{2.5} : ~4.4-855 (mean: 162)	~0.2-25	Zheng et al., 2015
Xi'an, Shaanxi (urban site)	23 December 2012 to 18 January 2013	PM _{2.5} : ~10-600	~0.3-44.5 (mean: 8.8)	Wang et al., 2014
Nanjing, Jiangsu (urban site)	1 January to 31 December 2015	PM ₁ : ~10-250 (mean: 48)	~0.5-20 (mean: 2.9)	Zhao et al., 2017
Shanghai (urban site)	5 to 10 December 2013	PM _{2.5} : ~40-636 (mean: 221)	~0.6-12.1 (mean: 3.2)	Gong et al., 2016
Jiaxing, Zhejiang (suburban site)	29 June to 15 July 2010 11 to 23 December 2010	PM ₁ : Summer ~4.6-104 (mean: 32.9) Winter 5.8-160 (mean: 41.9)	Summer ~0.4-11.7 (mean: 3.0) Winter ~0.52-49.5 (mean: 7.1)	Huang et al., 2013
Guangzhou, Guangdong (urban site)	5 October to 5	PM _{2.5} : ~63-152 (mean:103)	~3-20 (mean:103)	Andreae et al., 2008

	November 2004			
Heshan, Guangdong (suburban site)	From 21 November to 1 December 2010	PM _{2.5} : 23.5-145.2 (mean: 74.6)	2.9-13.8 (mean: 8.2)	Zhang et al., 2014

1

1 Table ~~S2~~ lists the BC and PM (PM₁ or PM_{2.5}) mass concentrations in China in
2 previous study. In this study, the PM₁ and rBC concentrations were 10-230 µg m⁻³ and
3 0.3-12µg m⁻³ in Beijing during the campaign period (17 to 30 November 2014), which
4 was consistent with previous studies in other polluted regions in China (Table ~~S2~~).
5 The consistency indicated that the enhancement of the light absorption capability of
6 BC-containing particles associated with air pollution not only occurred in Beijing but
7 also might be observed in other polluted regions in China.

8 **References**

9 Andreae, M. O., Schmid, O., Yang, H., Chand, D., Zhen Yu, J., Zeng, L.-M., and Zhang,
10 Y.-H.: Optical properties and chemical composition of the atmospheric aerosol in urban
11 Guangzhou, China, *Atmos. Environ.*, 42, 6335-6350, 2008.

12 Bond, T. C., and Bergstrom, R. W.: Light Absorption by Carbonaceous Particles: An
13 Investigative Review, *Aerosol Sci. Technol.*, 40, 27-67, 2006.

14 Cappa, C. D., Onasch, T. B., Massoli, P., Worsnop, D. R., Bates, T. S., Cross, E. S.,
15 Davidovits, P., Hakala, J., Hayden, K. L., Jobson, B. T., Kolesar, K. R., Lack, D. A.,
16 Lerner, B. M., Li, S.-M., Mellon, D., Nuaaman, I., Olfert, J. S., Petäjä, T., Quinn, P. K.,
17 Song, C., Subramanian, R., Williams, E. J., and Zaveri, R. A.: Radiative Absorption
18 Enhancements Due to the Mixing State of Atmospheric Black Carbon, *Science*, 337,
19 1078-1081, 2012.

20 [Chung, S. H., and Seinfeld, J. H.: Global distribution and climate forcing of
21 carbonaceous aerosols, *J. Geophys. Res.-Atmos.*, 107, AAC 14-11-AAC 14-33,
22 10.1029/2001JD001397, 2002.](#)

23 Drinovec, L., Močnik, G., Zotter, P., Prévôt, A., Ruckstuhl, C., Coz, E., Rupakheti, M.,
24 Sciare, J., Müller, T., and Wiedensohler, A.: The" dual-spot" Aethalometer: an
25 improved measurement of aerosol black carbon with real-time loading compensation,
26 *Atmos. Meas. Tech.*, 8, 1965-1979, 2015.

1 Gong, X., Zhang, C., Chen, H., Nizkorodov, S. A., Chen, J., and Yang, X.: Size
2 distribution and mixing state of black carbon particles during a heavy air pollution
3 episode in Shanghai, *Atmos. Chem. Phys.*, 16, 5399-5411, 2016.

4 [Hänel, G.: The real part of the mean complex refractive index and the mean density of](#)
5 [samples of atmospheric aerosol particles, *Tellus*, 20, 371-379, 1968.](#)

6 Huang, X.-F., Xue, L., Tian, X.-D., Shao, W.-W., Sun, T.-L., Gong, Z.-H., Ju, W.-W.,
7 Jiang, B., Hu, M., and He, L.-Y.: Highly time-resolved carbonaceous aerosol
8 characterization in Yangtze River Delta of China: Composition, mixing state and
9 secondary formation, *Atmos. Environ.*, 64, 200-207, 2013.

10 [Hyvärinen, A.-P., Vakkari, V., Laakso, L., Hooda, R. K., Sharma, V. P., Panwar, T. S.,](#)
11 [Beukes, J. P., van Zyl, P. G., Josipovic, M., Garland, R. M., Andreae, M. O., Pöschl,](#)
12 [U., and Petzold, A.: Correction for a measurement artifact of the Multi-Angle](#)
13 [Absorption Photometer \(MAAP\) at high black carbon mass concentration levels,](#)
14 [*Atmos. Meas. Tech.*, 6, 81-90, 2013.](#)

15 [Kim, D., Wang, C., Ekman, A. M. L., Barth, M. C., and Rasch, P. J.: Distribution and](#)
16 [direct radiative forcing of carbonaceous and sulfate aerosols in an interactive size-](#)
17 [resolving aerosol–climate model, *J. Geophys. Res.-Atmos.*, 113,](#)
18 [10.1029/2007JD009756, 2008.](#)

19 [Mallet, M., J.C. Roger, S. Despiiau, O. Dubovik and J.P. Putaud \(2003\), Microphysical](#)
20 [and optical properties of aerosol particles in urban zone during ESCOMPTE. *Atmos.*](#)
21 [*Res.*, 69\(1-2\), 73-97.](#)

22 [Marley, N.A., J.S. Gaffney, C. Baird, C.A. Blazer, P. J. Drayton and J. E. Frederick](#)
23 [\(2001\), An empirical method for the determination of the complex refractive index of](#)
24 [size fractionated atmospheric aerosols for radiative transfer calculations, *Aerospace.*](#)
25 [*Sci. Technol.* 34\(6\), 535-549.](#)

26 [Schkolnik, G., D. Chand, A. Hoffer, M.O. Andreae, C. Erlick, E. Swietlicki and Y.](#)
27 [Rudich \(2007\), Constraining the density and complex refractive index of elemental and](#)
28 [organic carbon in biomass burning aerosol using optical and chemical measurements,](#)
29 [*Atmos. Environ.*, 41, 1107-1118.](#)

1 [Schulz, M., Textor, C., Kinne, S., Balkanski, Y., Bauer, S., Berntsen, T., Berglen, T.,](#)
2 [Boucher, O., Dentener, F., Guibert, S., Isaksen, I. S. A., Iversen, T., Koch, D., Kirkevåg,](#)
3 [A., Liu, X., Montanaro, V., Myhre, G., Penner, J. E., Pitari, G., Reddy, S., Seland, Ø.,](#)
4 [Stier, P., and Takemura, T.: Radiative forcing by aerosols as derived from the AeroCom](#)
5 [present-day and pre-industrial simulations, *Atmos. Chem. Phys.*, 6, 5225-5246, 2006.](#)

6 Segura, S., Estellés, V., Titos, G., Lyamani, H., Utrillas, M. P., Zotter, P., Prévôt, A. S.
7 H., Močnik, G., Alados-Arboledas, L., and Martínez-Lozano, J. A.: Determination and
8 analysis of in situ spectral aerosol optical properties by a multi-instrumental approach,
9 *Atmos. Meas. Tech.*, 7, 2373–2387, 2014.

10 Taylor, J. W., Allan, J. D., Liu, D., Flynn, M., Weber, R., Zhang, X., Lefer, B. L.,
11 Grossberg, N., Flynn, J., and Coe, H.: Assessment of the sensitivity of core / shell
12 parameters derived using the single-particle soot photometer to density and refractive
13 index, *Atmos. Meas. Tech.*, 8, 1701-1718, 2015.

14 Wang, Q., Huang, R. J., Cao, J., Han, Y., Wang, G., Li, G., Wang, Y., Dai, W., Zhang,
15 R., and Zhou, Y.: Mixing State of Black Carbon Aerosol in a Heavily Polluted Urban
16 Area of China: Implications for Light Absorption Enhancement, *Aerosol Sci. Technol.*,
17 48, 689-697, 2014.

18 Weingartner, E., Saathoff, H., Schnaiter, M., Streit, N., Bitnar, B., and Baltensperger,
19 U.: Absorption of light by soot particles: determination of the absorption coefficient by
20 means of aethalometers, *J. Aerosol Sci.*, 34, 1445–1463, 2003.

21 Zhang, G., Bi, X., He, J., Chen, D., Chan, L. Y., Xie, G., Wang, X., Sheng, G., Fu, J.,
22 and Zhou, Z.: Variation of secondary coatings associated with elemental carbon by
23 single particle analysis, *Atmos. Environ.*, 92, 162-170, 2014.

24 [Zhang, H., Wang, Z., Wang, Z., Liu, Q., Gong, S., Zhang, X., Shen, Z., Lu, P., Wei, X.,](#)
25 [Che, H., and Li, L.: Simulation of direct radiative forcing of aerosols and their effects](#)
26 [on East Asian climate using an interactive AGCM-aerosol coupled system, *Clim. Dyn.*,](#)
27 [38, 1675-1693, 10.1007/s00382-011-1131-0, 2012.](#)

28 Zhao, Q., Shen, G., Li, L., Chen, F., Qiao, Y., Li, C., Liu, Q., and Han, J.: Ambient
29 Particles (PM₁₀, PM_{2.5} and PM_{1.0}) and PM_{2.5} Chemical Components in Western

1 Yangtze River Delta (YRD): An Overview of Data from 1-year Online Continuous
2 Monitoring at Nanjing, *Aerosol Sci. Eng.*, 2017.

3 Zheng, G. J., Duan, F. K., Su, H., Ma, Y. L., Cheng, Y., Zheng, B., Zhang, Q., Huang,
4 T., Kimoto, T., Chang, D., Pöschl, U., Cheng, Y. F., and He, K. B.: Exploring the severe
5 winter haze in Beijing: the impact of synoptic weather, regional transport and
6 heterogeneous reactions, *Atmos. Chem. Phys.*, 15, 2969-2983, 2015.

7